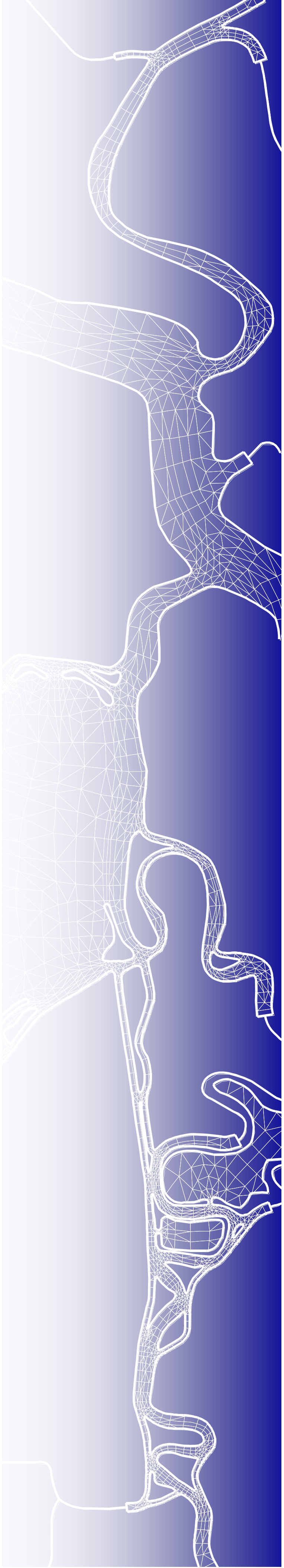

HYDRODYNAMIC AND SALINITY TRANSPORT MODELING OF THE HISTORICAL BAY-DELTA SYSTEM

TECHNICAL MEMORANDUM
APRIL 2014

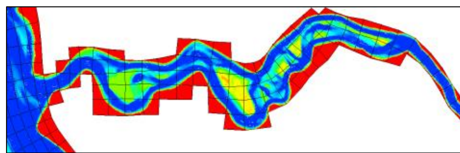

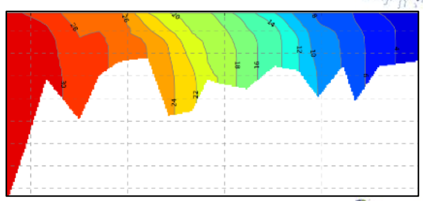

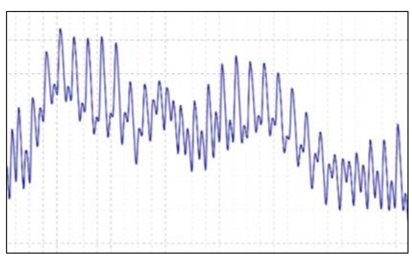

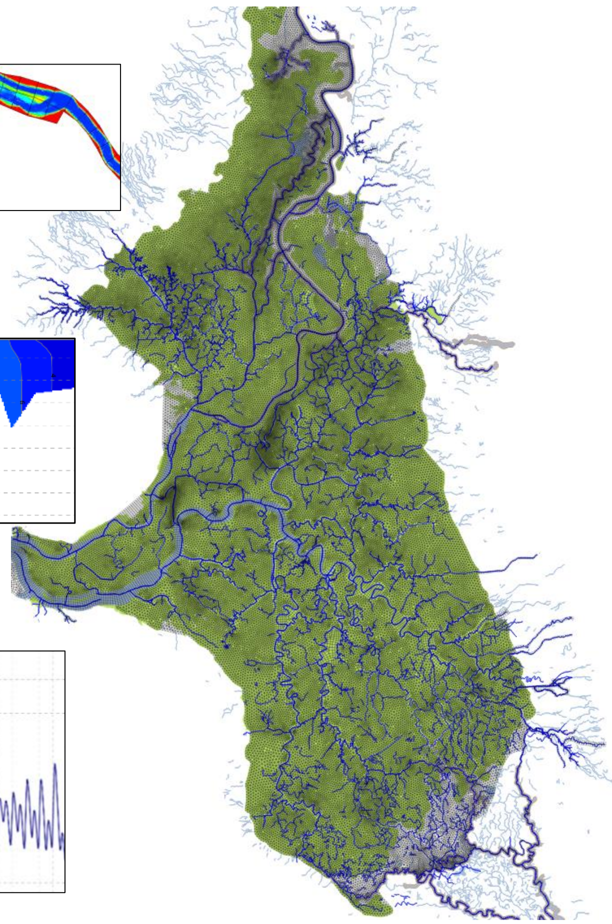

Prepared For:
Metropolitan Water District of Southern California
1121 L Street, Suite 900
Sacramento, CA 95814
Contact:
Paul Hutton
916-650-2620

Prepared By:
Resource Management Associates
4171 Suisun Valley Road, Suite J
Fairfield, CA 94534
Contact:
John DeGeorge
707-864-2950

RMA RESOURCE MANAGEMENT ASSOCIATES

Executive Summary

Human activities in the Sacramento and San Joaquin watersheds and Bay-Delta have changed inflow and outflow patterns and the geometry and connectivity of channels throughout the Delta. The purpose of this project is to model the historical Delta and characterize the salinity regime in comparison to that of the current Delta. The major project tasks undertaken to accomplish this objective were: 1) build a model grid for the contemporary Bay-Delta system, 2) calibrate the contemporary model using observed data in order to validate the computational engine, 3) build a model grid for the historical Delta based on reconstructed Delta channel configurations and geometries, 4) calibrate the historical model based on historical observed data, and 5) visualize and characterize the salinity regime of the historical Delta.

The three-dimensional hydrodynamic model UnTRIM was chosen as the computational engine for modeling because of its efficiency, stability, documentation, and demonstrated accuracy on similar estuarine circulation problems. Code was added to the user interface in order to handle time variable inflows and exports; spatially variable friction, evaporation, and precipitation; gate operations; time variable wind; Delta Island Consumptive Use; and a compact output file format for quick model data extraction.

The contemporary Bay-Delta grid was built using elements aligned to major flow paths through the system. It was calibrated for two time periods (in 1994 and 2010) by varying bottom friction values.

The historical Bay-Delta grid was constructed using the contemporary grid as a base. Cut channels and canals constructed in recent times were removed, and several historically important channels were added. The marsh plain areas within the channel network and on the Delta periphery were added to the grid. A historical Delta digital elevation model, developed through a collaborative effort with the San Francisco Estuary Institute (under subcontract with RMA) and the University of California, Davis, was used to set the historical Delta grid bathymetry.

The presence of bathymetric artifacts, unintentionally created as part of the digital elevation model construction process, caused severe flow constrictions in many of the important Delta channels. This rendered the results obtained with the historical flow model unusable for assessing changes in the salinity regime. Phase I of this project was concluded at this point in the work. Phase II is planned for the immediate future and will address fixes for the elevation model artifacts and then proceed to calibrate and run simulations using the historical model.

HYDRODYNAMIC AND SALINITY TRANSPORT MODELING OF THE HISTORICAL BAY AND DELTA SYSTEM – TECHNICAL MEMORANDUM

TABLE OF FIGURES

1 Introduction

Human activities in the Sacramento and San Joaquin watersheds and Bay-Delta have changed inflow and outflow patterns and the geometry and connectivity of channels throughout the Delta.

The purpose of this project is to model the historical Delta and characterize the salinity regime in comparison to that of the contemporary Delta.

This project is a joint effort between RMA, the San Francisco Estuary Institute (SFEI), the University of California, Davis (UCD), and MWH engineering. SFEI is responsible for translating research on historical Delta (Whipple, et al., 2013) into a shapefile representing the configuration of the historical Delta. UCD is responsible for translating this shapefile into a digital elevation model (DEM). RMA is responsible for using the historical DEM to create a three-dimensional (3D) model representing the historical Delta and performing model simulations to estimate the historical salinity regime. MWH is responsible for providing estimates of historical hydrology to be used as model boundary conditions.

Progress of work done by SFEI, UCD, and MWH are detailed in separate technical memorandums.

The steps necessary for RMA to complete the objectives of the project include the following.

1) Build a grid for contemporary Bay-Delta; the Bay configuration and much of the present day Delta channel configuration was the same in the historical condition.
2) Calibrate the contemporary Bay-Delta model in order to validate the chosen compute engine and boundary condition implementation; using the contemporary Bay-Delta model for this validation allows the use of observed data for model evaluation which is much more accurate and abundant.
3) Build a historical Bay-Delta grid based on the SFEI Delta channel configurations and the UCD historical DEM; the contemporary Bay-Delta planform grid is used as a base.
4) Calibrate the historical Bay-Delta model based on SFEI-collected, historical observed data.
5) Run the historical Bay-Delta model using historical hydrology based on MWH estimates.
6) Characterize the salinity regime of the historical Delta.

This report details Phase I of the project and presents preliminary results for steps 1–4. Steps 5 and 6 will be covered in Phase II of project.

2 Model Information

The computational model chosen for this project is UnTRIM (Casulli and Walters, 2000). UnTRIM is a 3D finite difference model that solves the shallow water equations to predict water velocities, water surface elevations, and scalar transport. The computations are performed over an unstructured orthogonal grid in order to accurately fit the boundaries of complex shorelines. UnTRIM is computationally efficient and stable; it may be run in parallel to utilize multiple compute threads. The model allows for the relevant physical processes necessary for modeling estuarine transport and circulation to be taken into account. Development and applications of UnTRIM have been extensively documented and verified in peer reviewed journals. Many of these applications have demonstrated its accuracy and efficiency in modeling estuarine circulation and salinity regimes (Cheng and Casulli, 2001). UnTRIM is currently developed and maintained by Vincenzo Casulli at the University of Trento, Italy.

2.1 Governing Equations

The UnTRIM computational engine solves the 3D equations governing conservation of fluid volume and momentum, and scalar transport:

$$\frac{\partial u}{\partial t} + u\,\frac{\partial u}{\partial x} + v\,\frac{\partial u}{\partial y} + w\,\frac{\partial u}{\partial z} - fv = -g\,\frac{\partial \eta}{\partial x} + \nu^h\left(\frac{\partial^2 u}{\partial x^2} + \frac{\partial^2 u}{\partial y^2}\right) + \frac{\partial}{\partial z}\left(\nu^v\frac{\partial u}{\partial z}\right)$$

$$\frac{\partial v}{\partial t} + u\,\frac{\partial v}{\partial x} + v\,\frac{\partial v}{\partial y} + w\,\frac{\partial v}{\partial z} + fu = -g\,\frac{\partial \eta}{\partial y} + \nu^h\left(\frac{\partial^2 v}{\partial x^2} + \frac{\partial^2 v}{\partial y^2}\right) + \frac{\partial}{\partial z}\left(\nu^v\frac{\partial v}{\partial z}\right)$$

$$\frac{\partial u}{\partial x} + \frac{\partial v}{\partial y} + \frac{\partial w}{\partial z} = 0$$

where *u*, *v*, and *w* are the velocities in the *x*, *y*, and *z* directions, *t* is time, *f* is the Coriolis frequency, *g* is the acceleration of gravity, η is the free surface elevation, and ν are the eddy viscosities. These equations are subject to the free surface boundary conditions:

$$\frac{\partial \eta}{\partial t} + \frac{\partial}{\partial x}\left[\int_{-h}^{\eta} u\,dz\right] + \frac{\partial}{\partial y}\left[\int_{-h}^{\eta} v\,dz\right] = 0$$

$$\nu^v\,\frac{\partial u}{\partial z} = \gamma_T(u_a - u), \qquad \nu^v\,\frac{\partial v}{\partial z} = \gamma_T(v_a - v), \qquad \text{at } z = \eta$$

where γ_T is the wind stress coefficient at the water surface, *h* is the water depth measured positive downward from a constant vertical datum, and u_a and v_a are the components of the wind velocity.

The bottom boundary condition is:

$$\nu^v\,\frac{\partial u}{\partial z} = \gamma_B\,u, \qquad \nu^v\,\frac{\partial v}{\partial z} = \gamma_B\,v, \qquad \text{at } z = -h$$

where γ_T is the bottom friction coefficient. In the implementation of UnTRIM for this project, the bed friction coefficient is specified as a function of the bed roughness height, following Gross (2010).

2.2 UnTRIM Model Interface

The UnTRIM model is provided as a computational engine with a Fortran-based API that allows users to customize their implementations of boundary conditions in order to account for relevant physical processes in the modeled hydrodynamic environment. This allows for a great range of flexibility in the modeling environments that UnTRIM is able to handle, but requires significant work from the user in setting boundary conditions and getting model output. These tasks are handled through the interface using a series of routines that are documented in BAW (2010). In collaboration with the UCD Watershed Science Center, the model interface code was built up for this project in order to for UnTRIM to account for:

- Time variable river inflows and exports boundary conditions
- Time variable ocean water surface boundary condition
- Time variable salinity boundary conditions
- Delta Island Consumptive Use (DICU)
- Gate operations
- Vertical turbulence closure scheme
- Spatially variable bottom roughness coefficients
- Wind stress forcing at the water surface
- Spatially variable evaporation and precipitation
- Spatially variable initial conditions for the water surface elevation and salinity
- Restart and model log file creation
- Compact output file creation

2.3 Documentation and Model Validation

The development of UnTRIM has been tracked through several peer reviewed journal articles. A brief list of the major ones is given below:

- Original TRIM 3D model – Casulli and Catani (1994)
- UnTRIM model, use of unstructured grids – Casulli and Walters (2000)
- Scalar advection – Casulli and Zanolli (2005)
- Wetting and drying of grid cells – Casulli (2008)
- Subgrid methodology – Casulli and Stelling (2010)

Additionally, the German Bundesanstalt für Wasserbau (BAW) Federal Waterways Engineering and Research Institute has documented the model details, assumptions, and verification studies under a broad range of 3D environmental flows (BAW, 2004).

2.4 Unstructured Orthogonal Grid

An unstructured orthogonal grid is required to run UnTRIM. The model domain must be covered by set of non-overlapping convex polygons. In order for the grid to be classified as orthogonal, lines joining the centers of adjacent elements must intersect the element edge at right angles. An example of an orthogonal grid is shown in Figure 2-1. Although grid orthogonality for areas with complex boundaries is difficult to achieve, it greatly increases the accuracy and efficiency of the UnTRIM computational algorithm.

The software program Janet[1], developed by Smile Consultants and recommended for use with UnTRIM, was chosen for grid generation.

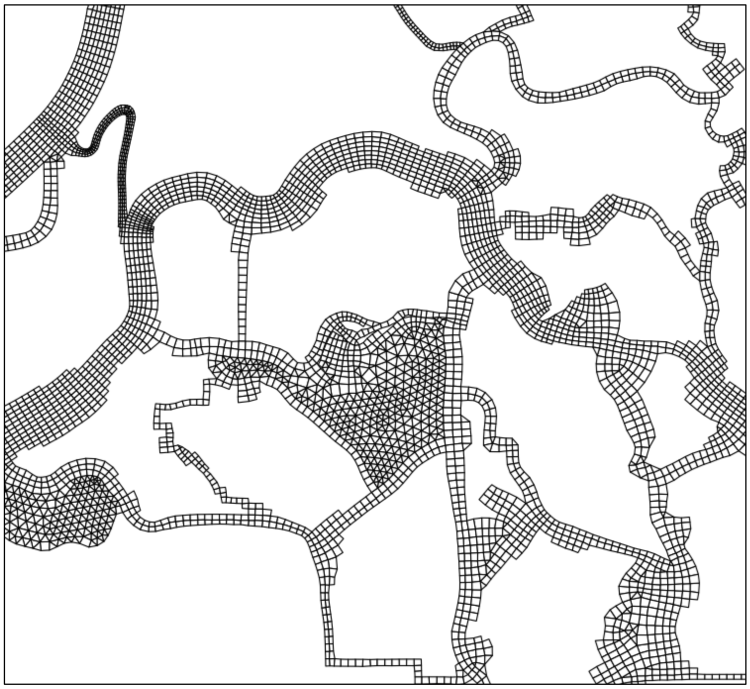

Figure 2-1 Orthogonal grid example of the Central Delta around Franks Tract.

2.4.1 Subgrid

An important feature of UnTRIM is ability to use subgrid algorithms. Without subgrid methods, only one value is used to represent bathymetry within a computational cell (Figure 2-2, left). With subgrid, additional information about the bathymetry within cell at a much finer discretization level is stored (Figure 2-2, right). This information is used by the model to get better estimates of element volume and face area, and leads to more accurate solutions of the equations conserving fluid volume and momentum. An example of subgrid set with Janet is shown in Figure 2-3.

UnTRIM uses the subgrid information in a bulk bathymetry distribution sense. The model has no explicit knowledge of where along an edge certain subgrid depths are found, and UnTRIM does not solve the equations for volume and momentum conservation at each subgrid cell. Therefore, care must be taken when constructing a grid for use with subgrid bathymetry to prevent aliasing. Aliasing occurs when disconnected hydrological features at the subgrid scale are united in a single element. For example, if a levee separating two adjacent but disconnected channels ran through the center of an element, the UnTRIM model would have no knowledge that the channels were separate and would allow flow between them. Careful grid construction is the only way to prevent these aliasing errors.

[1] http://www.smileconsult.de/index.php?article_id=24&clang=0

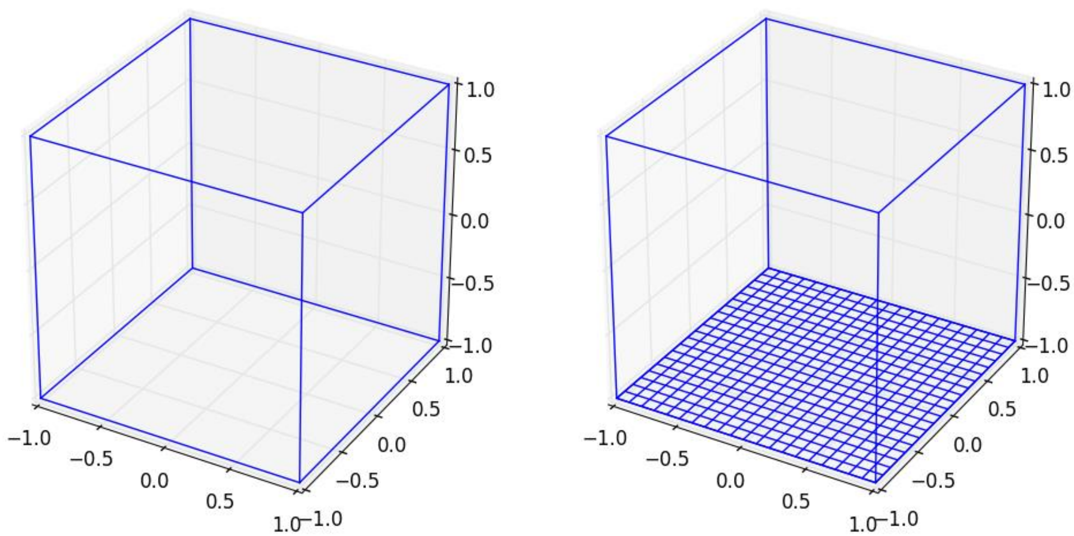

Figure 2-2 Three-dimensional element bathymetry diagram showing bottom discretization without the use of subgrid (left) and with subgrid (right).

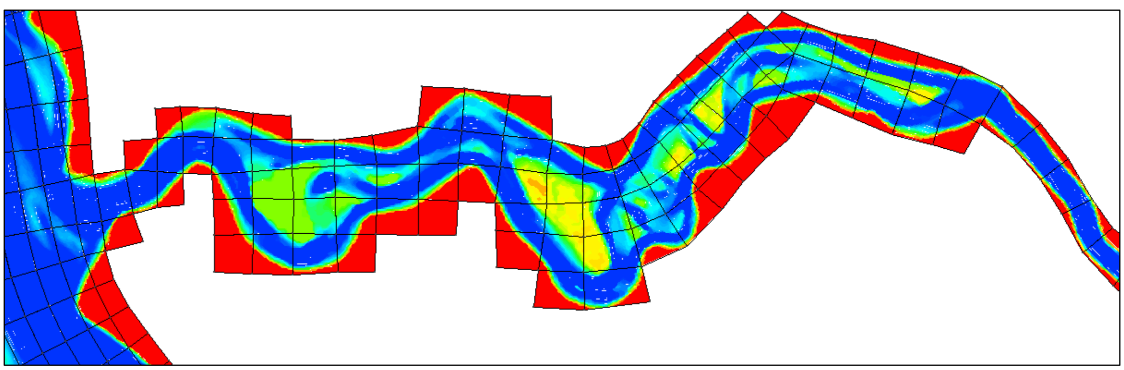

Figure 2-3 Subgrid example for section of Potato Slough, Central Delta. Subgrid bathymetry is color contoured according to depth. Black lines show element boundaries.

3 Contemporary Bay-Delta Model Grid

The first step of the modeling process was to build a grid for the Bay-Delta in its present state. This was useful for two main reasons: 1) the historical grid uses the same Bay configuration and much of the same channel configuration for the major rivers and sloughs, and thus the contemporary Bay-Delta grid could serve as a base for the historical Bay-Delta grid, and 2) before the simulation of the historical Bay-Delta, it was necessary to ensure that UnTRIM model and its interface implementations were functioning correctly; this is easier to accomplish using simulations of the contemporary Bay-Delta, where much more observed data are available for model comparison.

3.1 Planform Grid Generation

The grid developed for the contemporary Bay-Delta is shown in Figure 3-1. The ocean boundary was chosen to be arc approximately 50 kilometers from Golden Gate, in order to prevent reflection and interference of ocean stage boundary condition with Pacific coast. The extents of Delta channels were chosen to include tidally inundated areas and to approximately match the locations of data observation stations for use as boundary conditions.

For model accuracy, it is best to construct as much of the grid as possible using flow-aligned quadrilateral elements. This was done for major Delta channels and flow paths. Triangular elements were used for tidal flats, areas in between flow paths, transition areas between diverging or merging flow paths, and areas where there was no clear flow direction. Screenshots of the grid through Suisun Bay and the Central Delta are shown in Figure 3-2 and Figure 3-3 to illustrate these concepts.

The resulting grid included:

- 31775 elements (28973 quadrilateral, 2802 triangular)
- 36829 nodes
- 68695 sides
- 54 vertical layers
- Approximately 330,000 active 3D prisms during a typical simulation
- Approximately 175 m between adjacent element centers (Figure 3-4)

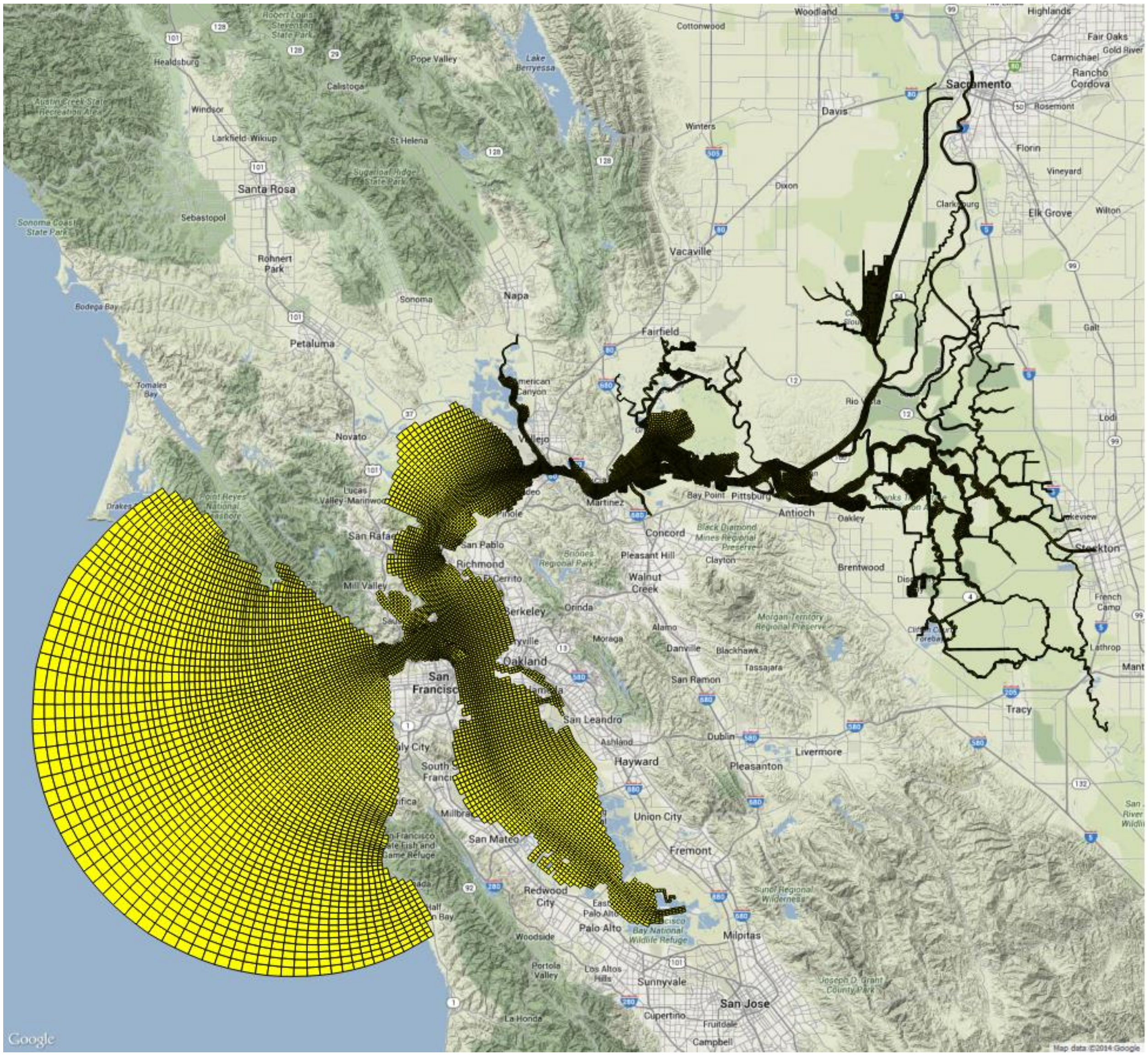

Figure 3-1 Contemporary Bay-Delta grid extents.

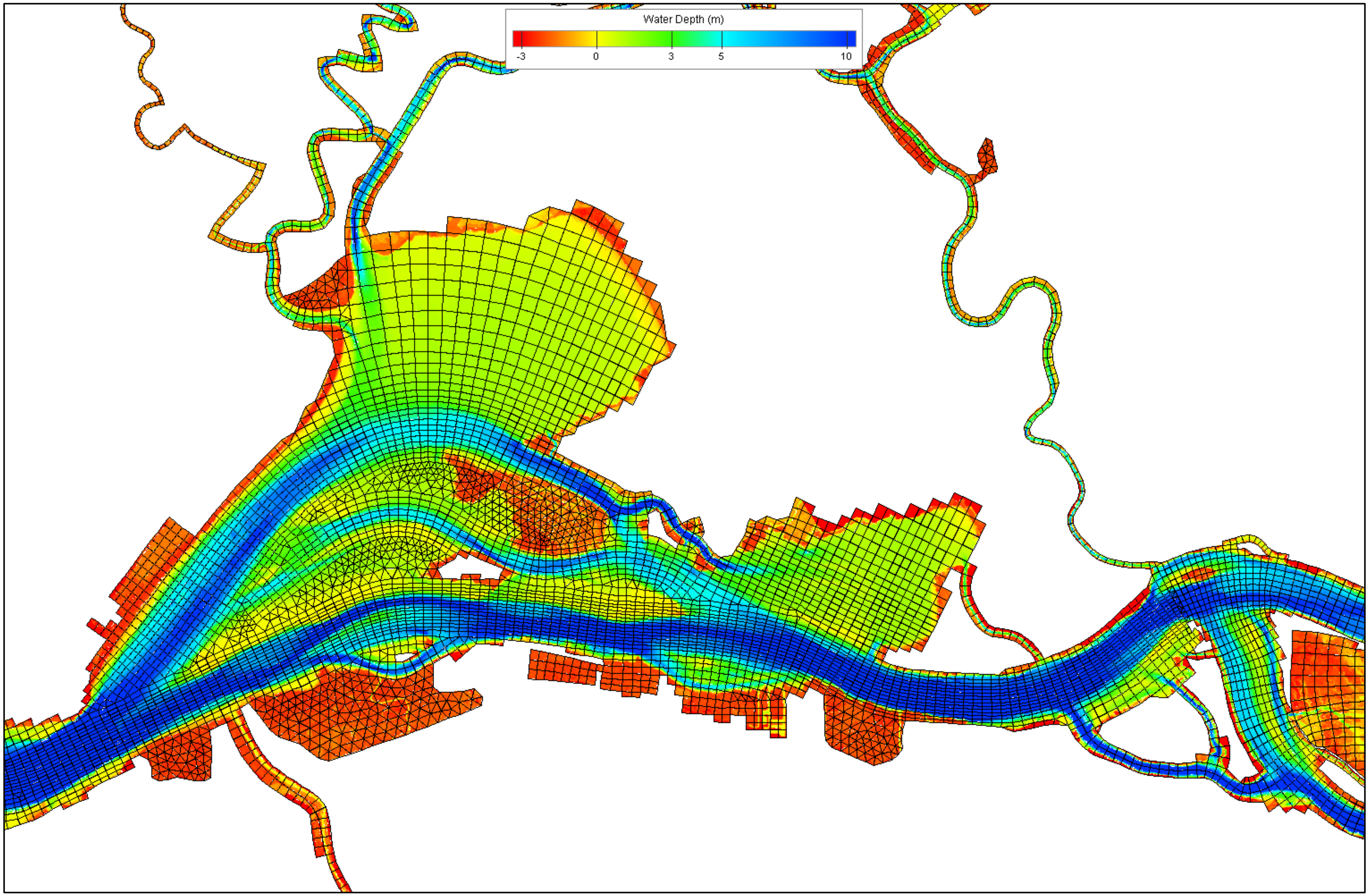

Figure 3-2 Contemporary Bay-Delta grid section through Suisun Bay. Quadrilateral elements were constructed to follow the contours of main channels. Triangular elements fill the intervening areas.

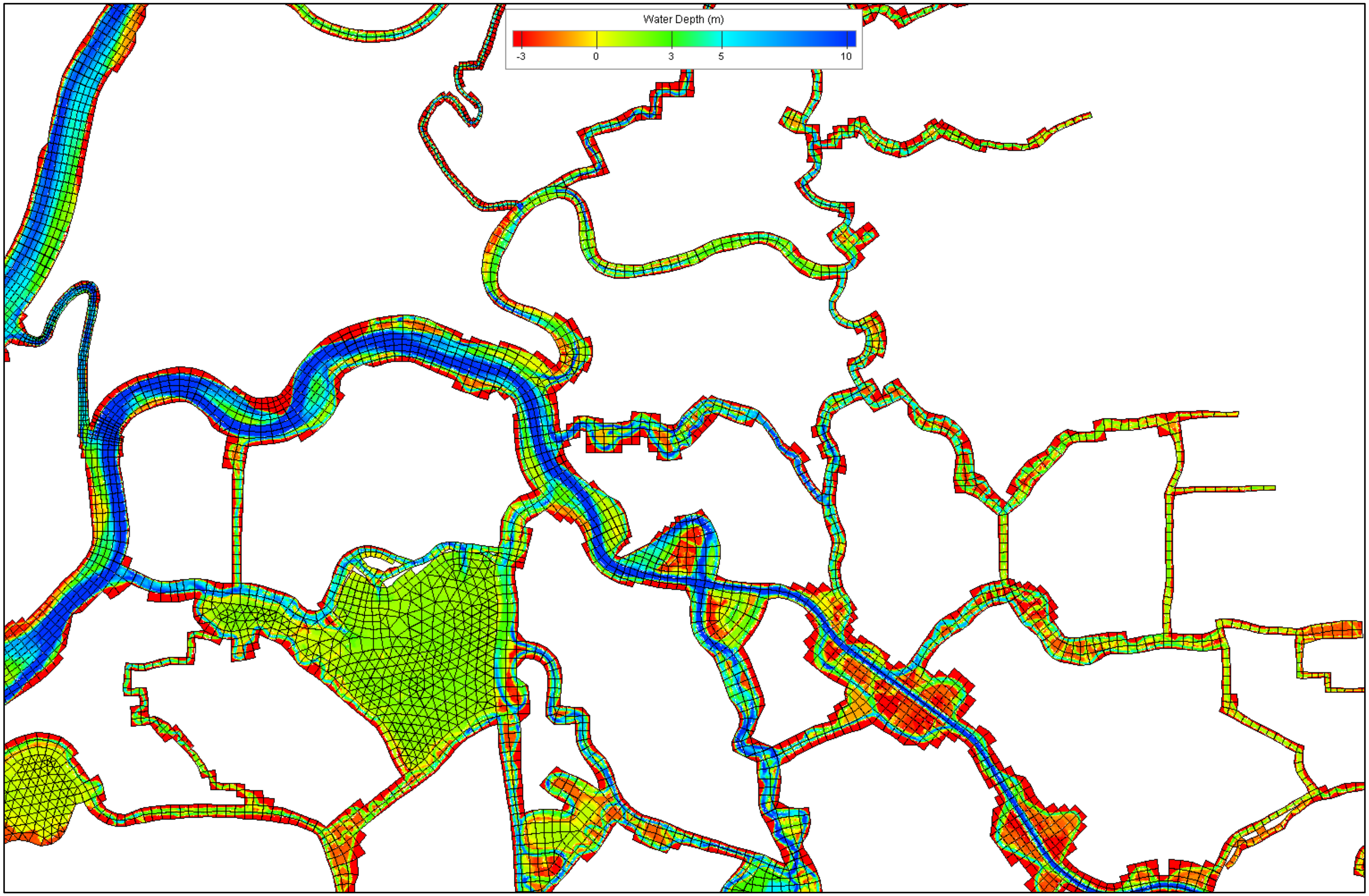

Figure 3-3 Contemporary Bay-Delta grid section through the Central Delta. Quadrilateral elements were constructed to follow the contours of main channels. Triangular elements fill the intervening areas.

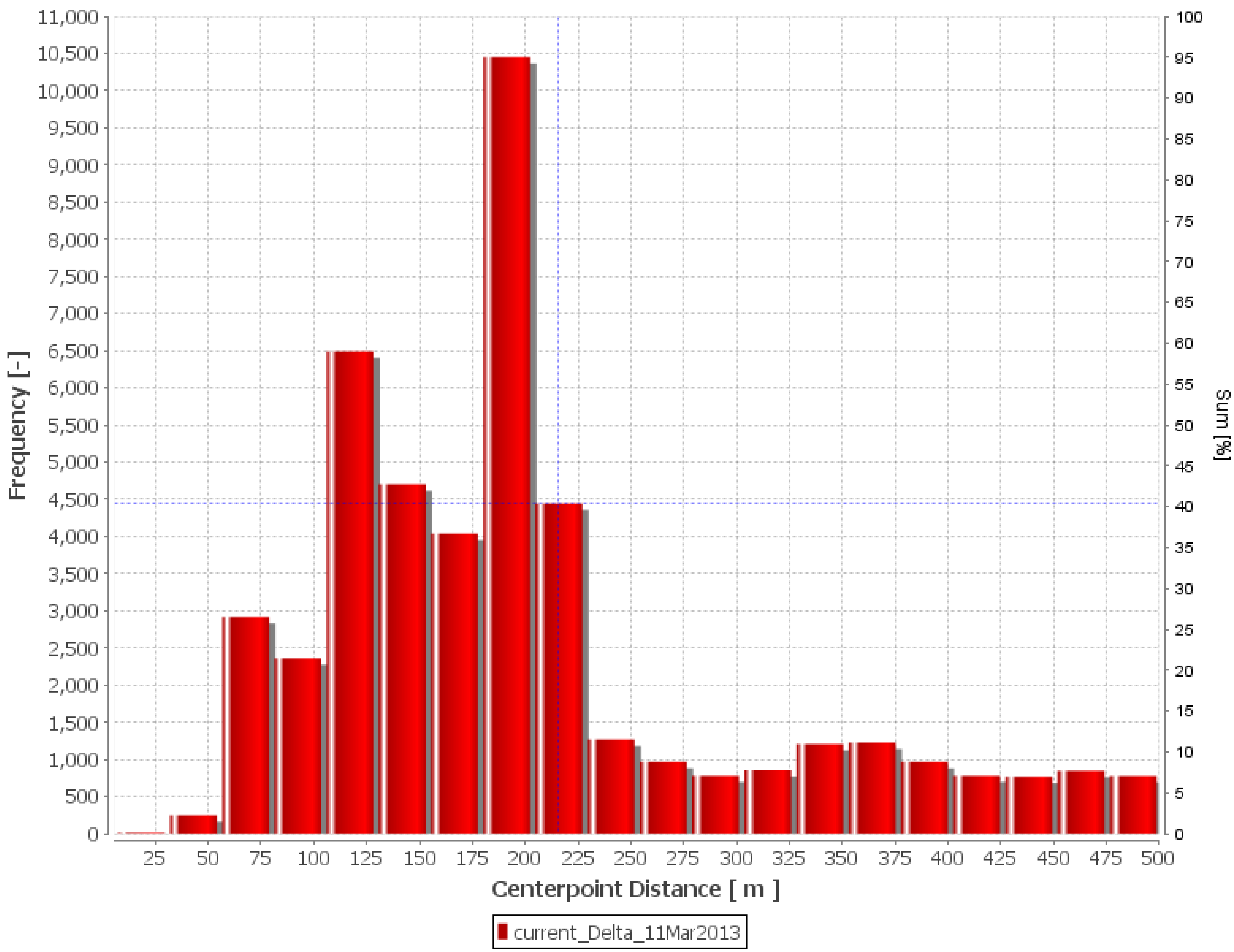

Figure 3-4 Adjacent element distance histogram for contemporary Bay-Delta model grid.

3.2 Bathymetry

Bathymetry for the contemporary Delta was provided by UCD. The Delta DEM was based on a DEM released by DWR[2] (Wang and Ateljevich, 2012). Modifications were made to clean up DEM artifacts in upper reaches of Yolo Bypass. Non-flooded Delta islands had their bathymetry raised in order to prevent subgrid aliasing of element volumes in areas adjacent to levees. Without the raised islands, cell volumes at high tides would substantially overpredict cell volume. Figure 3-5 illustrates the DEM provided by UCD. Horizontal resolution is 10 m. Outside of the Delta, another DEM released by DWR (Wang and Ateljevich, 2012) was used (Figure 3-6). Horizontal resolution was 10 m for this DEM as well. Additional bathymetry data sets were used where 2 m data was available in the South Delta and Threemile Slough.

Subgrid elevations were set using the Janet program and an option of 20 subedges per edge. Figure 3-7 and Figure 3-8 illustrate the resulting model grid bathymetry.

[2] Available at http://baydeltaoffice.water.ca.gov/modeling/deltamodeling/modelingdata/DEM.cfm

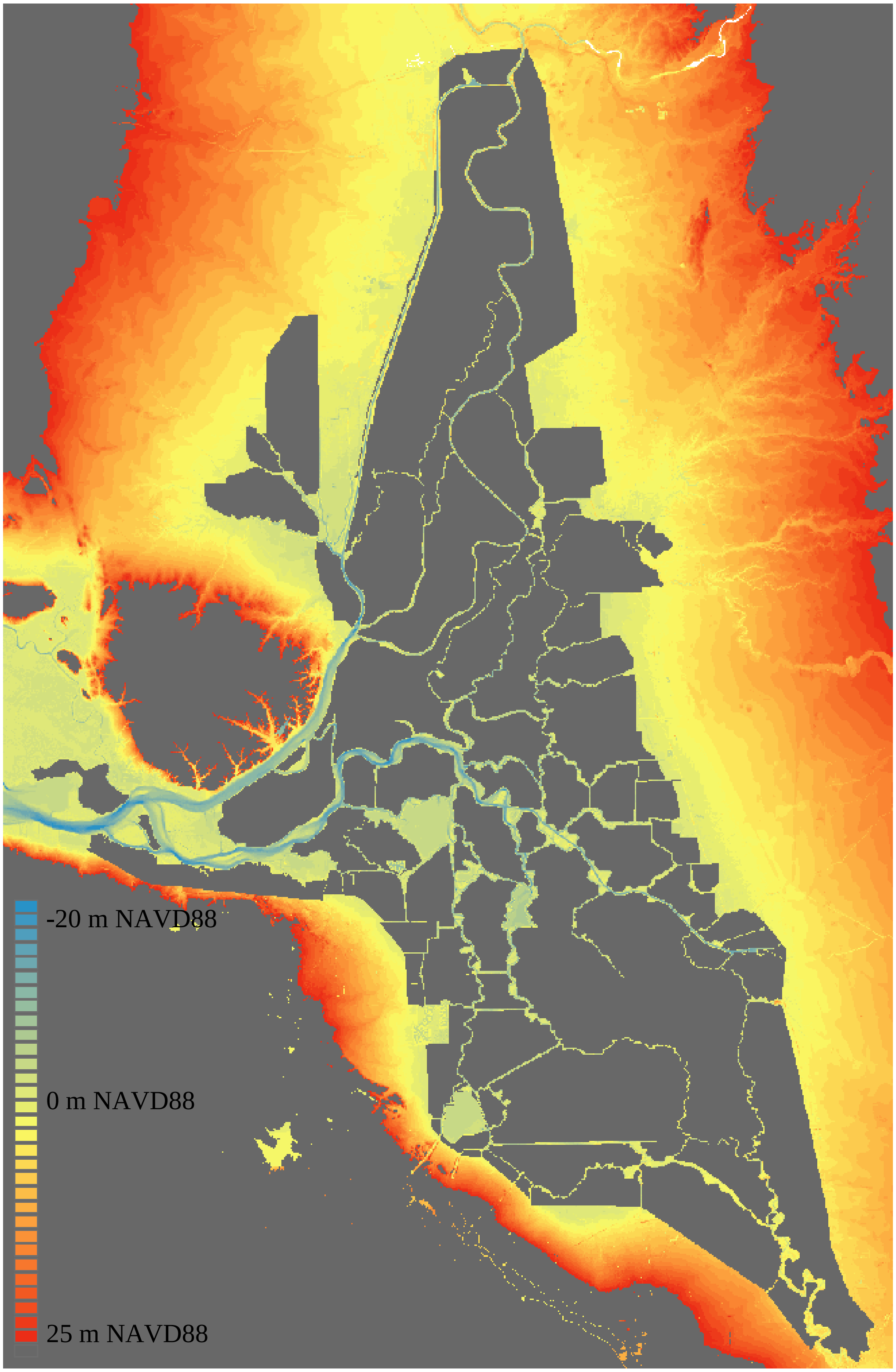

Figure 3-5 Contemporary Delta DEM. Gray areas have elevations greater than 25 m NAVD88.

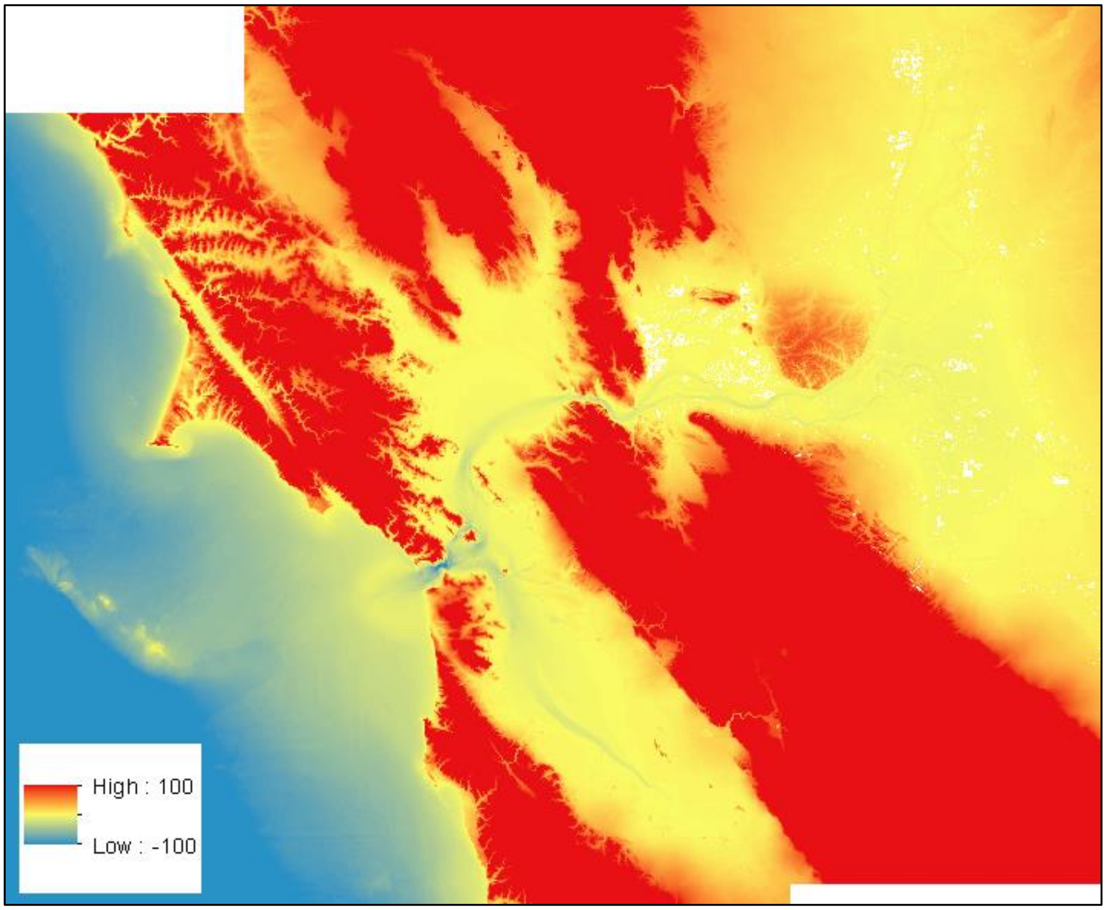

Figure 3-6 DWR released Bay-Delta DEM. This DEM was used to set the grid bathymetry in areas outside of the Delta.

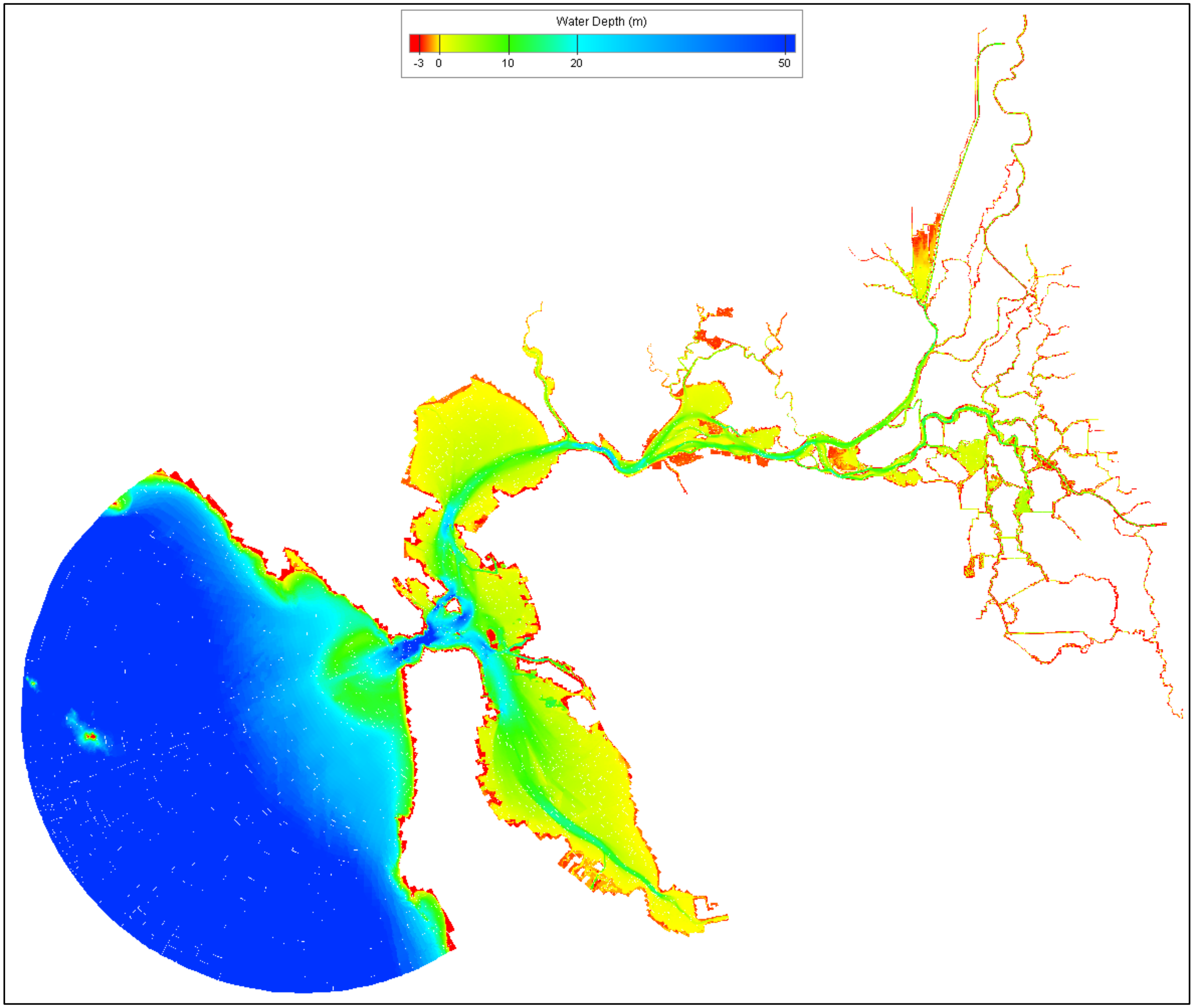

Figure 3-7 UnTRIM grid for contemporary Bay-Delta. Subgrid bathymetry contours shown.

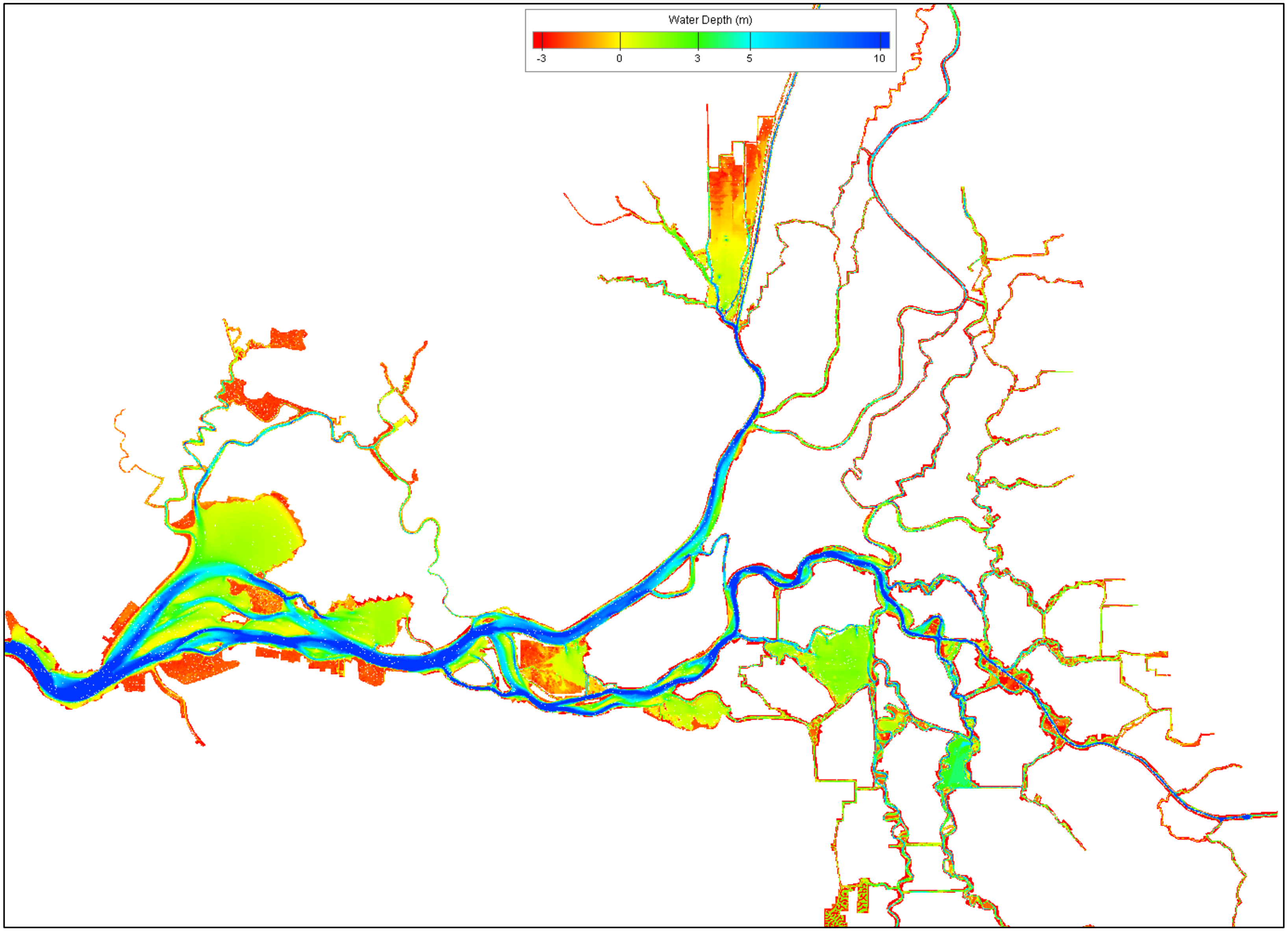

Figure 3-8 UnTRIM grid for contemporary Bay-Delta. Close-up of Delta area. Subgrid bathymetry contours shown. Note the different color contour scale than was used in Figure 3-7.

3.3 Boundary Conditions

Boundary conditions in the contemporary Bay-Delta model include:

- Stage at Point Reyes
- Inflows
  - Sacramento River below the American River confluence
  - Yolo Bypass at northern reach
  - Cosumnes River at Delta boundary
  - Mokelumne River at Delta boundary
  - Calaveras River at Delta boundary
  - San Joaquin River at Vernalis
  - Napa River at Napa
- Exports
  - North Bay Aqueduct at Barker Slough Pumping Plant
  - State Water Project Intake to Clifton Court Forebay
  - Central Valley Project Intake at Harvey Banks Pumping Plant
  - Contra Costa Water District Intakes at Rock Slough, Old River, and Victoria Canal
- Delta Island Consumptive Use (DICU) at 257 locations throughout the Delta
- Delta Cross Channel Gate
- Salinity at all inflow boundaries and for DICU return flows

The locations of these boundary conditions are presented in Figure 3-9. Because of its relatively complex configuration and operation, the Suisun Marsh Salinity Control Gate was not included in the Phase I contemporary Delta grid or simulations. Its integration in planned for Phase II of this project.

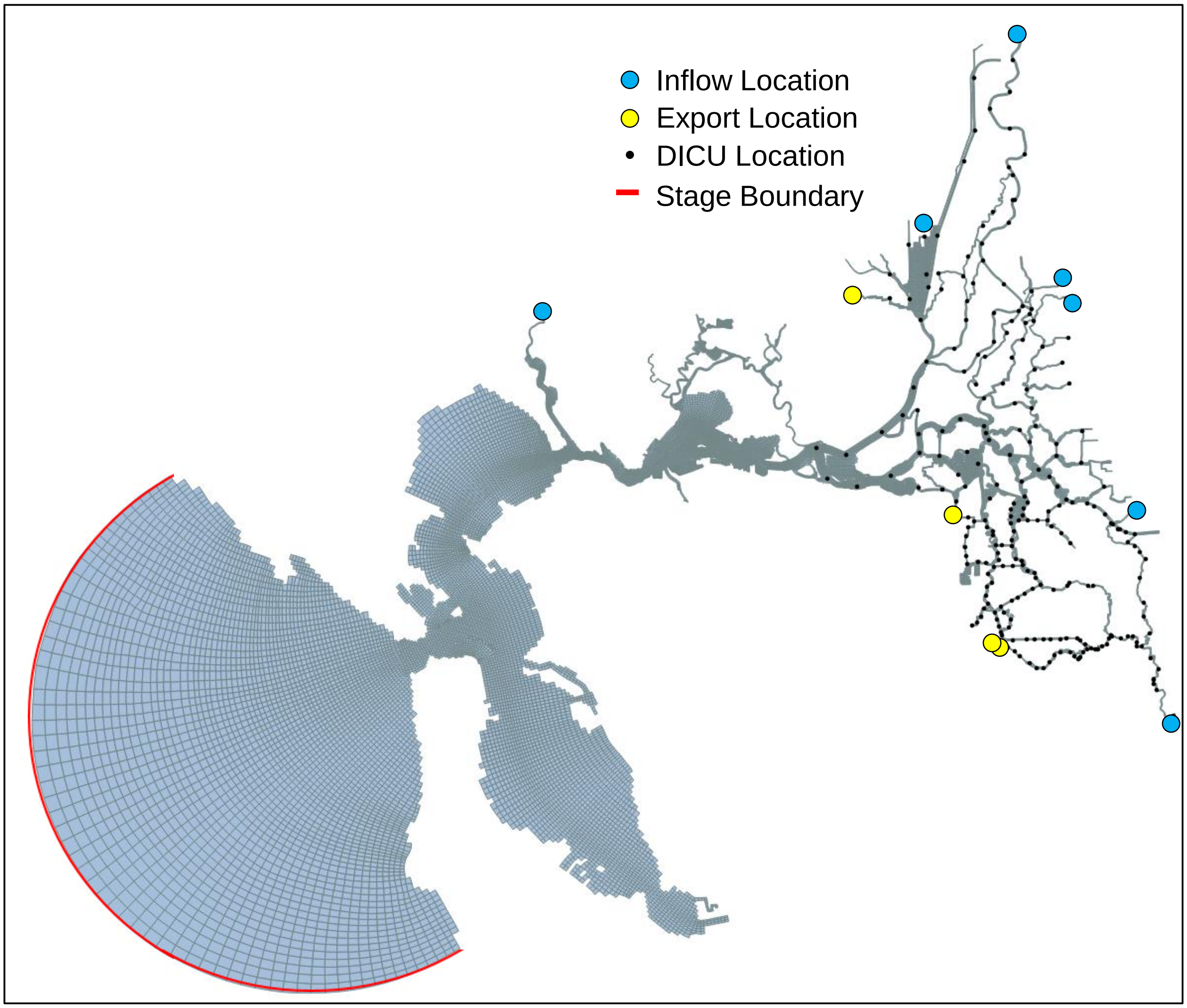

Figure 3-9 UnTRIM contemporary Bay-Delta model boundary condition locations.

4 Contemporary Bay-Delta Model Calibration

The contemporary Bay-Delta model was calibrated using observed data from 2010 and 1994. The 2010 calibration period was much more comprehensive because of the availability of observed data for model comparisons. The 1994 calibration focused on detailed salinity transect data collected for a particular study in the Suisun Bay region.

4.1 Observed Data

Calibration data included observed stage, flow and salinity time series collected from various agencies throughout the Bay and Delta. Data were obtained either from NOAA, USGS, DWR, CIMIS, and local water agencies from agency websites, from direct contact with agencies, or from an environmental data repository sites such as the California Data Exchange Center (CDEC) or the DWR Water Data Library (WDL). Vertical salinity profiles from USGS Polaris water quality cruises were also used for calibration. Vertical profiles at the locations shown in Figure 4-1 were taken approximately monthly. These data characterize the salinity stratification through system.

For the 1994 calibration period, data collected from a detailed study of the Delta entrapment zone were used. The entrapment zone is an area of low-salinity water from the north San Francisco Bay into the western Delta. It is ecologically important because of its high concentrations of particles, plankton, and fish. The 2 PSU salinity isohaline is also found in this region, and its position has important regulatory implications. Vertical profiles of salinity were collected along a transect through this region on a relatively fine time scale over two 36 hour study periods (Burau et al., 1998).

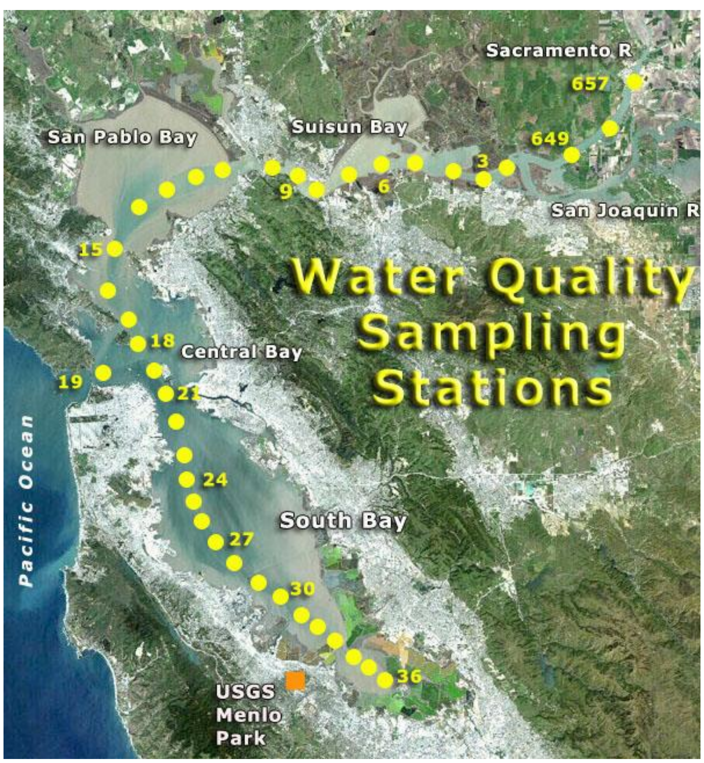

Figure 4-1 USGS Polaris cruise water quality sampling stations. Figure obtained from http://sfbay.wr.usgs.gov/access/wqdata/index.html.

4.2 2010 Calibration Period

The 2010 calibration modeling period was 12 April 2010 – 31 October 2010. The period was chosen to allow high flow conditions in the early part of the run to quickly wash out any effects due to incomplete knowledge of the initial 3D salinity field.

4.2.1 Boundary Conditions

Stage, inflow, and export boundary condition time series are shown in Figure 4-2 through Figure 4-5. Salinity boundary conditions are shown for the Sacramento and San Joaquin inflows in Figure 4-6. The Calaveras inflow salinity was set at a constant value of 0.3 PSU based on average historical values. All other inflows were set at a constant salinity value of 0.08 PSU. In setting salinity boundary conditions, electrical conductivity (EC) data were obtained and then converted to salinity using the relationship:

$$salinity\ [PSU] = \frac{0.583793 * EC\ [\mu S/cm] - 2.67}{1000}$$

Meteorological boundary conditions are shown in Figure 4-7 and Figure 4-8. The wind stress boundary condition was set using NOAA observed wind speed and direction at Port Chicago and was applied to the entire model domain.

Evaporation and precipitation data were obtained from CIMIS stations and were set according to whether the element was located within one of three regions:

- South Bay (Union City CIMIS station)
- Central and North Bay (Oakland Foothills CIMIS station)
- San Pablo and Suisun Bay (Carneros CIMIS station)

DICU was used to account for evaporation and precipitation within the Delta. Net flows and return flow EC values were provided by the DWR Delta Modeling Section (DMS).

The DCC was opened for the season on 18 June and closed 13 October[3].

Other pertinent boundary condition and model information used for the simulation included:

- Turbulence closure scheme based on generic length scale model (Warner, 2005)
    - Neumann boundary conditions used for the surface and bottom boundaries
    - Kantha-Clayson stability function used
- Roughness height (z_0) specification of bottom boundary friction based on bottom elevation, following Gross (2010)
    - elevation -10 m NAVD88: z_0 0.0001
    - elevation -8 m: z_0 0.0002
    - elevation -4 m: z_0 0.001
    - elevation 1 m: z_0 0.004
- Interpolated 3D initial salinity field set based on Polaris transect data

[3] http://www.usbr.gov/mp/cvo/vungvari/Ccgates.pdf

- Model time step: 60 seconds

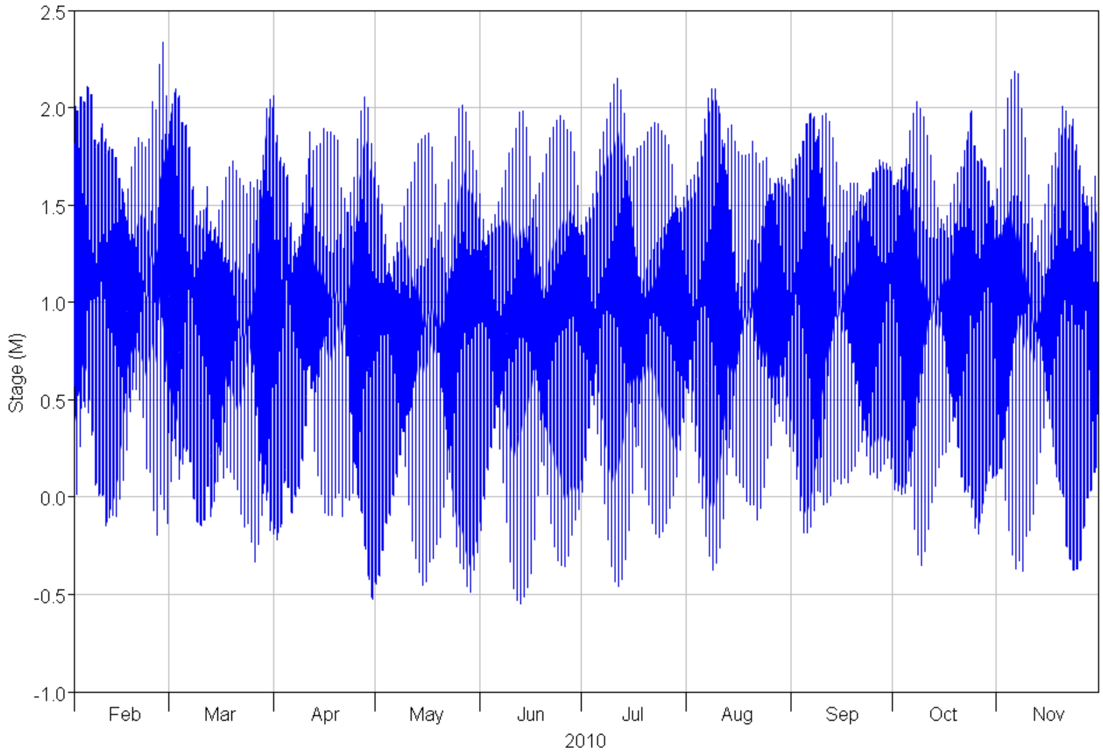

Figure 4-2 2010 contemporary Bay-Delta calibration period stage boundary condition at Point Reyes.

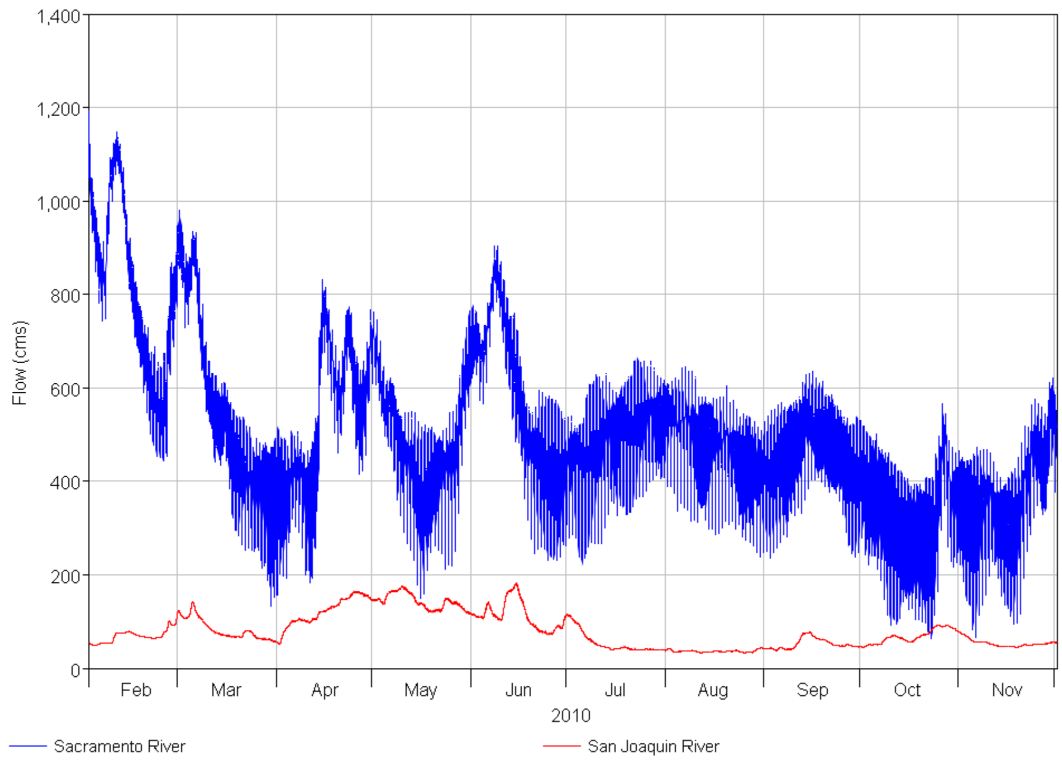

Figure 4-3 2010 contemporary Bay-Delta calibration period flow boundary conditions at the Sacramento River at Freeport and the San Joaquin River at Vernalis.

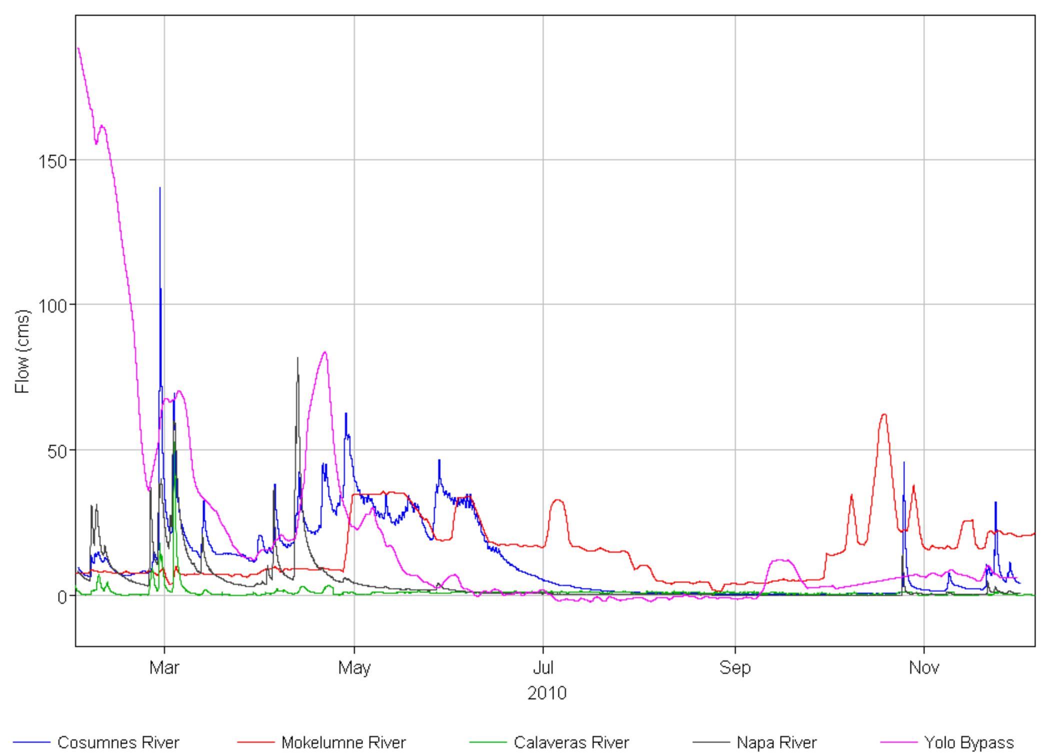

Figure 4-4 2010 contemporary Bay-Delta calibration period flow boundary conditions at the Yolo Bypass and Cosumnes, Mokelumne, and Napa Rivers.

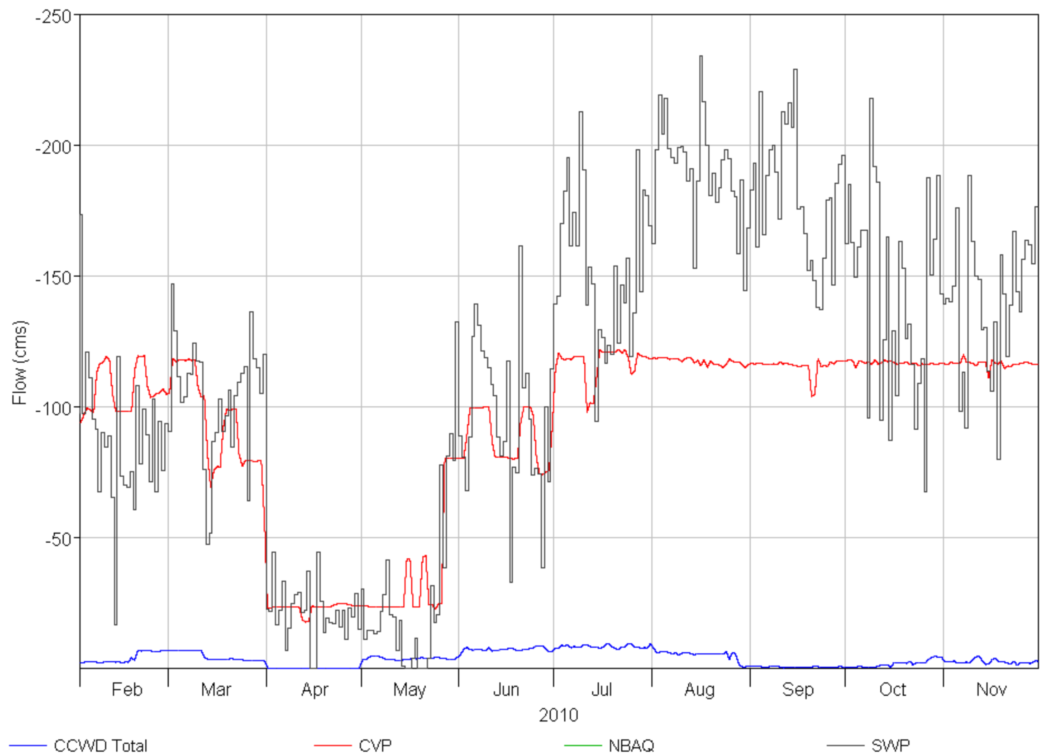

Figure 4-5 2010 contemporary Bay-Delta calibration period export flow boundary conditions at SWP, CVP, and North Bay Aqueduct pumps, and the CCWD withdrawals.

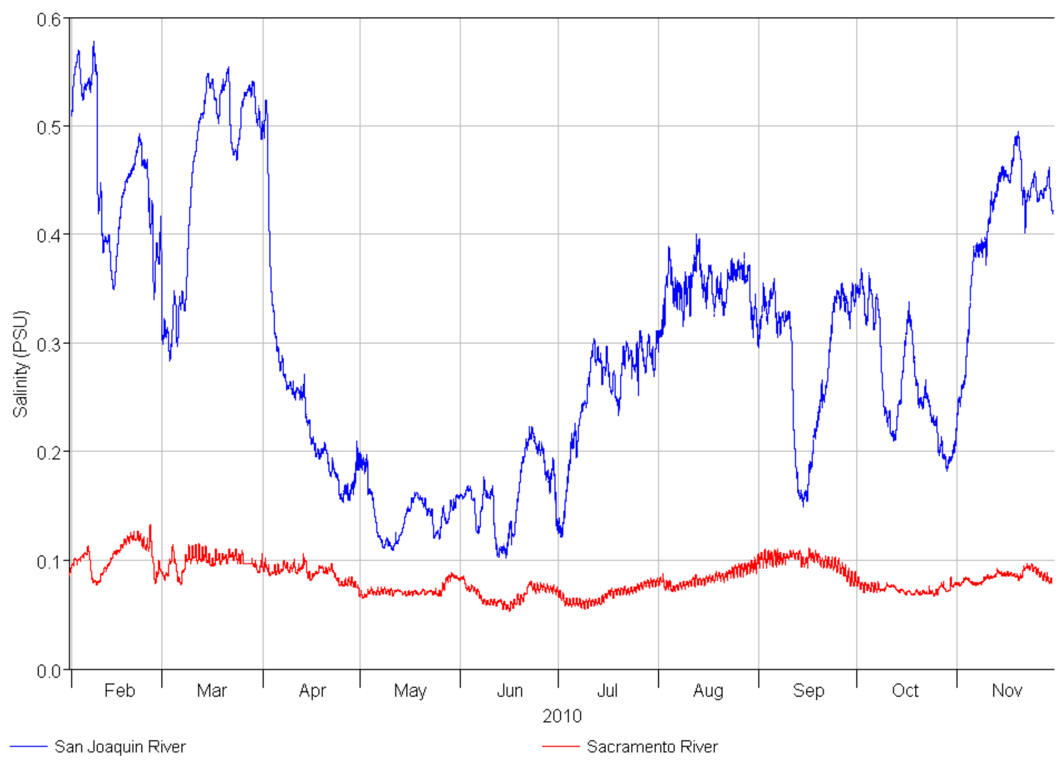

Figure 4-6 2010 contemporary Bay-Delta calibration period salinity boundary conditions at the Sacramento River at Freeport and the San Joaquin River at Vernalis.

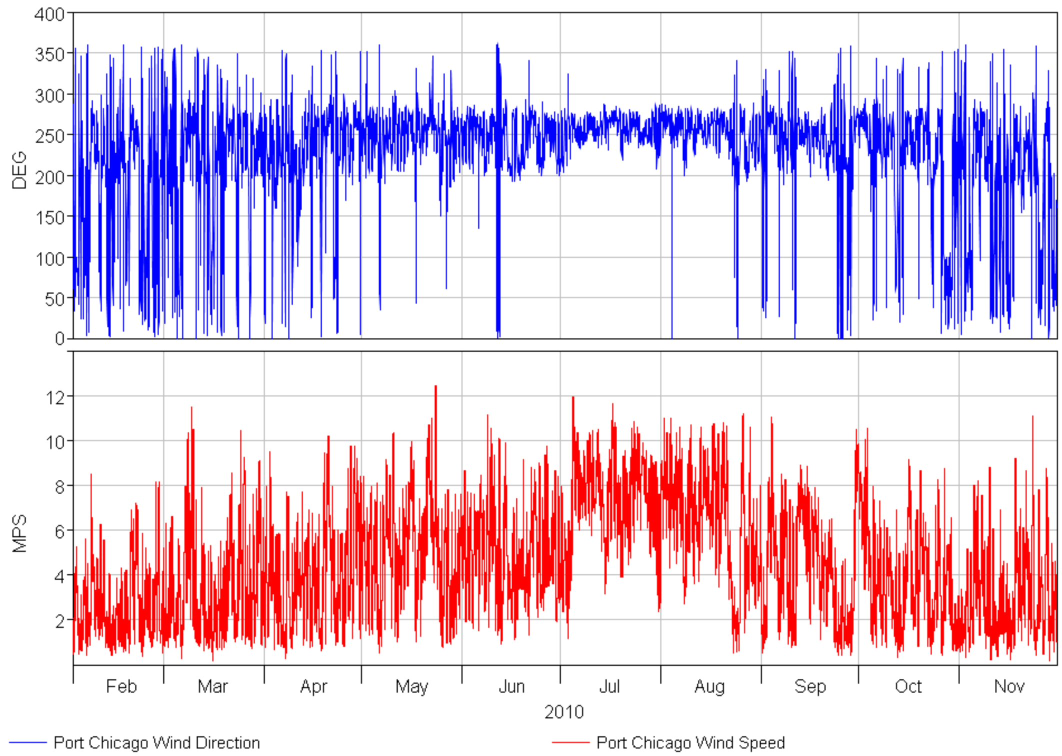

Figure 4-7 2010 contemporary Bay-Delta calibration period wind boundary conditions at Port Chicago.

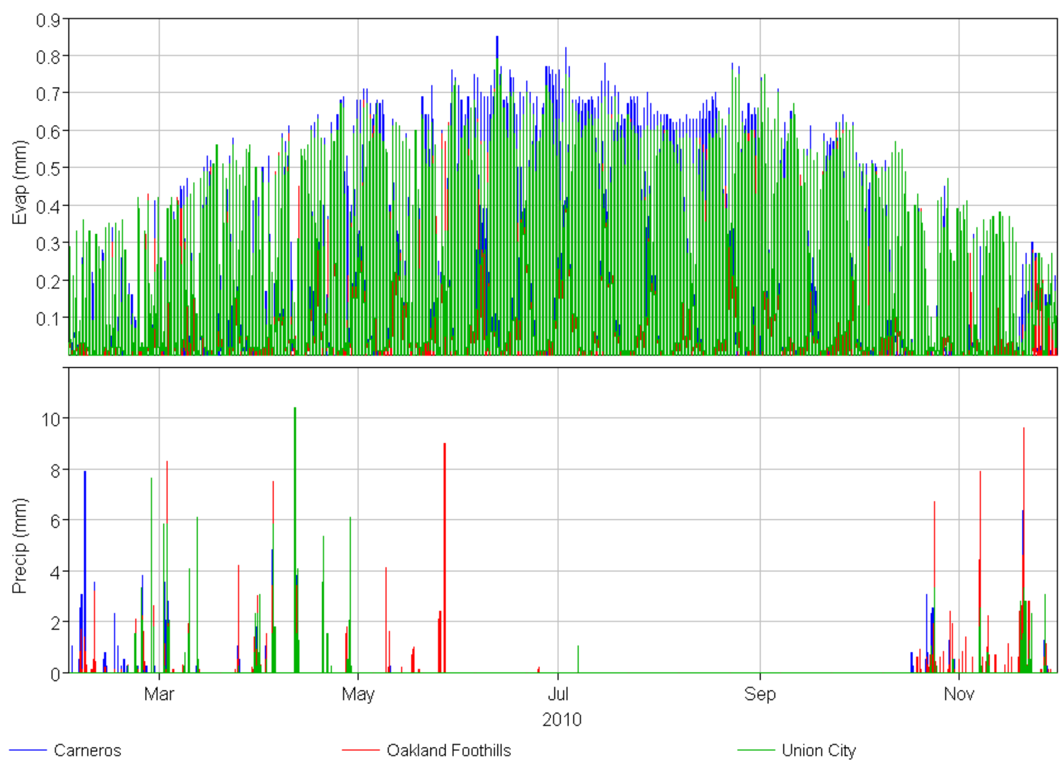

Figure 4-8 2010 contemporary Bay-Delta calibration period evaporation and precipitation boundary conditions.

4.2.2 Interim Calibration Results

Interim model calibration results are presented in detail in Appendix A. The major calibration coefficient that was used to match the observed data was the bottom roughness height, z_0.

4.3 1994 Calibration Period

The 1994 calibration modeling period was 17 April 1994 – 19 May 1994. A shorter period was chosen to just overlap with the entrapment zone study observations.

4.3.1 Boundary Conditions

Boundary conditions for the 1994 runs were similar to those used for the 2010 runs and are presented in Figure 4-9 through Figure 4-15.

The DCC was closed for the duration of the simulation.

Because of data availability, NOAA wind data at the Pittsburg station was used instead of at Port Chicago. Evaporation and precipitation data from the Novato station was used for South Bay, North Bay, and San Pablo Bay.

4.3.2 Interim Calibration Results

1994 calibration results are presented in detail in Appendix B. The same bottom roughness heights obtained from the 2010 interim calibration were used for the 1994 runs.

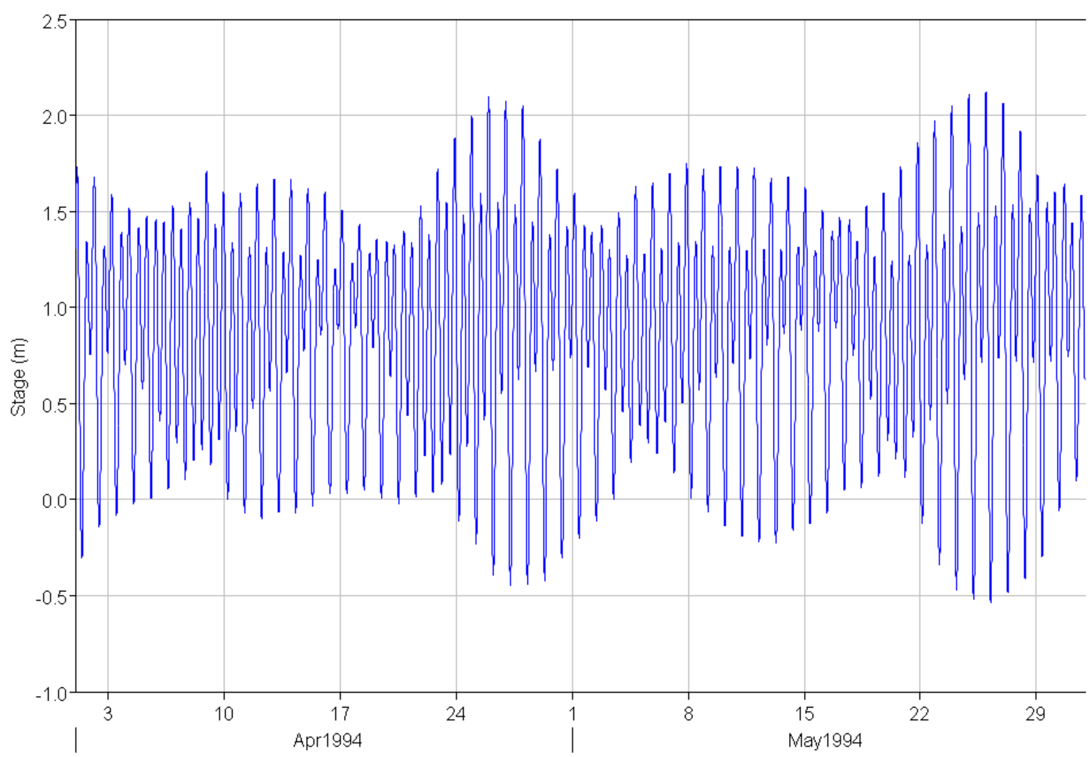

Figure 4-9 1994 contemporary Bay-Delta calibration period stage boundary condition at Point Reyes.

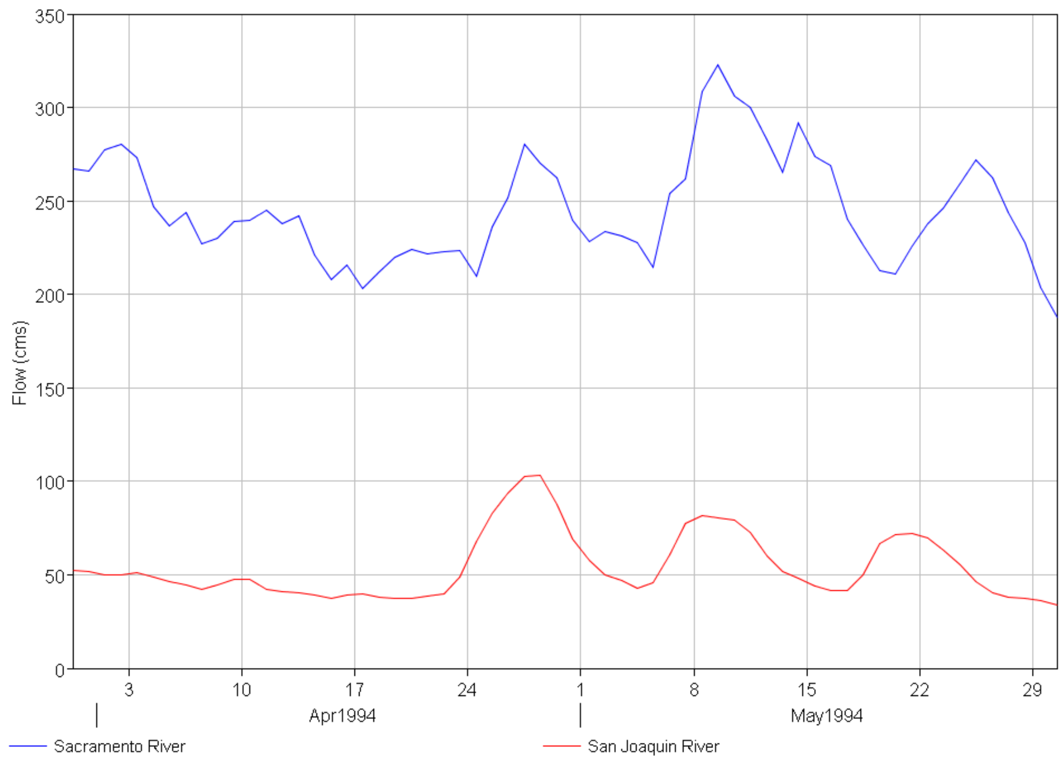

Figure 4-10 1994 contemporary Bay-Delta calibration period flow boundary conditions at the Sacramento River at Freeport and the San Joaquin River at Vernalis.

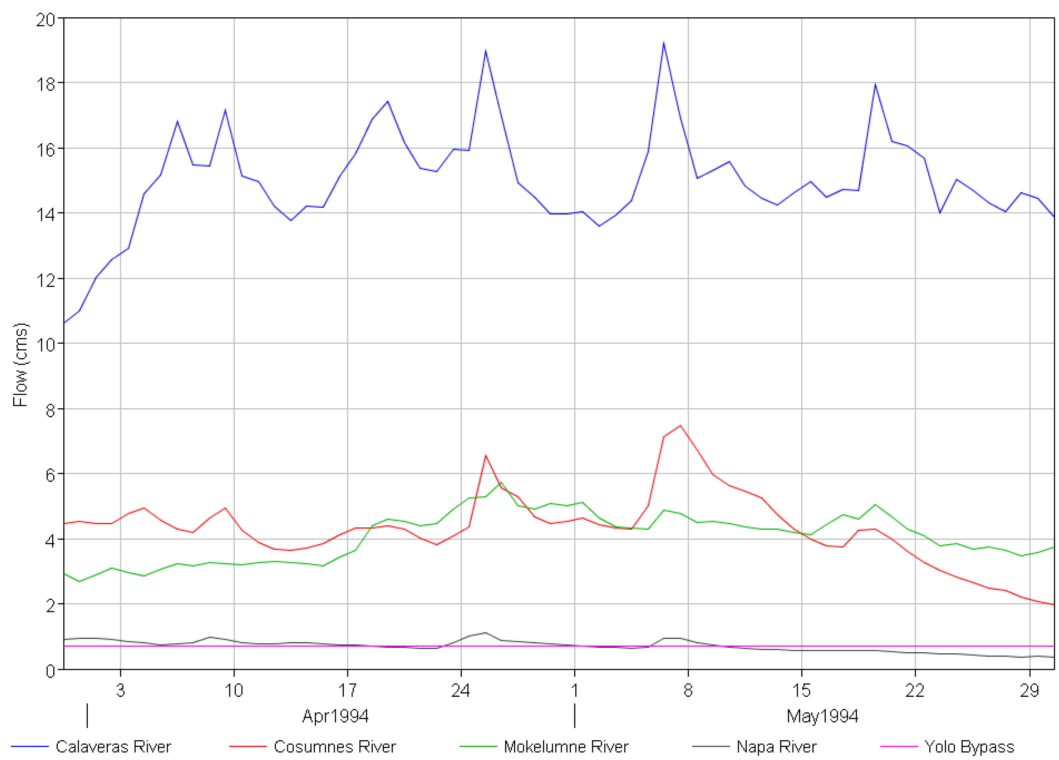

Figure 4-11 1994 contemporary Bay-Delta calibration period flow boundary conditions at the Yolo Bypass and Cosumnes, Mokelumne, and Napa Rivers.

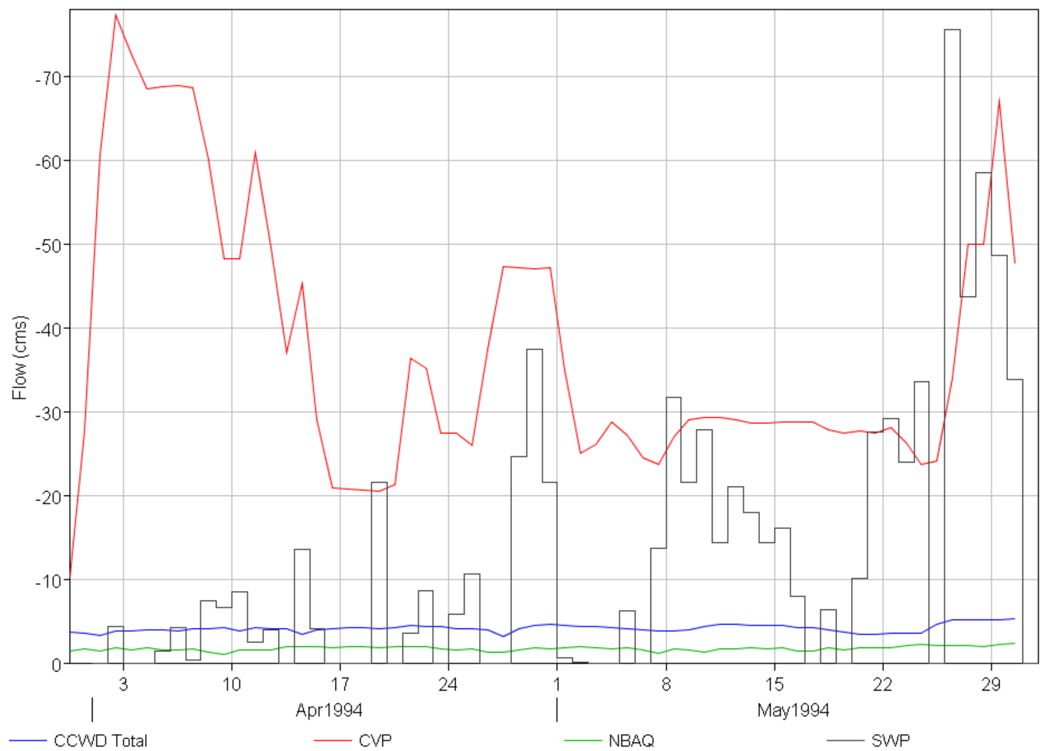

Figure 4-12 1994 contemporary Bay-Delta calibration period export flow boundary conditions at SWP, CVP, and North Bay Aqueduct pumps, and the CCWD withdrawals.

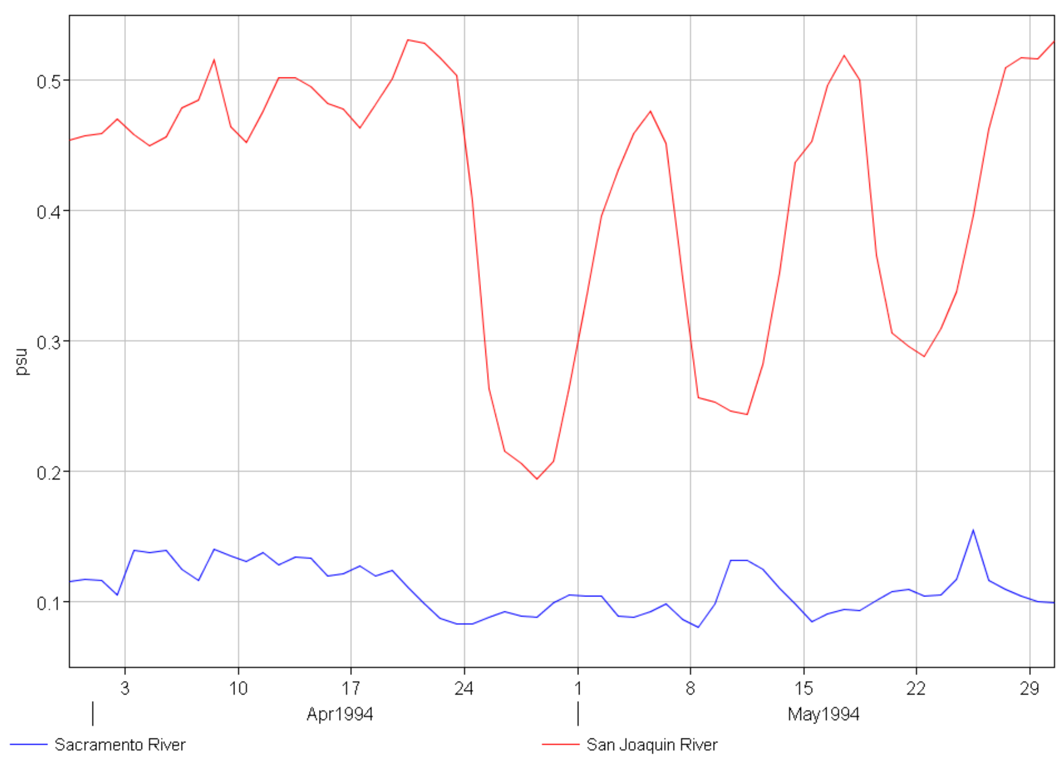

Figure 4-13 1994 contemporary Bay-Delta calibration period salinity boundary conditions at the Sacramento River at Freeport and the San Joaquin River at Vernalis.

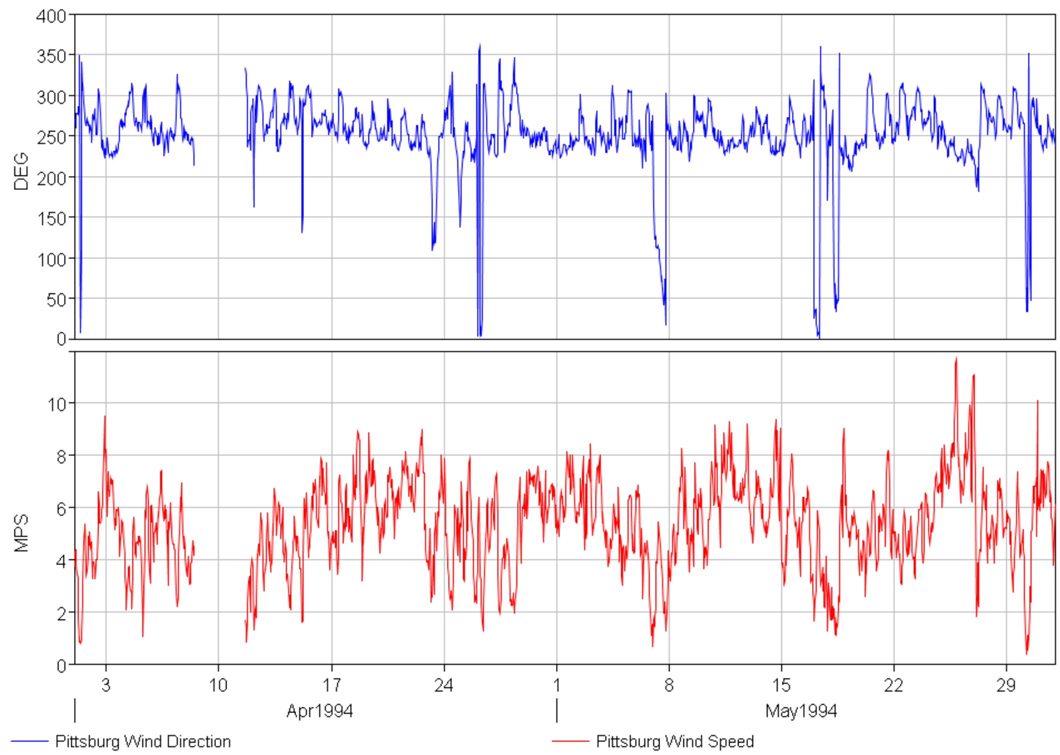

Figure 4-14 1994 contemporary Bay-Delta calibration period wind boundary conditions at Pittsburg.

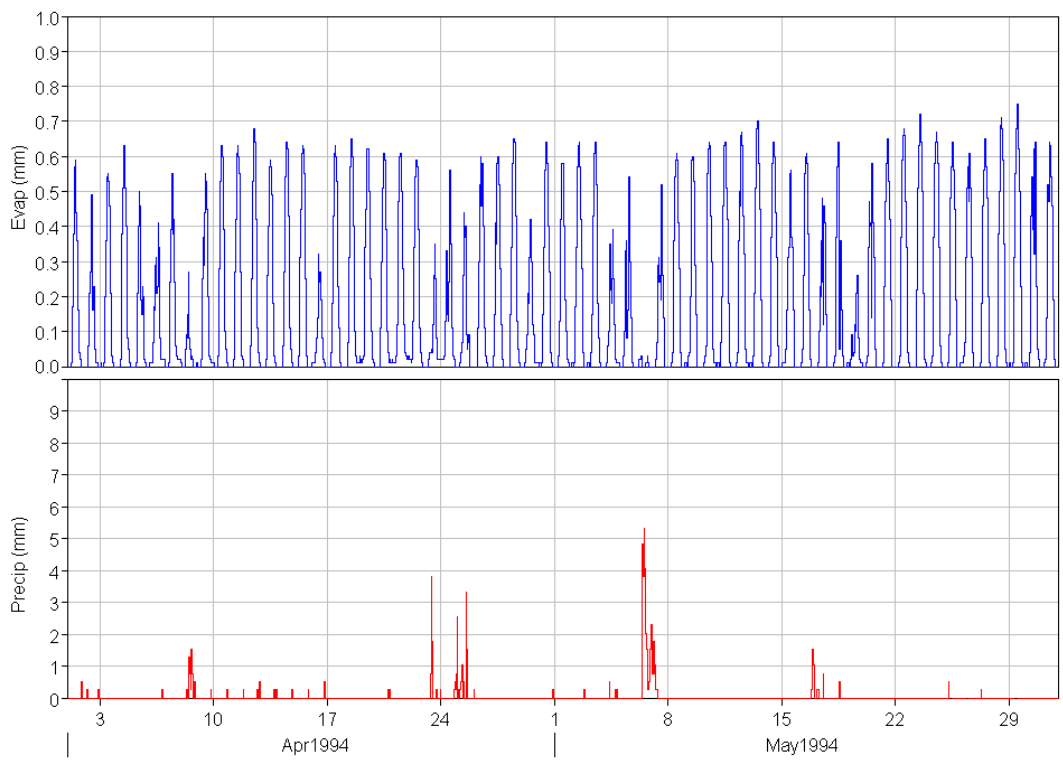

Figure 4-15 1994 contemporary Bay-Delta calibration period evaporation and precipitation boundary conditions at Novato.

5 Historical Bay-Delta Model Grid

5.1 Planform Grid Generation

The historical Bay-Delta planform grid was constructed starting with the contemporary Bay-Delta grid. Canals and cuts that were constructed in recent time were removed from the grid. These were mainly located in the South and East Delta and included Grantline Canal, Victoria Canal, and the Delta Cross Channel. Following the strategy used in making the contemporary Bay-Delta grid, flow-aligned quadrilaterals were constructed for the major historical channels, as identified by SFEI. Once the major channel network through the Delta had been constructed, tidal marsh areas located between the channels were filled in using triangular elements. Triangular elements were also used to add grid to the periphery of the Delta, in order to completely cover the area identified by SFEI as tidal marsh. The grid downstream of the Sacramento-San Joaquin confluence was the same as the contemporary Bay-Delta grid.

The final historical Bay-Delta grid is shown in Figure 5-1 through Figure 5-4 overlaid above SFEI-provided shapefiles of the major channels, minor channels, and tidal marsh extents.

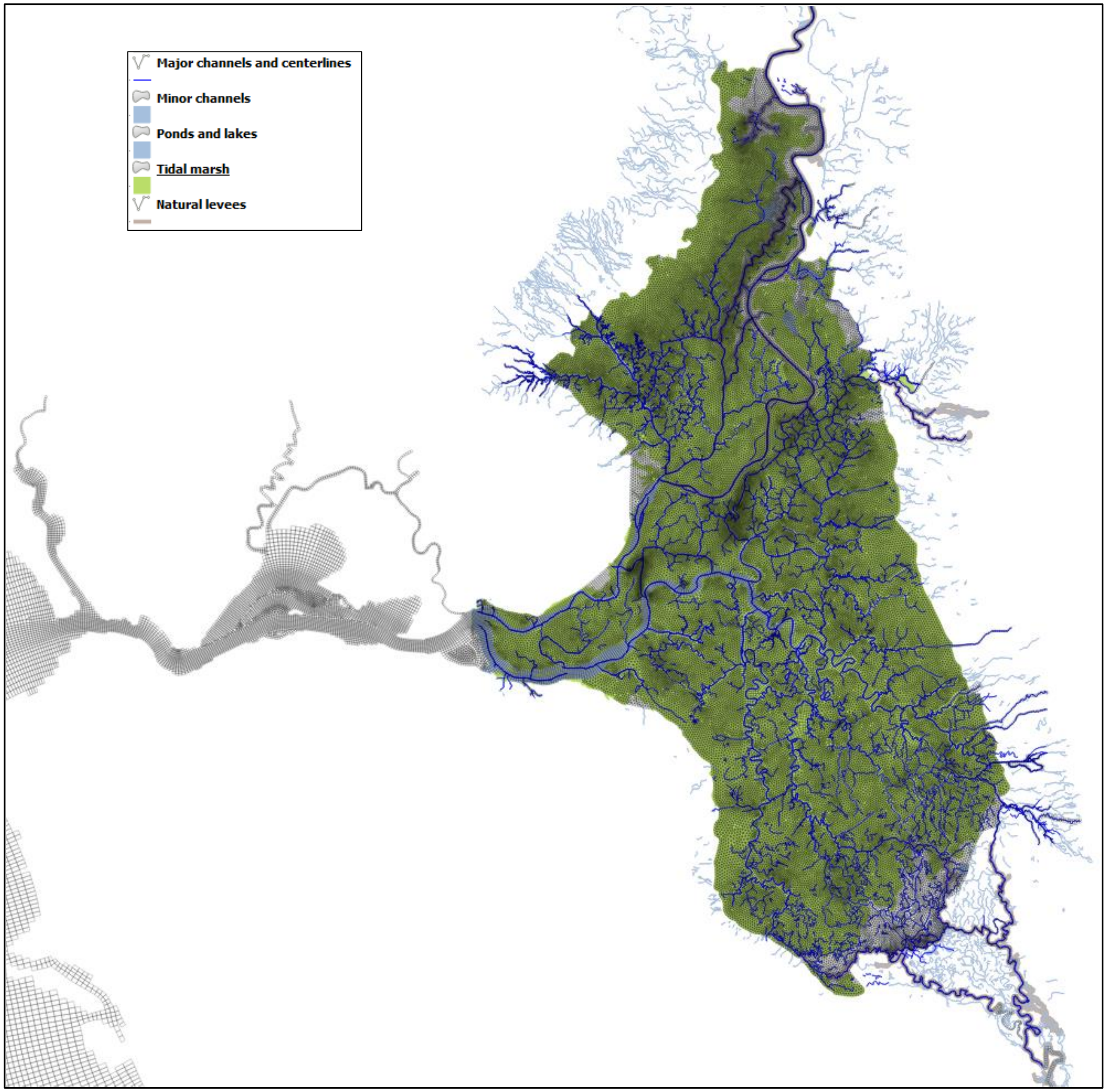

Figure 5-1 Historical Bay-Delta grid. Grid extends beyond the limits of this figure to include the same ocean boundary as shown in Figure 3-1.

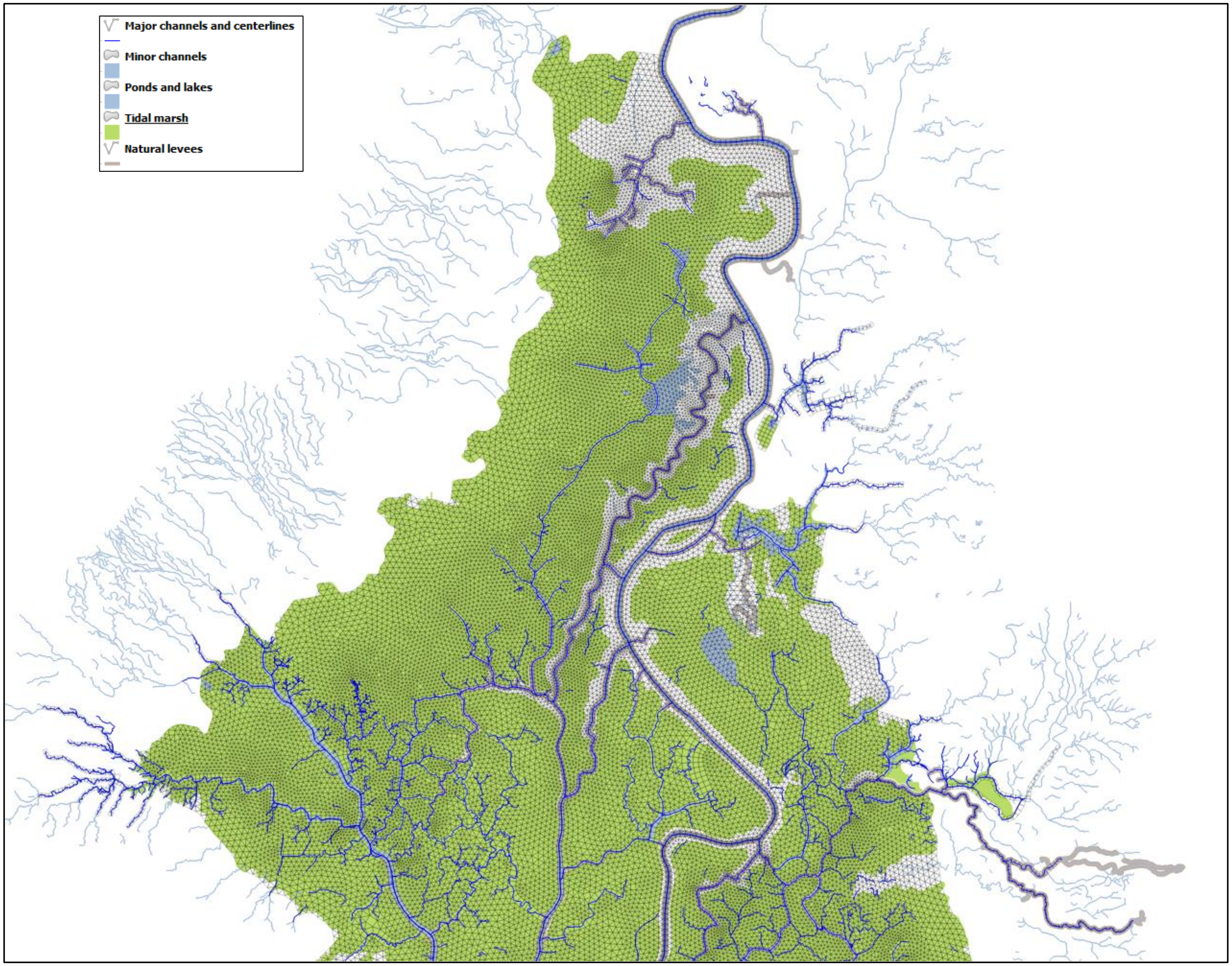

Figure 5-2 Historical Bay-Delta grid, North Delta.

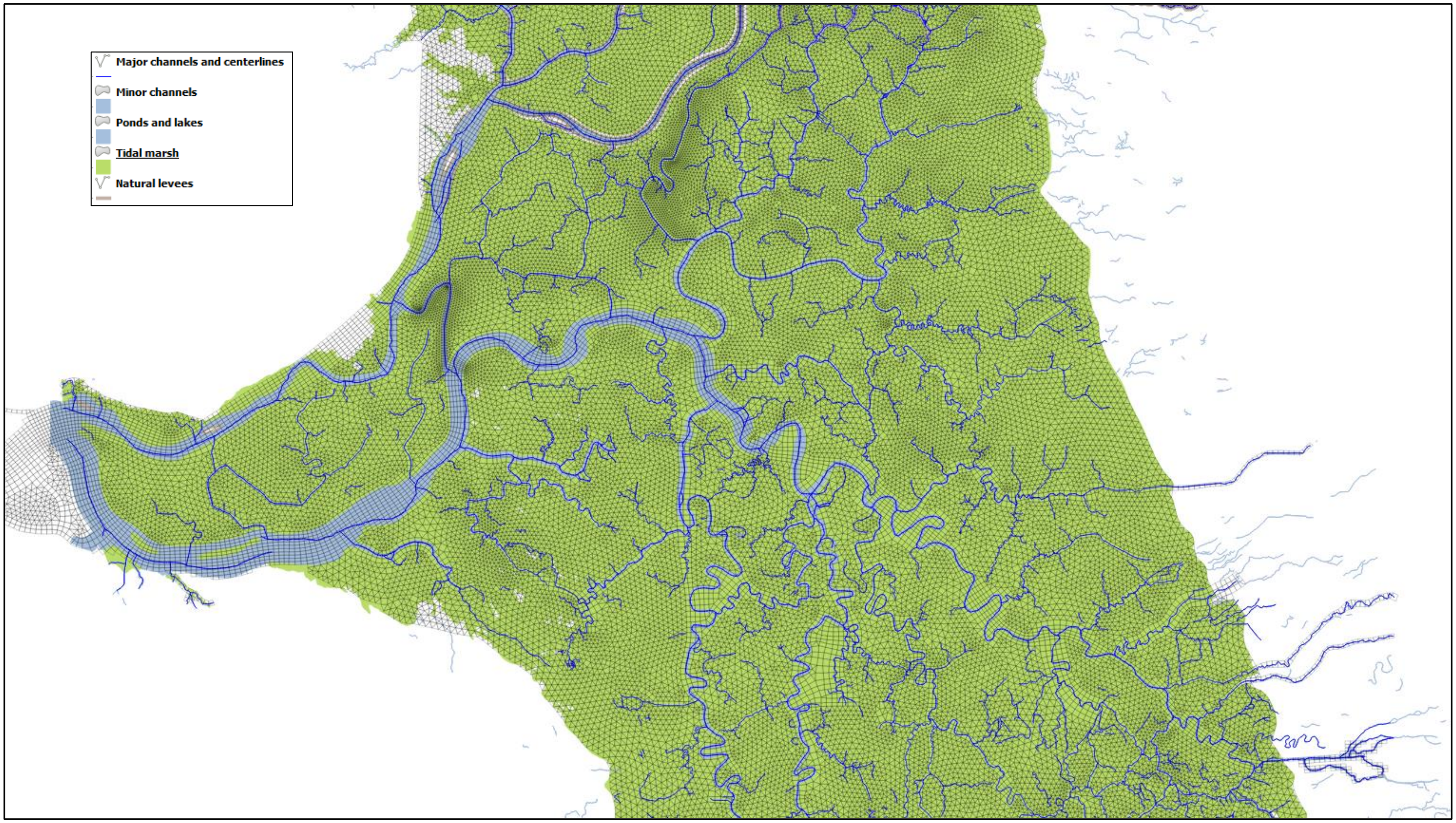

Figure 5-3 Historical Bay-Delta grid, Central Delta.

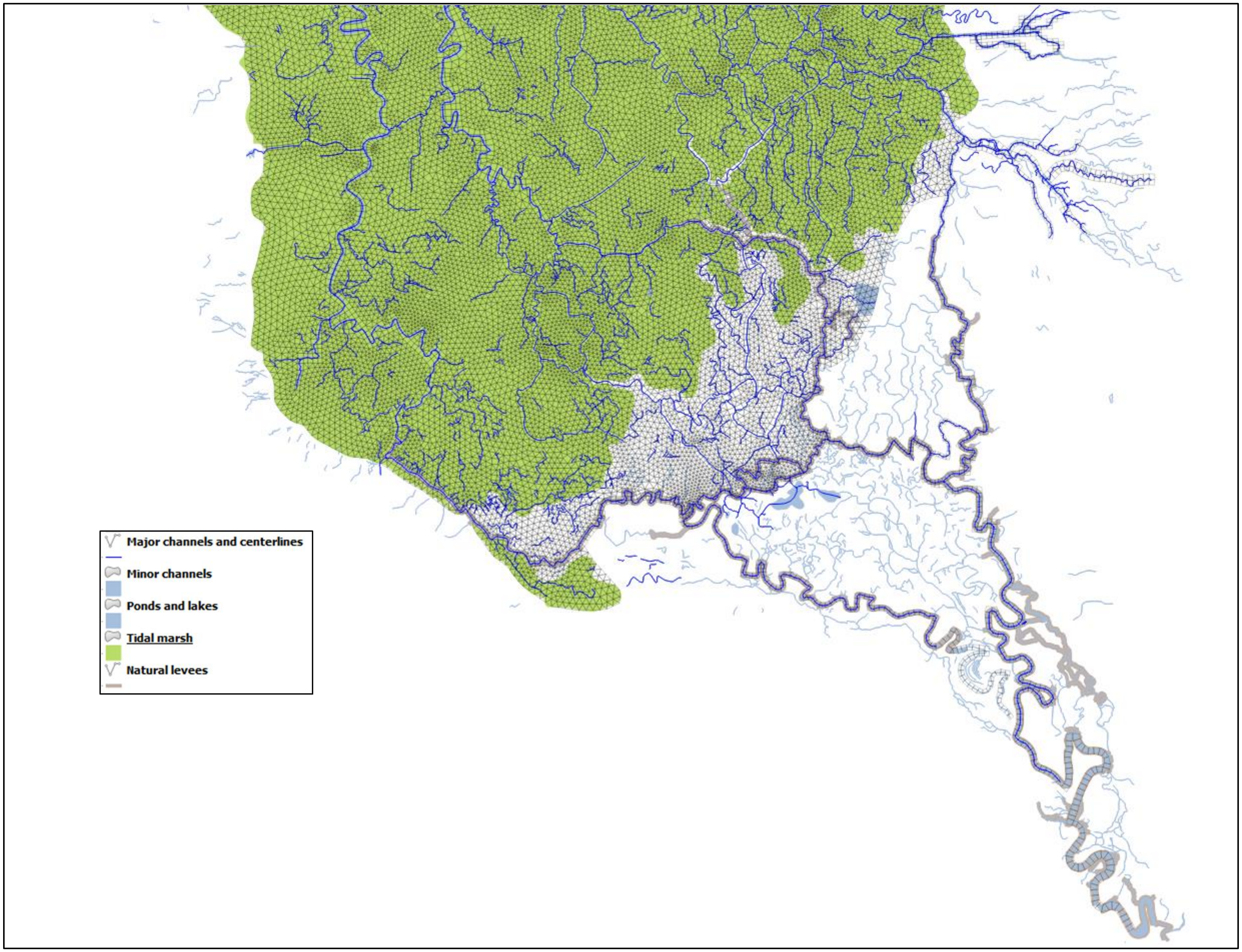

Figure 5-4 Historical Bay-Delta grid, South Delta.

5.2 Bathymetry

The historical Delta DEM was created by UCD based on the SFEI channel geometry data. Its development is documented in a separate technical memorandum, but some brief details are provided here.

Absolute elevations are necessary for the hydrodynamic model. However when the early Delta measurements of bathymetry and channel geometry were made, there was no standardized vertical datum. Most measurements used mean sea level (MSL) as a reference elevation. It is expected that MSL may have changed substantially at different locations throughout the Delta between the present and when the early measurements were taken because of large changes to the Delta geometry, hydrologic regime, and sea level rise. For this reason, an MSL correction to NAVD88 was applied as a first layer of historical DEM.

Where channel sounding data were available in the western Delta, these values were interpolated to set the channel bathymetries. These data were only available for the largest channels. For smaller channels, a regression was developed based on point measurements of channel width and depth. Using this regression, channel depth was set assuming a parabolic channel cross-section with a maximum depth calculated based on the local channel width.

Marsh plain elevations were sloped away from the channel on major rivers in the North Delta to account for natural levees. Marsh plains in the central and south parts of the Delta gradually increased in elevation with distance away from the channel.

Figure 5-5 shows the historical Delta DEM.

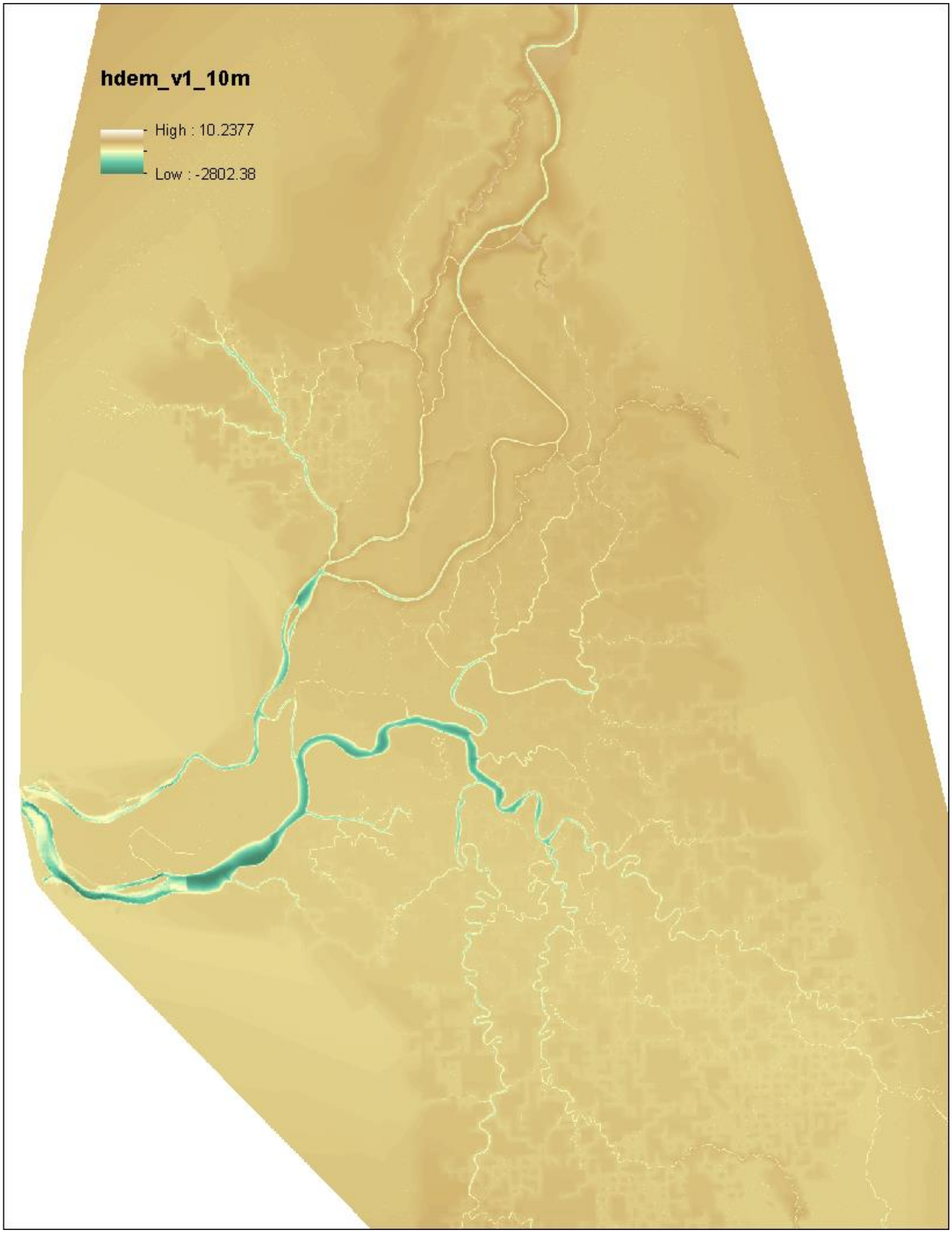

Figure 5-5 Historical Delta DEM.

5.3 Boundary Conditions

Boundary conditions mostly overlapped with the contemporary Bay-Delta locations and included:

- Stage at Point Reyes
- Inflows
  - Sacramento River below the American River confluence
  - Yolo Bypass at northern reaches of the basin
  - Cosumnes River at Delta boundary
  - Mokelumne River at Delta boundary
  - Calaveras River at Delta boundary
  - French Camp Slough at Delta boundary
  - San Joaquin River at Vernalis
  - Napa River at Napa
- Exports
  - None
- Delta Island Consumptive Use (DICU) at 257 locations throughout the Delta
  - Based only on evaporation and precipitation estimates

The Delta Cross Channel gate was removed. French Camp Slough was added as a major inflow location. No exports were modeled. DICU was provided for the historical simulations by MWH as a bulk estimate of precipitation gain and evaporation loss over the entirety of the Delta. In order to evenly distribute this gain/loss, the 257 DICU locations from the contemporary Delta were used as water source/sinks locations. The bulk DICU gain/loss was distributed evenly over these locations.

6 Historical Bay-Delta Model Calibration

6.1 Observed Data

Historical observed data for comparison with model output were provided by SFEI. The locations of the observed data are shown in Figure 6-1. Data were collected from historical accounts and were generally observations of tidal range in channels and depth of water on tidal marshes during specific time periods. A few examples of these measurement data are given below:

- "The tide rises and falls at Sacramento City, causing a variation in the depth between high and low tides of from six to fourteen inches."
- "The average difference between high and low tide is 6.12 feet and the average overflow at high tide is 0.492 feet or nearly 6 inches on the banks of the streams, the land gradually falling as you go back from the banks."
- An account from a farmer at Horseshoe Bend on the Sacramento River stated that his two and one half foot (0.76 m) high levee was "about one foot above the spring-tide mark," meaning that the pre-leveed marsh was likely overflowed by a foot and a half (0.46 m) of water at spring tides.

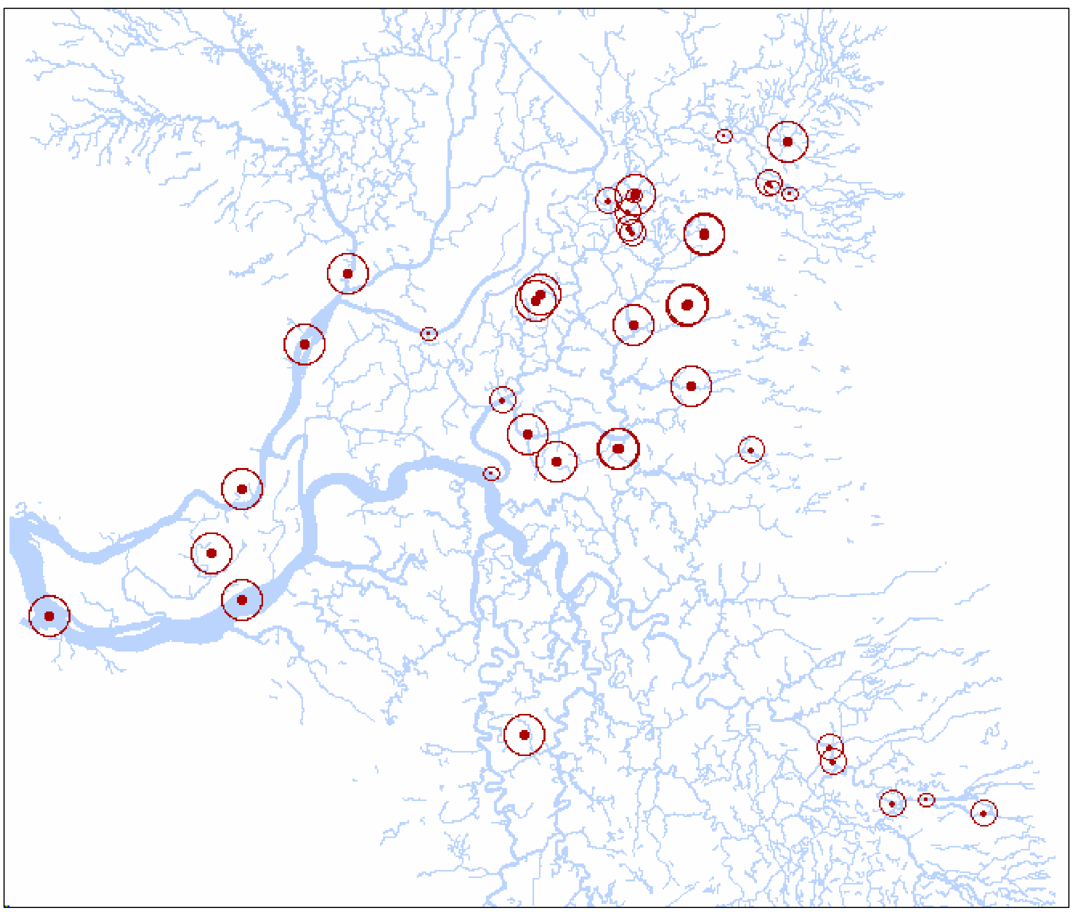

Figure 6-1 Locations of observed historical stage, inundation depth, or tidal range data for calibration of historical Bay-Delta model. Radius of circle provides an estimate of the accuracy of the estimated measurement location, with smaller circles representing greater accuracy.

6.2 Calibration Strategy

Because of the difficulty involved in calculating historical Delta absolute bathymetry values, the calibration strategy for the historical Bay-Delta model differs significantly from the contemporary Bay-Delta model. The contemporary Bay-Delta model varied bottom friction in order to calibrate to observed data. The historical Bay-Delta model is calibrated by varying the relative elevations of the marsh plains to the adjacent channels in order to match observed tidal ranges and marsh plain inundation depths. An initial guess at the MSL values is made based on contemporary MSLs. Then the historical model is run and MSLs and tidal marsh inundation depths are calculated and compared to the observed data. Changes are then made to the assumed MSL-NAVD88 offset values used to create the DEM and the marsh plain elevations relative to the adjacent channels. The historical Bay-Delta model is re-run with the updated DEM, and the process is repeated. An illustration of the iterative calibration cycle is given in Figure 6-2.

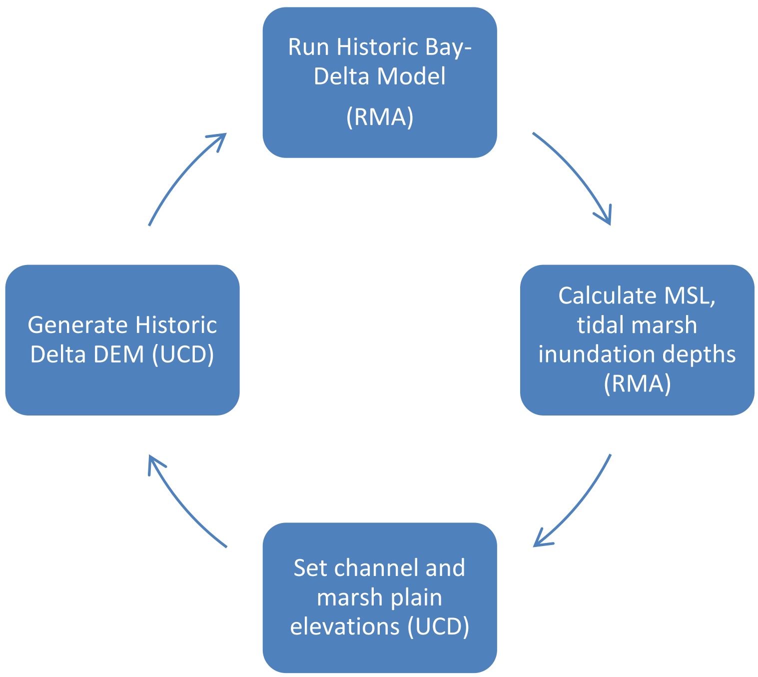

Figure 6-2 Iterative calibration strategy for the historical Bay-Delta model.

6.3 DEM Artifacts

Phase I of the historical Bay-Delta modeling project closed with an initial attempt at modeling historical Delta flows. However, the DEM creation process introduced artifacts into the model grid that resulted in unrealistic flows predicted for the Delta. These DEM artifacts were mainly a result of the interpolation methods used to translate the SFEI data into 3D channel geometries and are explained in detail in Appendix C.

The first task of the Phase II modeling work will be to fix the DEM artifacts in order to obtain a realistic first attempt at predicting the historical Delta flow and salinity regime.

7 Salinity Regime Analysis

A detailed analysis of the salinity regime could not be performed as part of the Phase I work because of the lack of reliable historical Bay-Delta model flow results (see Section 6.3). Phase II work will include analysis to evaluate the X2 bottom salinity position along with several surface isohaline positions. The model results will be used to develop regressions relating the isohaline positions to net Delta outflow conditions, similar to the work done by Gross (2010).

8 References

Bundesanstalt für Wasserbau (BAW). 2004. Mathematical Model UnTRIM Validation Document, Version June 2004 (1.0). Federal Waterways Engineering and Research Institute. Hamburg, Germany.

Bundesanstalt für Wasserbau (BAW). 2010. Mathematical Model UnTRIM^2 User Interface Description, Version May 2010 (1.1). Federal Waterways Engineering and Research Institute. Hamburg, Germany.

Burau J.R., Gartner J.W., and M.T. Stacey. 1998. Results for the hydrodynamic element of the 1994 entrapment zone study in Suisun Bay. In: Kimmerer WJ, editor. Report of the 1994 entrapment zone study. Sacramento (CA): Interagency Ecological Program for the San Francisco Bay/Delta Estuary. Pages 13-53.

Casulli, V. and E. Cattani. 1994. Stability, accuracy and efficiency of a semi-implicit method for three-dimensional shallow water flow. Computers and Mathematics with Applications 27(4): 99–112.

Casulli, V. and R.A. Walters. 2000. An unstructured grid, three-dimensional model based on the shallow water equations. International Journal for Numerical Methods in Fluids 32: 331–348.

Casulli, V. and P. Zanolli. 2005. High resolution methods for multidimensional advection-diffusion problems in free-surface hydrodynamics. Ocean Modeling 10: 137–151. DOI: 10.1016/j.ocemod.2004.06.007.

Casulli, V. 2008. A high-resolution wetting and drying algorithm for free-surface hydrodynamics. International Journal for Numerical Methods in Fluids. DOI: 10.1002/fld.1896.

Casulli, V. and G.S. Stelling. 2010. Semi-implicit subgrid modelling of three-dimensional free-surface flows. International Journal for Numerical Methods in Fluids. DOI: 10.1002/fld.2361.

Cheng, R.T. and V. Casulli. 2001. Evaluation of the UnTRIM model for 3-D tidal circulation. Proceedings of the 7th International Conference on Estuarine and Coastal Modeling. St. Petersburg, Florida.

Gross, E., MacWilliams, M.L., and W.J. Kimmerer. 2010. Three-dimensional modeling of tidal hydrodynamics in the San Francisco Estuary. San Francisco Estuary and Watershed Science 7(2).

Wang, R. and E. Ateljevich. (2012). A Continuous Surface Elevation Map for Modeling (Chapter 6). In Methodology for Flow and Salinity Estimates in the Sacramento-San Joaquin Delta and Suisun Mars, 23rd Annual Progress Report to the State Water Resources Control

Board. California Department of Water Resources, Bay-Delta Office, Delta Modeling Section.

Warner, J.C., Sherwood, C.R., Arango, H.G., and R.P. Signell. 2005. Performance of four turbulence closure models implemented using a generic length scale method. Ocean Modeling 8: 81–113. DOI: 10.1016/j.ocemod.2003.12.003.

Whipple A.A., Grossinger R.M., Rankin D., Stanford B., and R.A. Askevold. 2012. Sacramento-San Joaquin Delta Historical Ecology Investigation: Exploring Pattern and Process. Prepared for the California Department of Fish and Game and Ecosystem Restoration Program. A Report of SFEI-ASC's Historical Ecology Program, Publication #672, San Francisco Estuary Institute-Aquatic Science Center, Richmond, CA.

9 Appendix A: Contemporary Bay-Delta Model Calibration Data and Interim Calibration Results: 2010 Modeling Period

9.1 *Stage Time Series*

Figure 9-1 shows the locations of observed stage data that were used for model comparison. Observed-modeled time series plots are shown in Figure 9-2 through Figure 9-16. Table 9-1 summarizes the error between the observed and the modeled data. In all of the plots that follow, modeled results are shown in green and are overlaid on observed data, shown in blue.

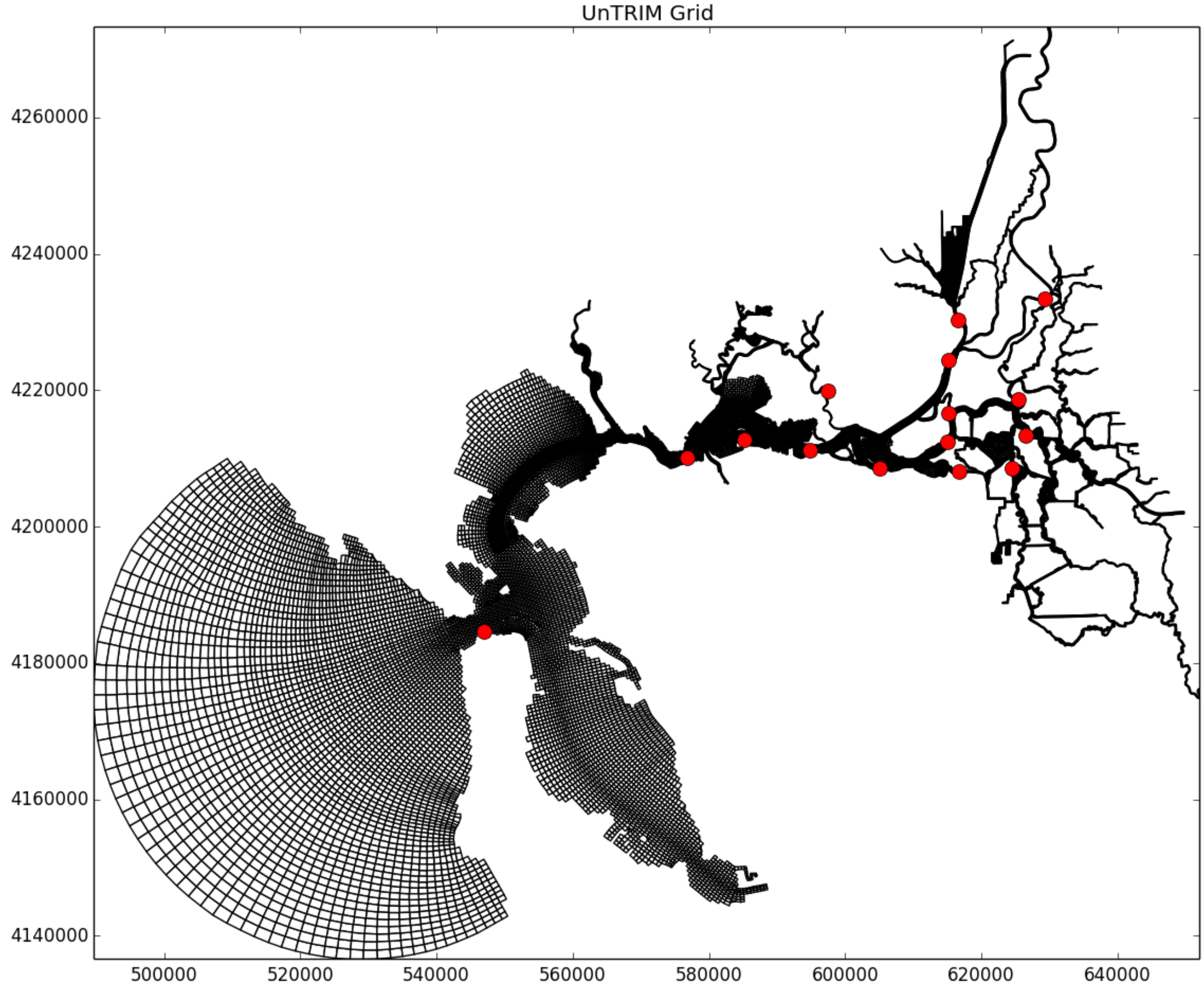

Figure 9-1 UnTRIM model-observed comparison locations for stage. 2010 calibration.

Table 9-1 UnTRIM stage error metrics.

Station	MeanE	AmpE	PhaseE	MHHWE	MLLWE	TRE	TRO	TRC
Golden Gate	0.011	1.016	4	-0.004	0.044	-0.003	1.237	1.235
Martinez	-0.061	0.956	-15	0.039	-0.115	0.131	1.033	1.164
Port Chicago	-0.007	0.963	11	-0.001	0.045	-0.058	1.088	1.030
Mallard Is	-0.040	0.946	15	-0.056	0.010	-0.076	0.973	0.897
Antioch	-0.117	0.994	17	-0.108	-0.104	-0.024	0.844	0.820
Mont Sl Nat Steel	-0.084	0.949	19	-0.101	-0.030	-0.065	1.097	1.032
SJR at Jersey Pt	-0.077	1.036	8	-0.042	-0.092	0.016	0.706	0.721
Threemile Sl	-0.160	1.121	9	-0.109	-0.208	0.059	0.690	0.749
Sac R at Rio Vista	-0.190	1.071	13	-0.146	-0.213	0.040	0.833	0.873
Cache Sl at Ryer	-0.117	1.088	2	-0.063	-0.146	0.056	0.850	0.906
Sac R Below DXC	-0.060	1.000	-6	-0.061	-0.023	-0.032	0.550	0.518
Dutch Sl	-0.077	1.052	-9	-0.034	-0.099	0.019	0.722	0.741
Holland Cut	-0.042	1.074	-6	0.004	-0.073	0.036	0.704	0.740
Mok Rvier at SJR	0.030	1.077	1	0.073	0.001	0.034	0.687	0.721
SJR at Pris Pt	0.082	1.068	9	0.128	0.061	0.033	0.713	0.746

MeanE, Mean Error [m] → $1/n \sum_i comp_i - 1/n \sum_i obs_i$
AmpE, Amplitude Error [m] → Slope of phase corrected regression line
PhaseE, Phase Error [min] → Highest correlated time shift of model data [±90 min]
MHHWE, Mean Higher High Water Error [m] → MHHW(comp) - MHHW(obs)
MLLWE, Mean Lower Low Water Error [m] → MLLW(comp) - MLLW(obs)
TRE, Tidal Range Error [m] → (MHW(comp)-MLW(comp)) - (MHW(obs)-MLW(obs))
TRO, Tidal Range Observed [m] → MHW(obs)-MLW(obs)
TRC, Tidal Range Computed [m] → MHW(comp)-MLW(comp)
comp = UnTRIM Computed Results
obs = Observed Data

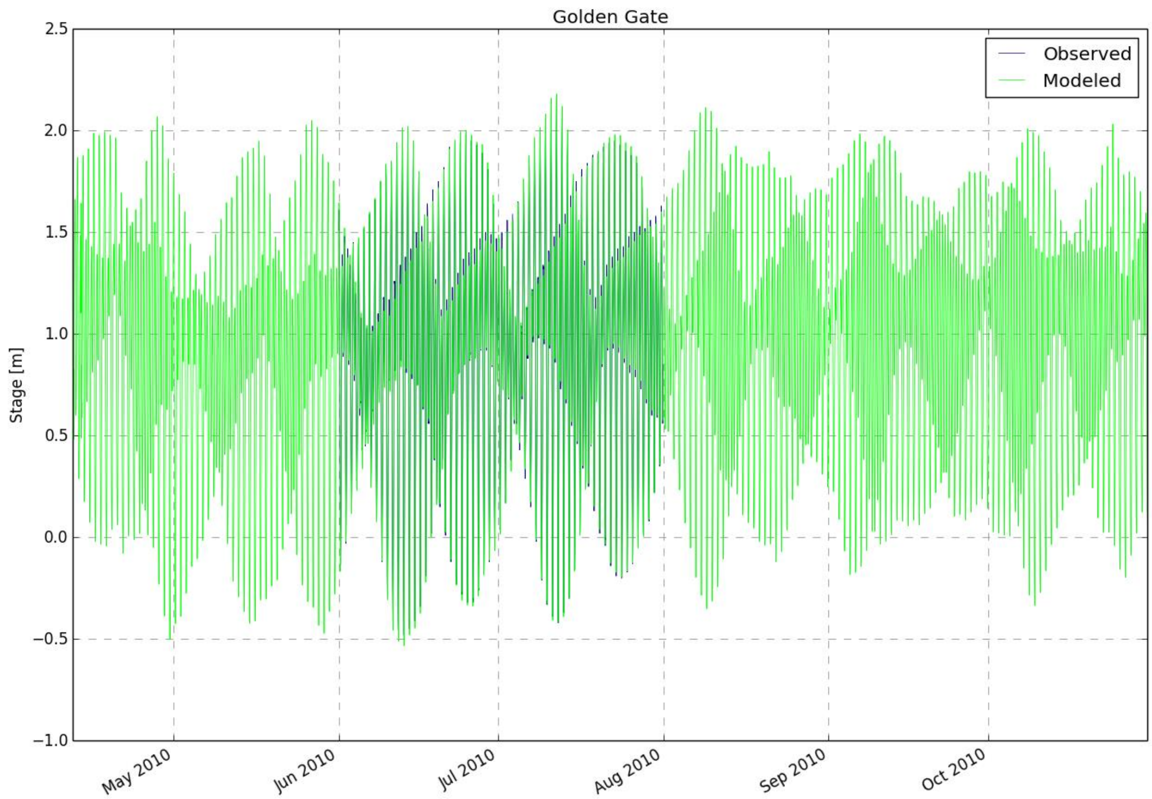

Figure 9-2 UnTRIM results and observed stage at Golden Gate station. 2010 calibration period.

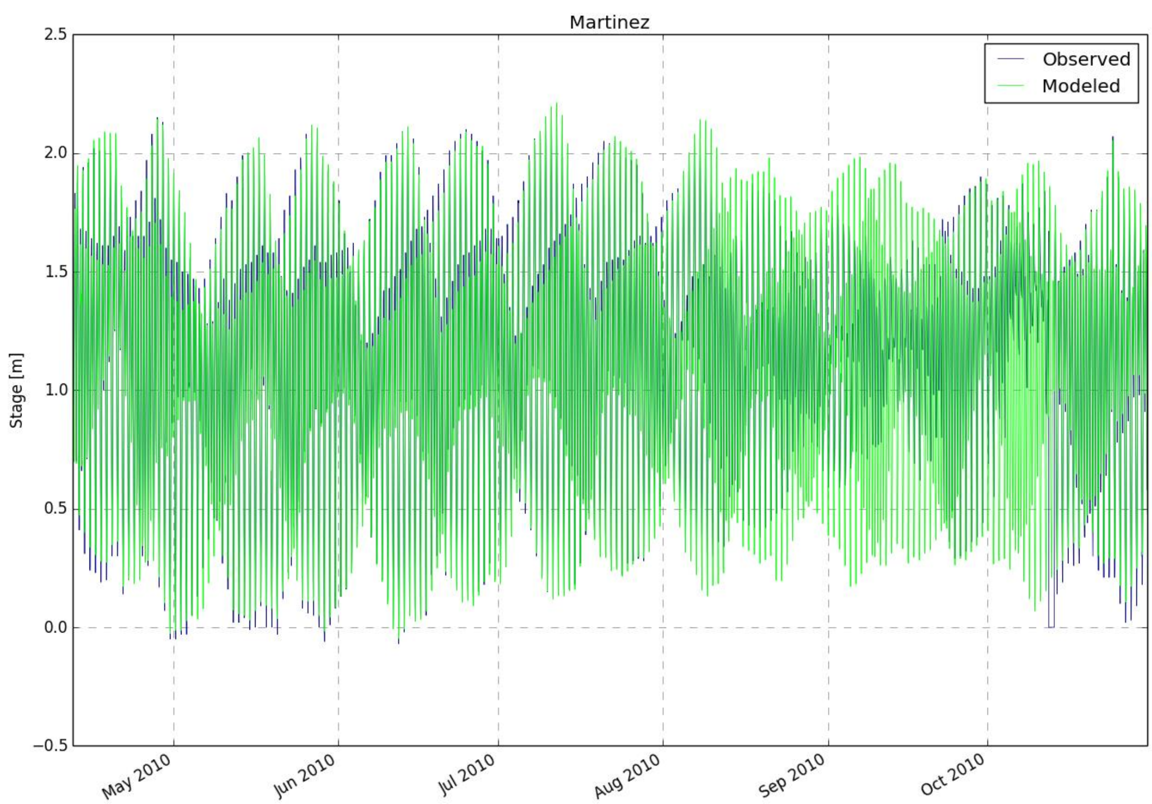

Figure 9-3 UnTRIM results and observed stage at Martinez station. 2010 calibration period.

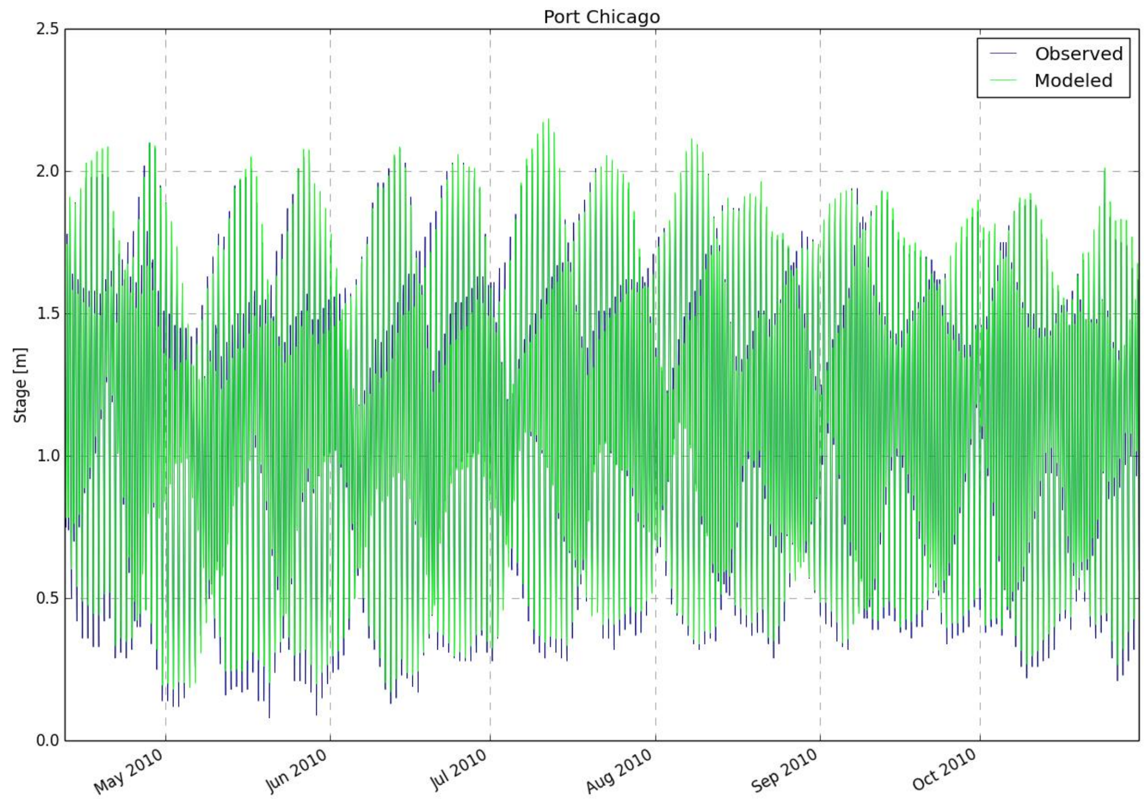

Figure 9-4 UnTRIM results and observed stage at Port Chicago station. 2010 calibration period.

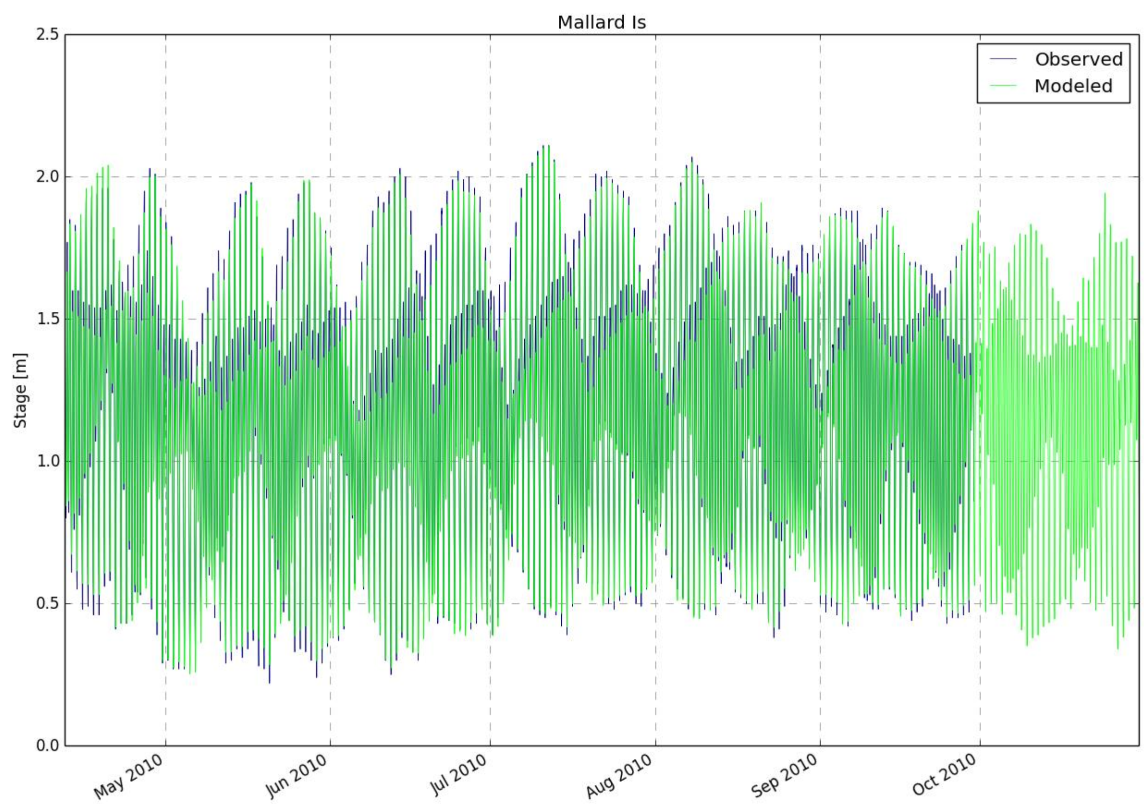

Figure 9-5 UnTRIM results and observed stage at Mallard Island station. 2010 calibration period.

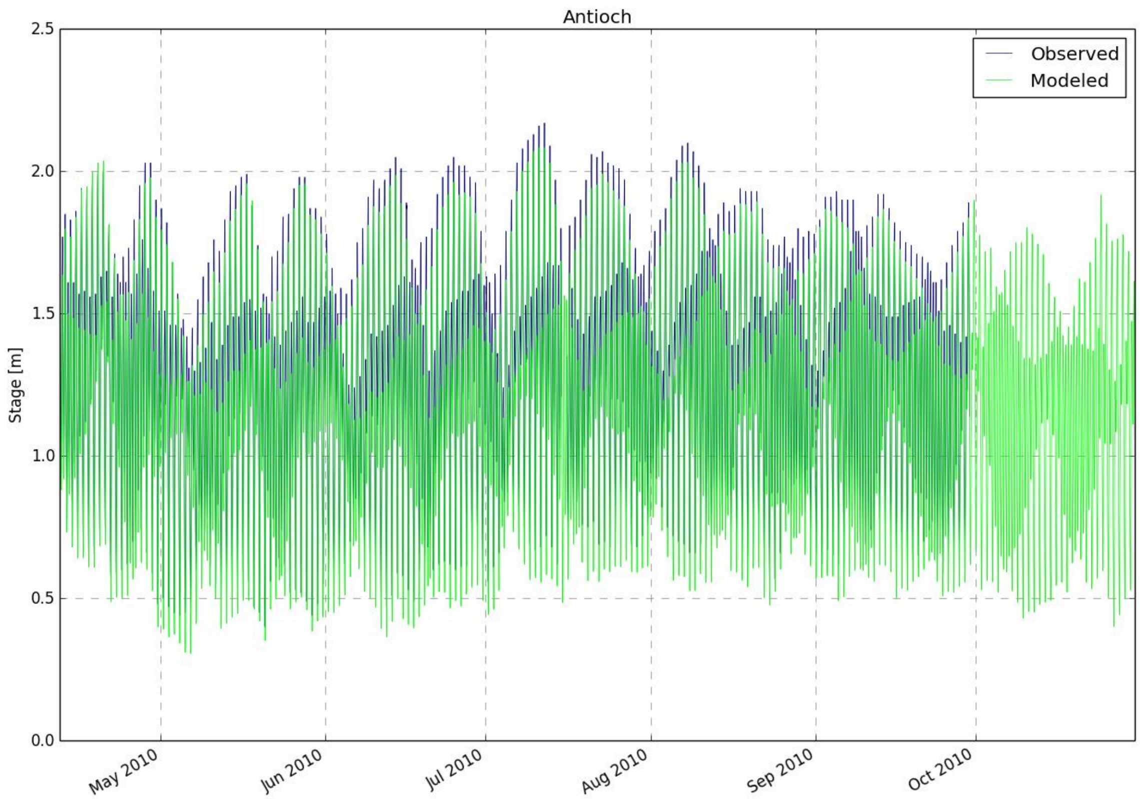

Figure 9-6 UnTRIM results and observed stage at Antioch station. 2010 calibration period.

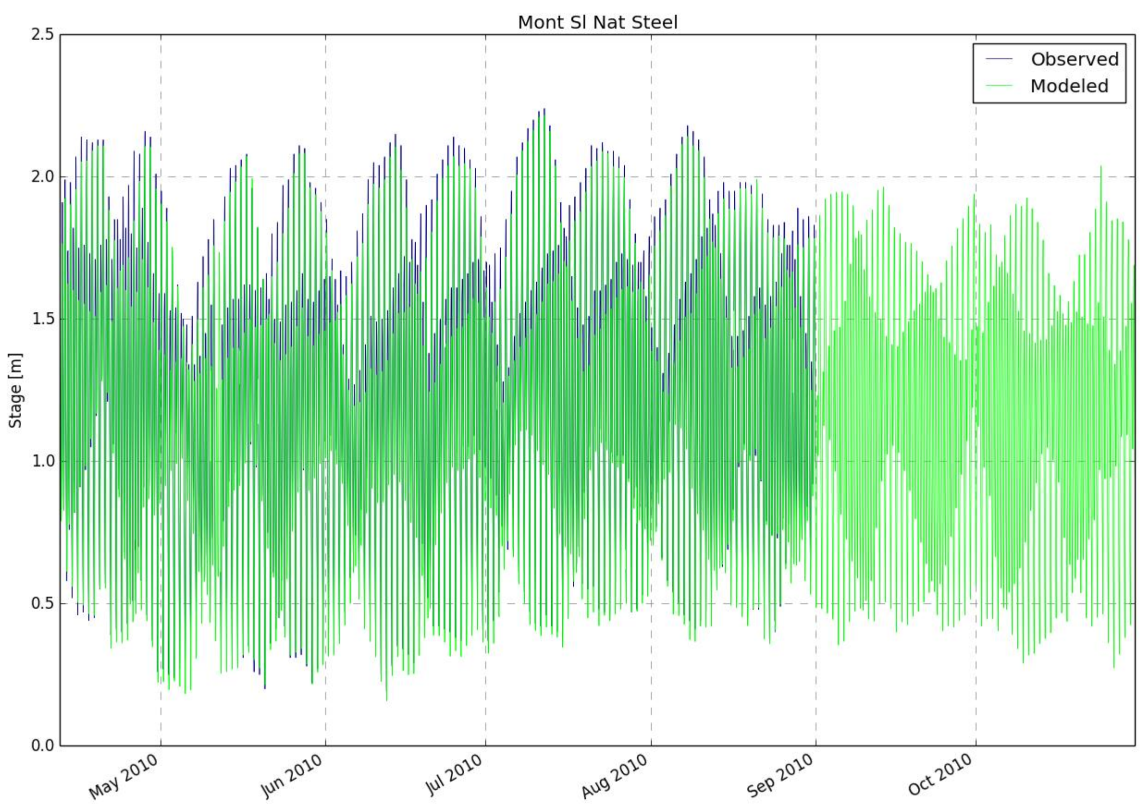

Figure 9-7 UnTRIM results and observed stage at Montezuma Slough station. 2010 calibration period.

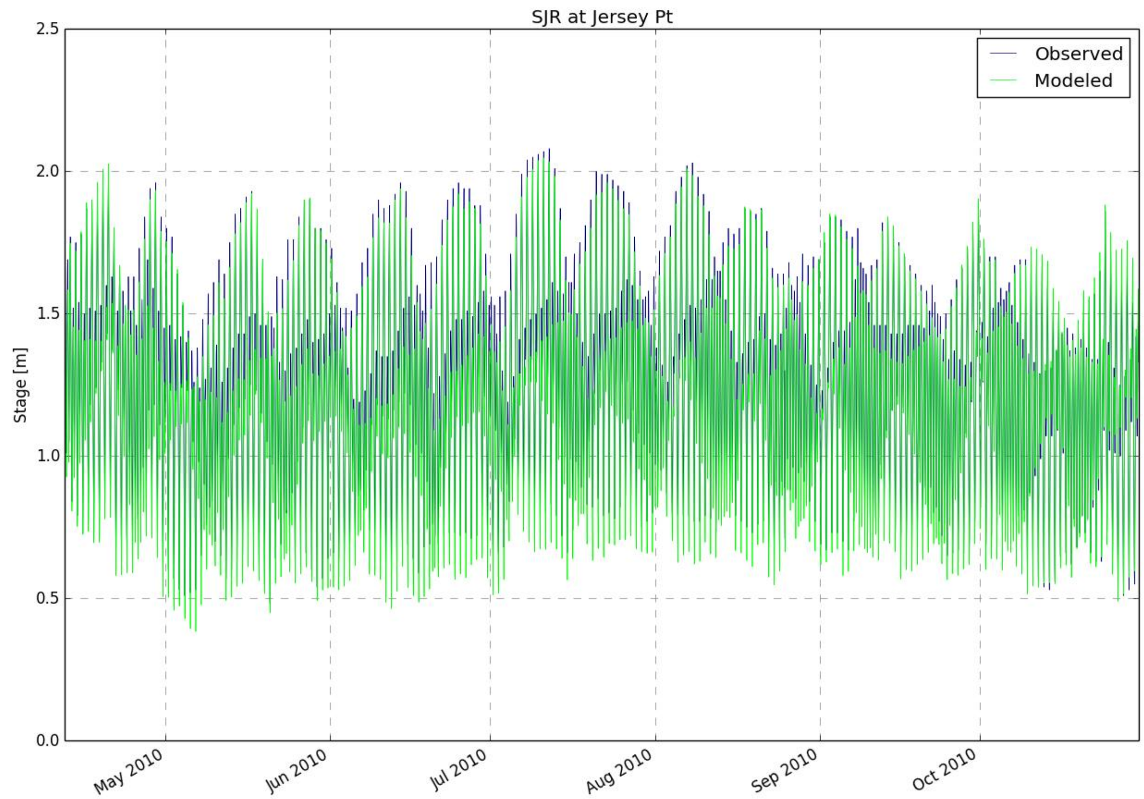

Figure 9-8 UnTRIM results and observed stage at Jersey Point station. 2010 calibration period.

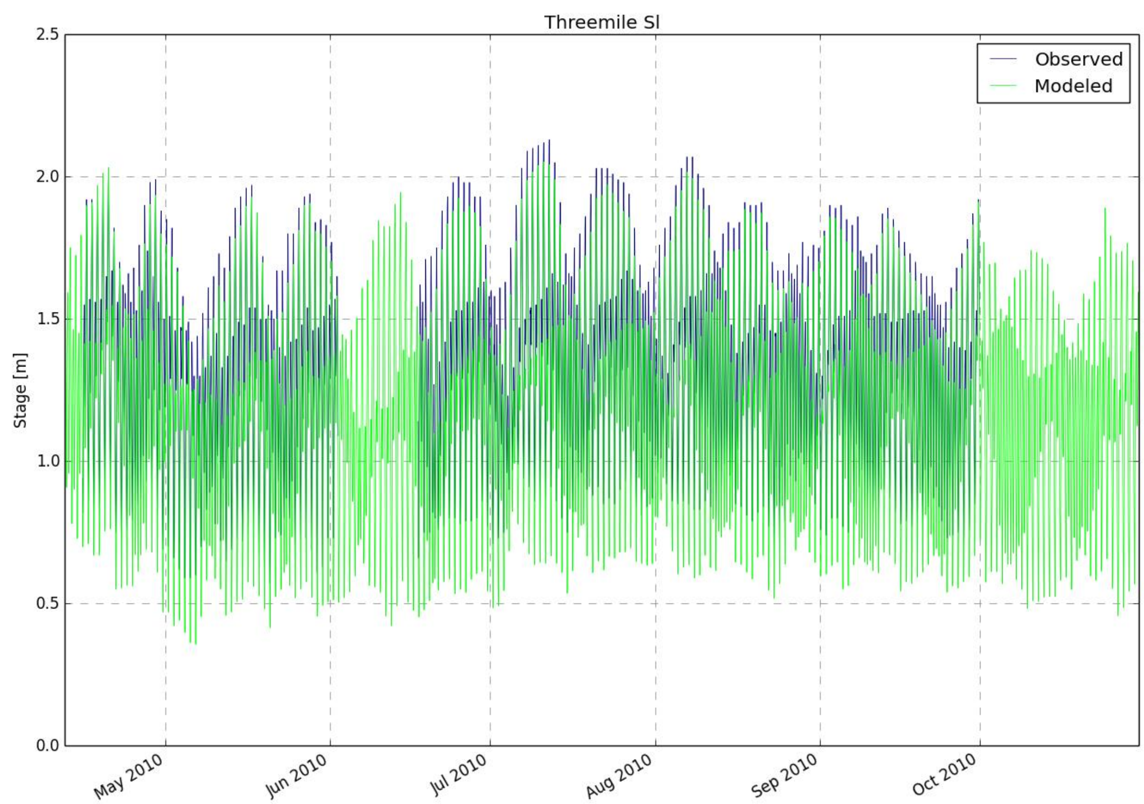

Figure 9-9 UnTRIM results and observed stage at Threemile Slough station. 2010 calibration period.

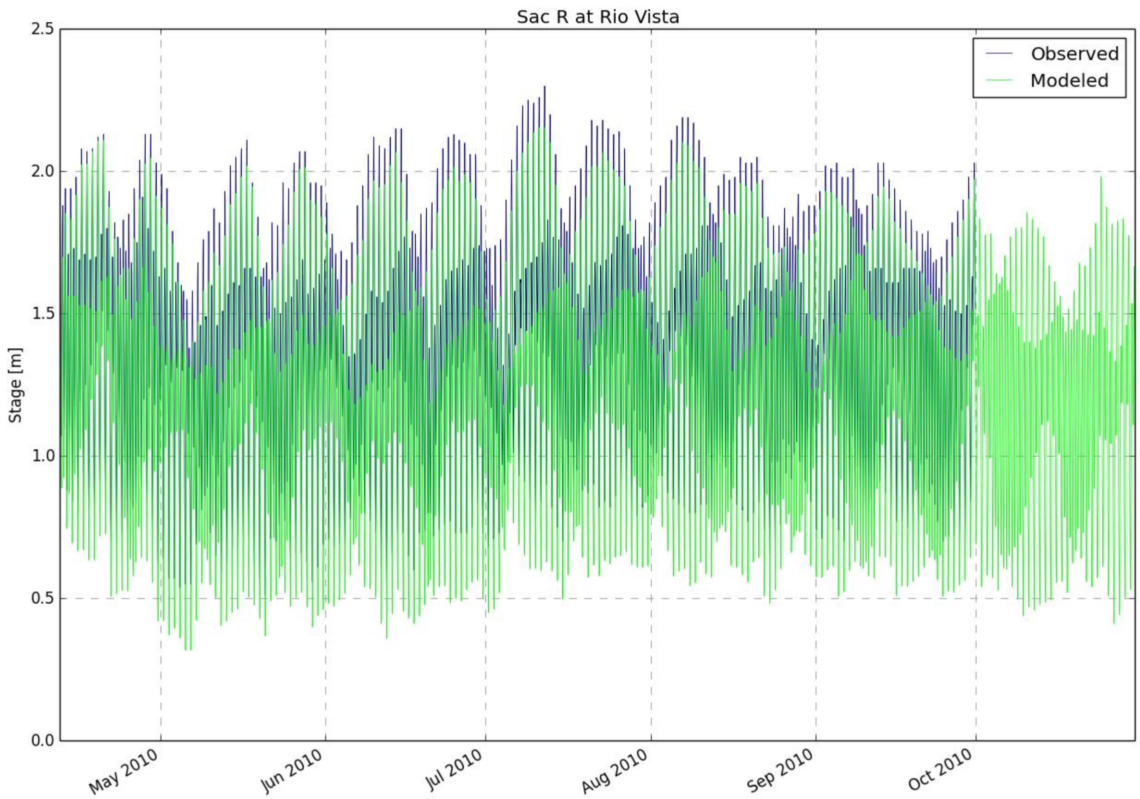

Figure 9-10 UnTRIM results and observed stage at Rio Vista station. 2010 calibration period.

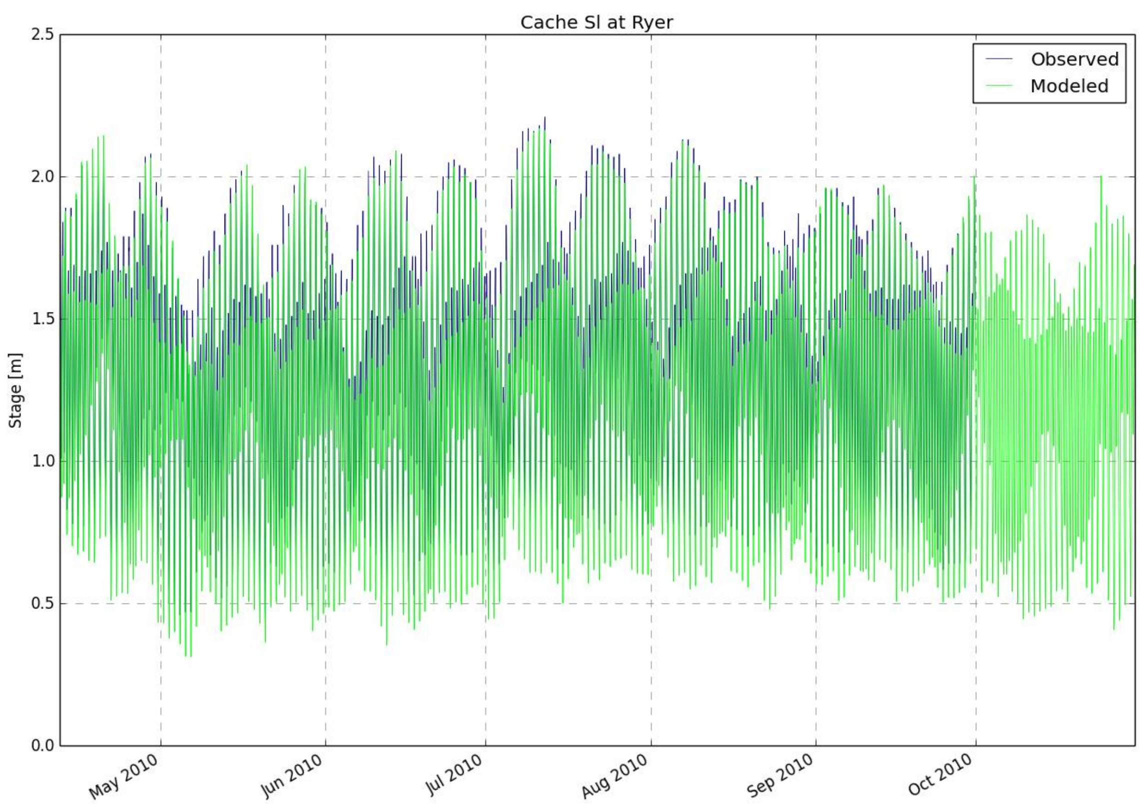

Figure 9-11 UnTRIM results and observed stage at Cache Slough station. 2010 calibration period.

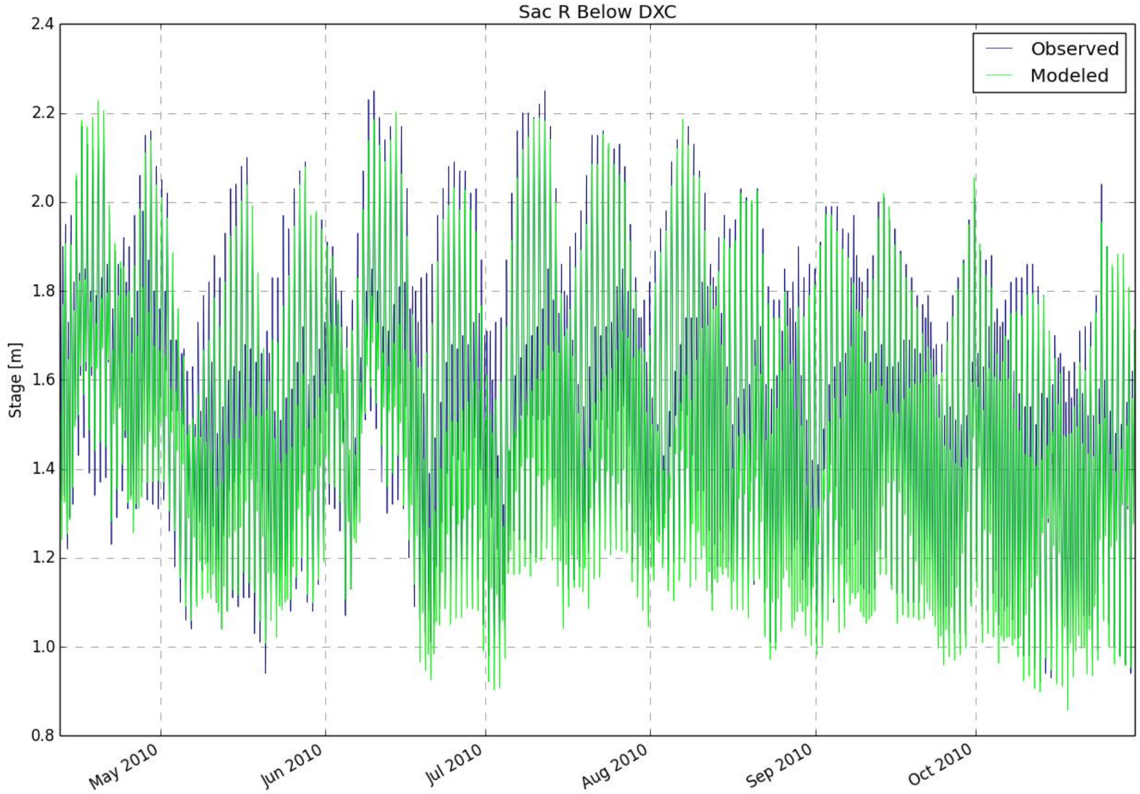

Figure 9-12 UnTRIM results and observed stage at Sacramento River below DCC station. 2010 calibration period.

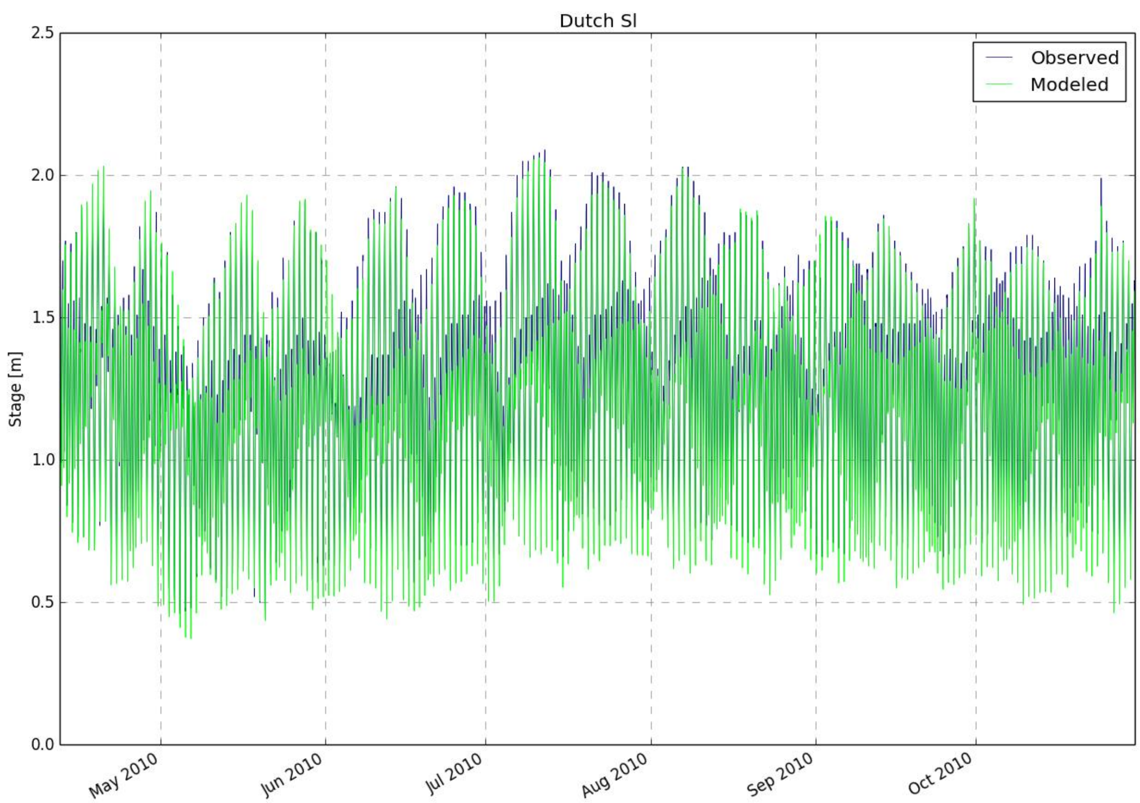

Figure 9-13 UnTRIM results and observed stage at Dutch Slough station. 2010 calibration period.

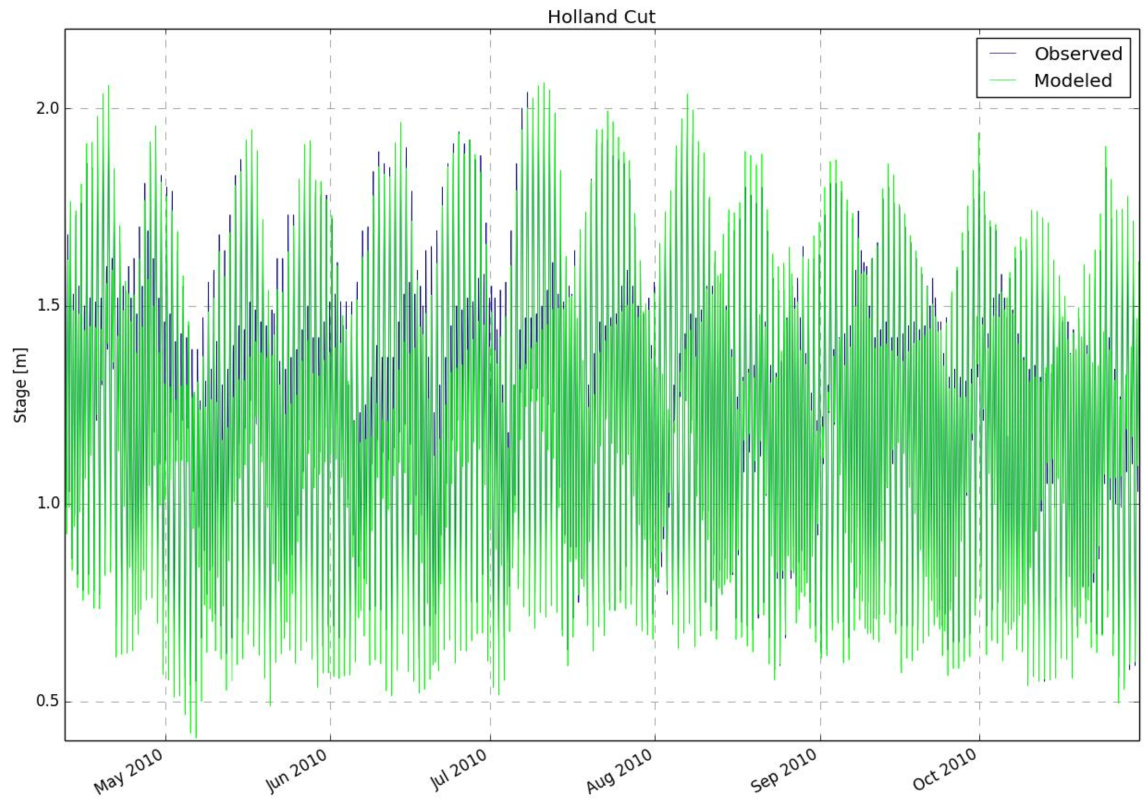

Figure 9-14 UnTRIM results and observed stage at Holland Cut station. 2010 calibration period.

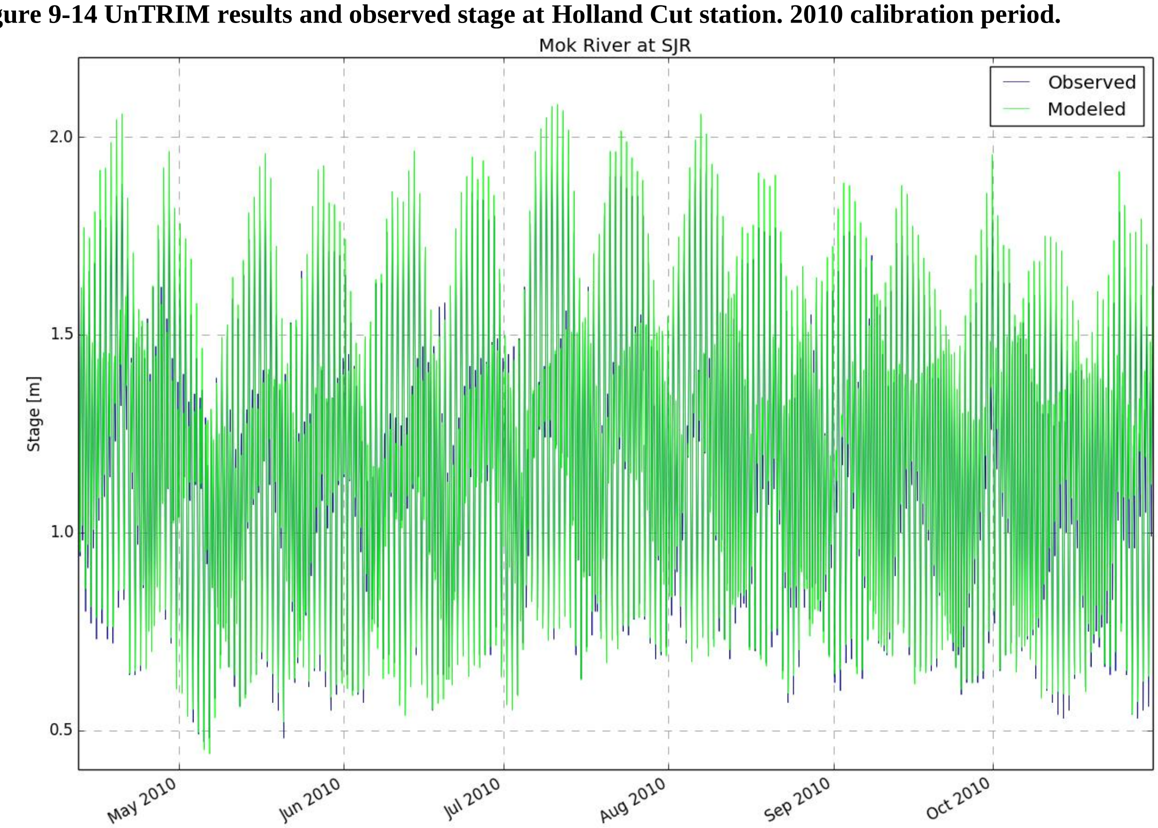

Figure 9-15 UnTRIM results and observed stage at Mokelumne River at San Joaquin River station. 2010 calibration period.

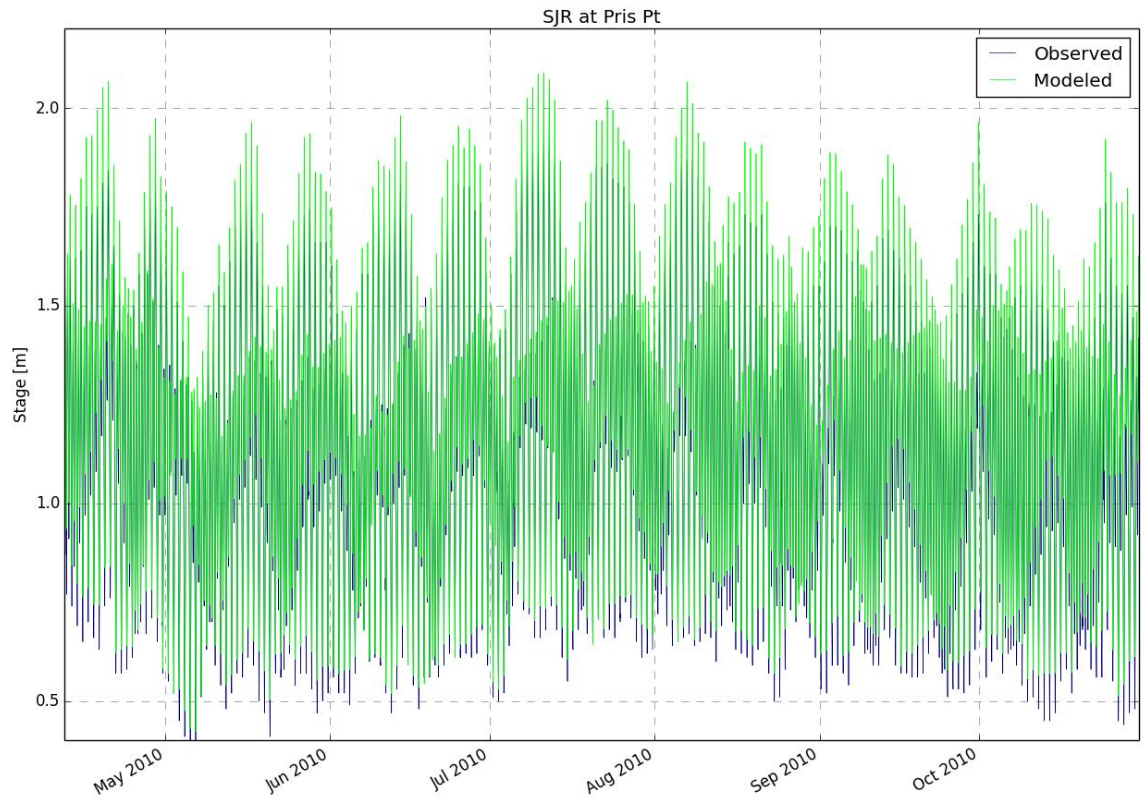

Figure 9-16 UnTRIM results and observed stage at Prisoners Point station. 2010 calibration period.

9.2 Flow Time Series

Figure 9-17 shows the locations of observed flow data that were used for model comparison. Observed-modeled time series plots are shown in Figure 9-19 through Figure 9-29. In all of these plots, modeled results are shown in green and are overlaid on observed data, shown in blue. Table 9-2 summarizes the error between the observed and the modeled data.

Figure 9-18 shows the UnTRIM computed tidally averaged flow at Chipps Island compared to the Dayflow[4] estimated Net Delta Outflow. The filling and draining of the Delta related to the spring-neap cycle is a prominent feature in the UnTRIM results. The Dayflow estimated NDO has this effect removed[5].

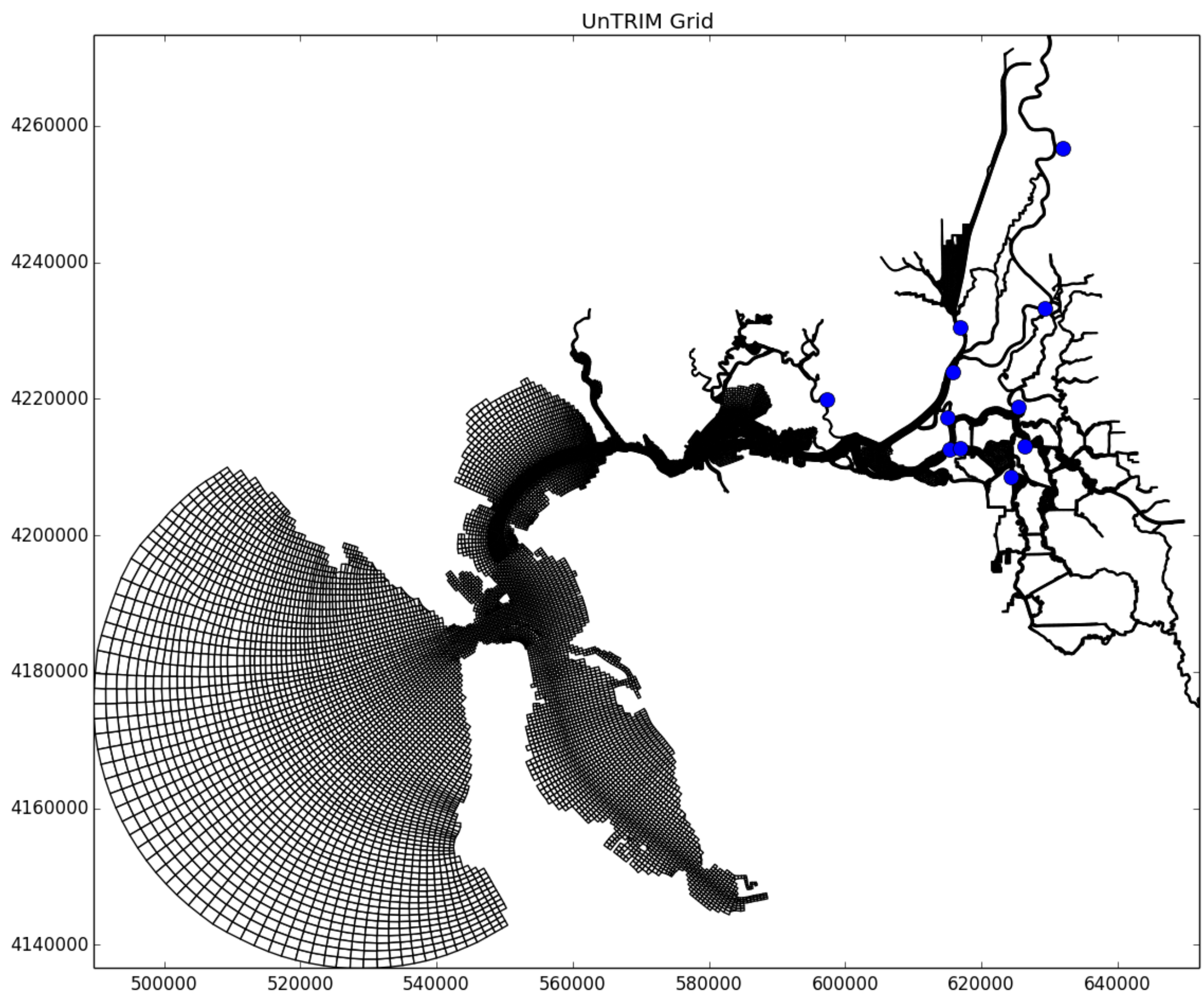

Figure 9-17 UnTRIM model-observed comparison locations for flow. 2010 calibration.

[4] http://www.water.ca.gov/dayflow/
[5] http://www.water.ca.gov/dayflow/ndoVsNdoi/

Table 9-2 UnTRIM flow error metrics.

Station	MeanE	AmpE	PhaseE
Mont Sl Nat Steel	-12.3	0.723	10
SJR at Jersey Pt	94.5	0.023	-10
Threemile Sl	1.8	1.203	7
False River	39.8	1.077	-2
Sac R at Rio Vista	-51.9	0.920	-15
Cache Sl at Ryer	14.1	0.902	-12
Sac R Below DCC	-2.6	0.867	-1
Sac R at Freeport	-37.0	1.215	-5
Holland Cut	-36.7	0.903	-5
Mok River at SJR	-13.1	1.049	-3
SJR at Pris Pt	61.6	0.886	-21

MeanE, Mean Error [m^3/s] → $1/n \sum_i comp_i - 1/n \sum_i obs_i$
AmpE, Amplitude Error [m] → Slope of phase corrected regression line
PhaseE, Phase Error [min] → Highest correlated time shift of model data [90 min]
comp = UnTRIM Computed Results
obs = Observed Data

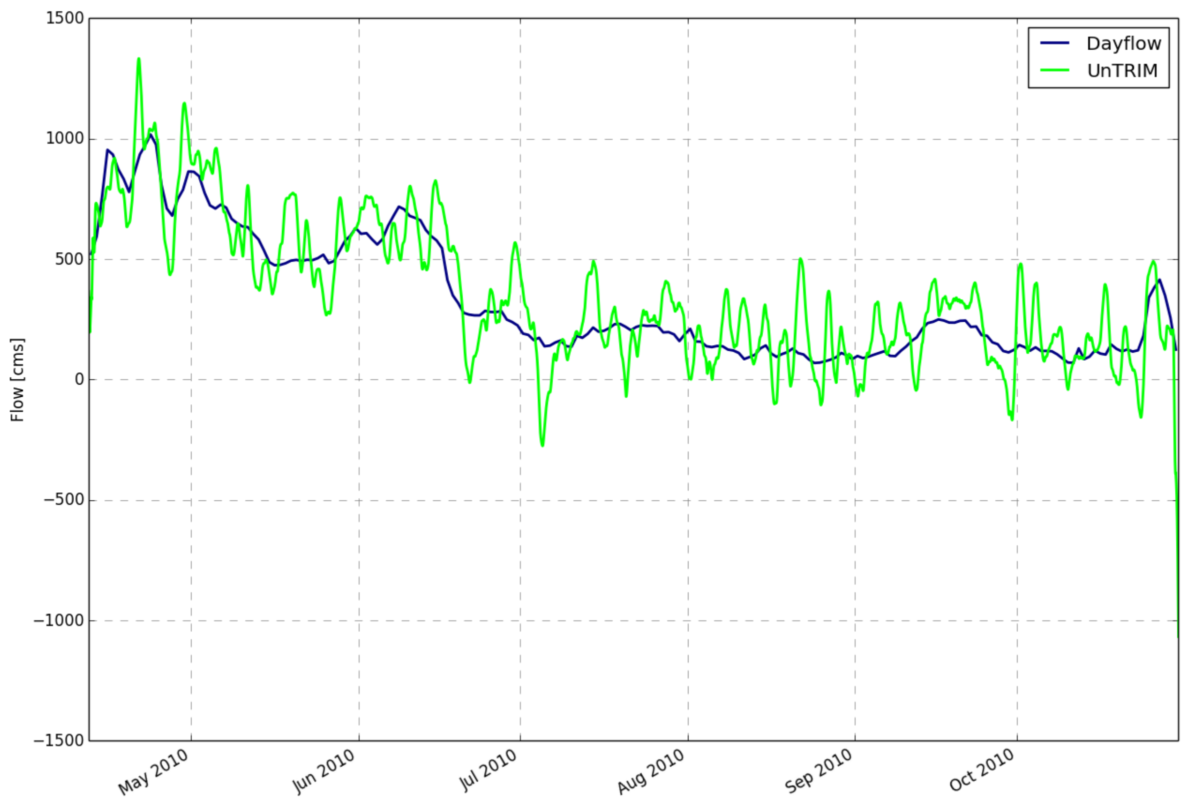

Figure 9-18 UnTRIM results for tidally-averaged Net Delta Outflow at Chipps Island and Dayflow calculated NDO. 2010 calibration period.

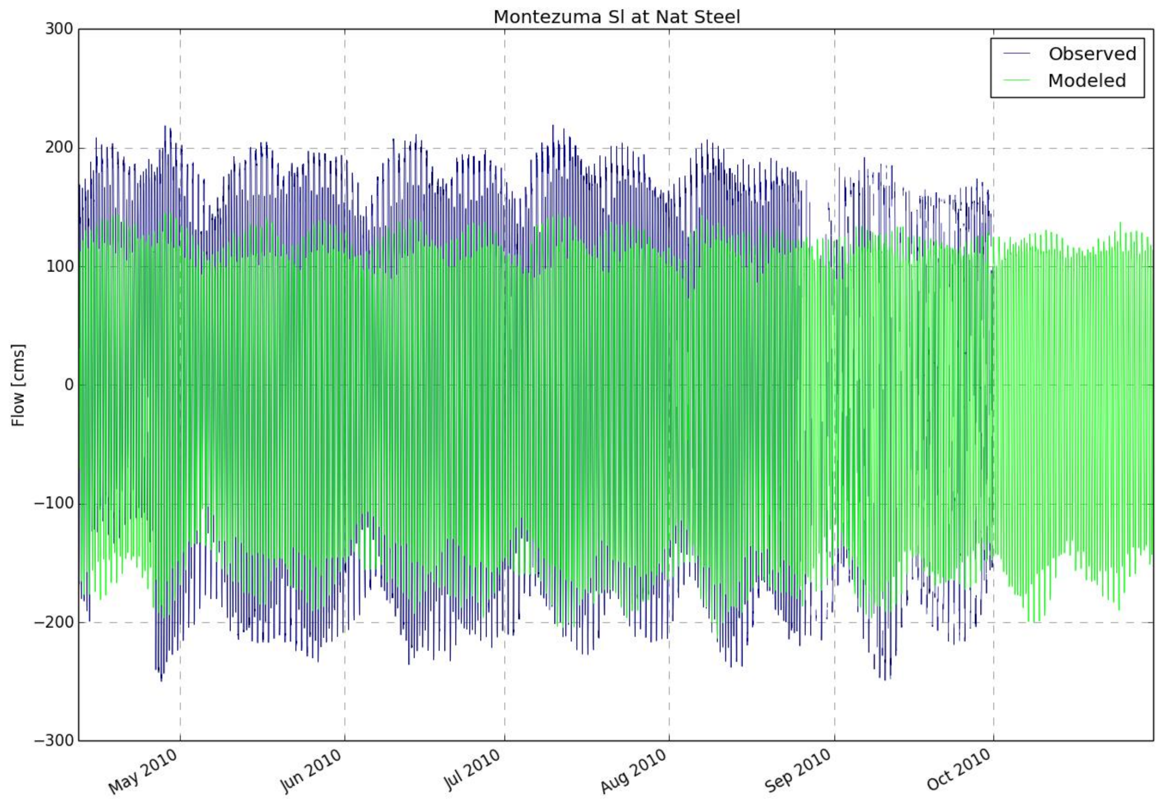

Figure 9-19 UnTRIM results and observed flow at Montezuma Sl station. 2010 calibration period.

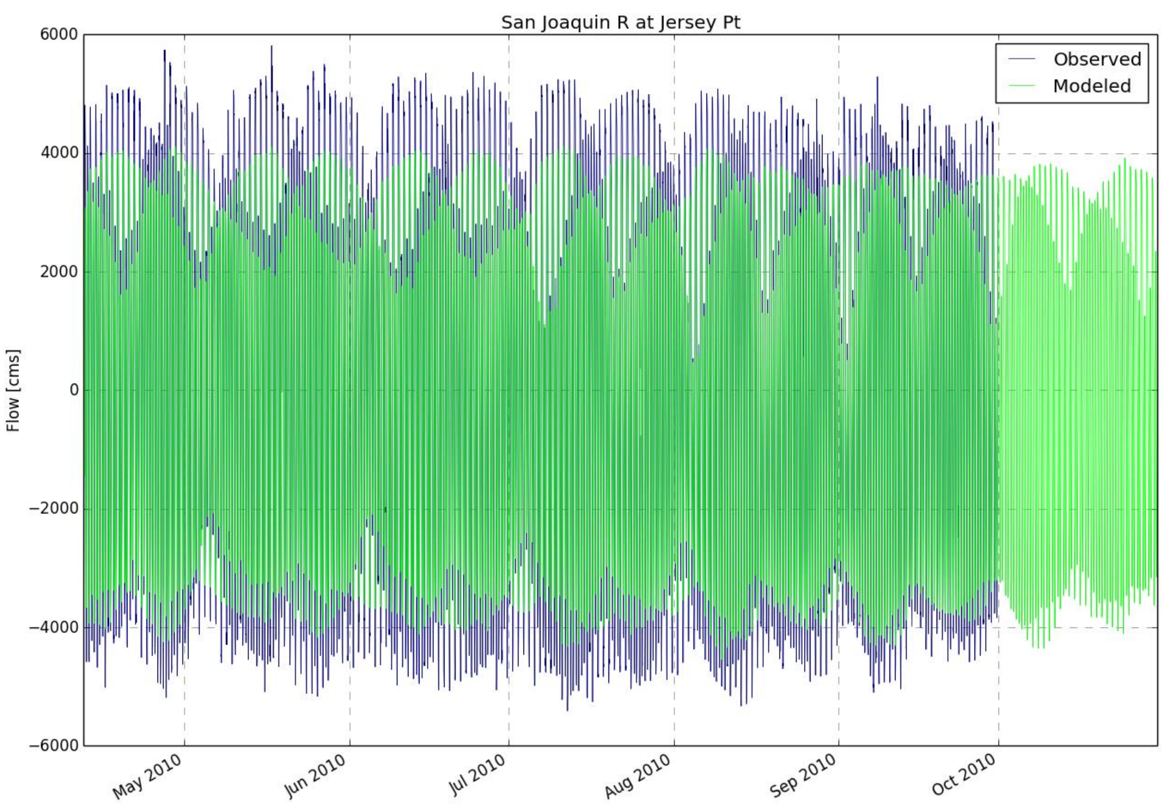

Figure 9-20 UnTRIM results and observed flow at Jersey Point station. 2010 calibration period.

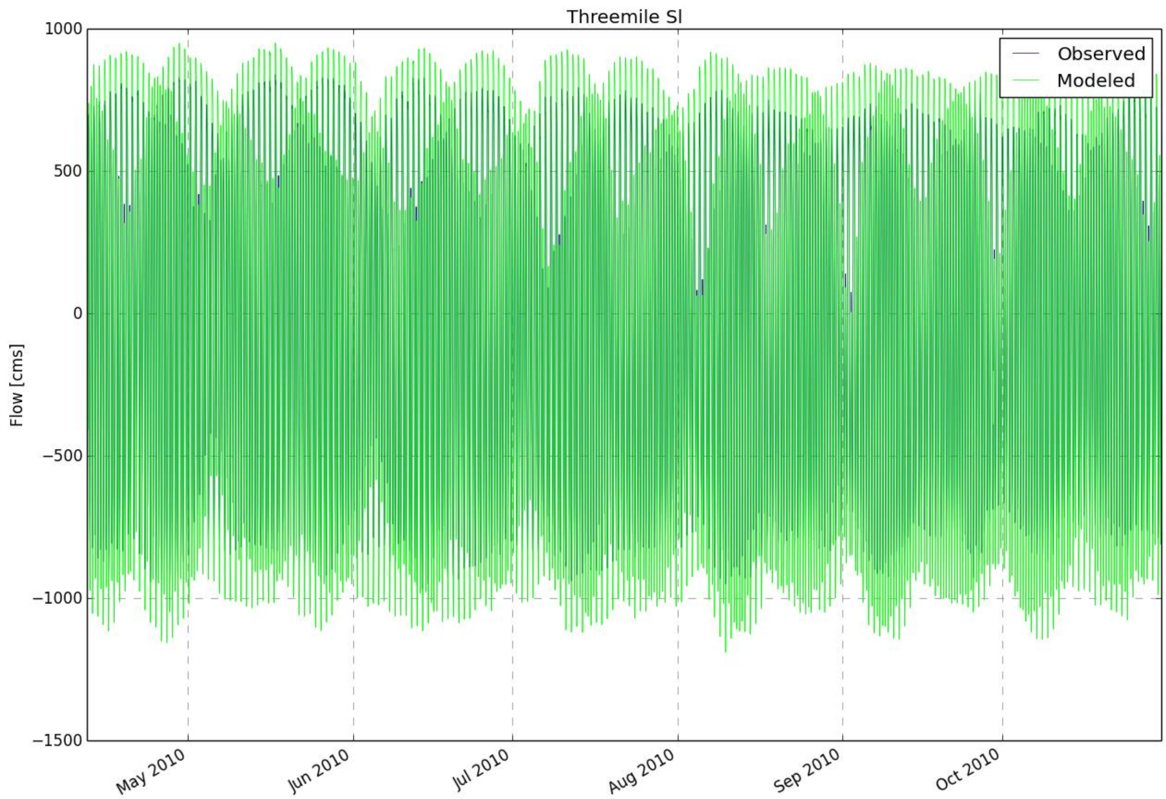

Figure 9-21 UnTRIM results and observed flow at Threemile Slough station. 2010 calibration period.

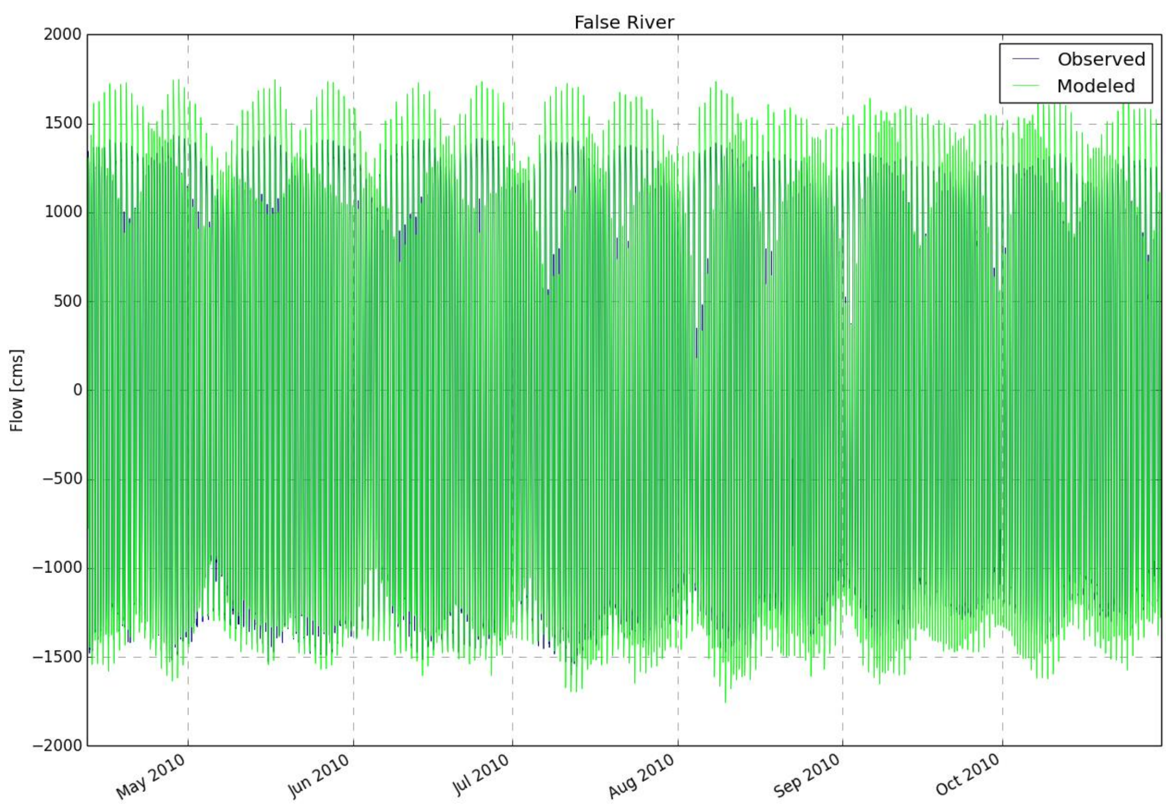

Figure 9-22 UnTRIM results and observed flow at False River station. 2010 calibration period.

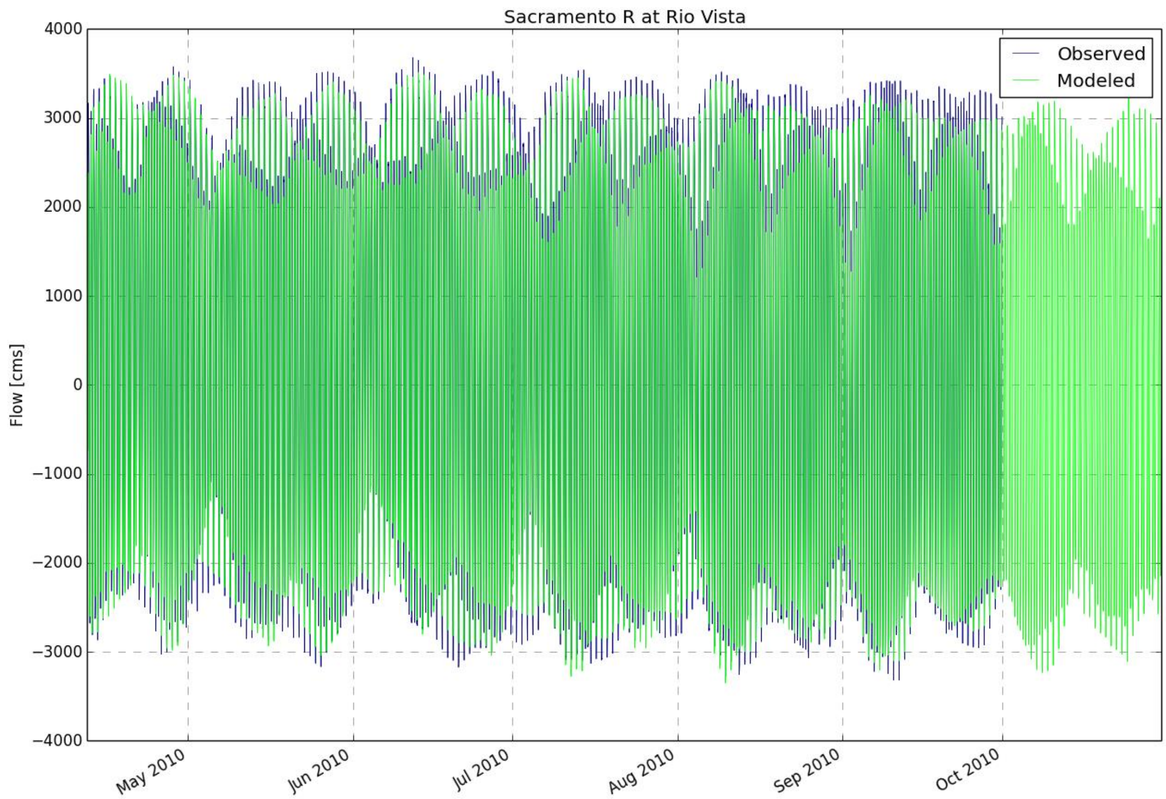

Figure 9-23 UnTRIM results and observed flow at Rio Vista station. 2010 calibration period.

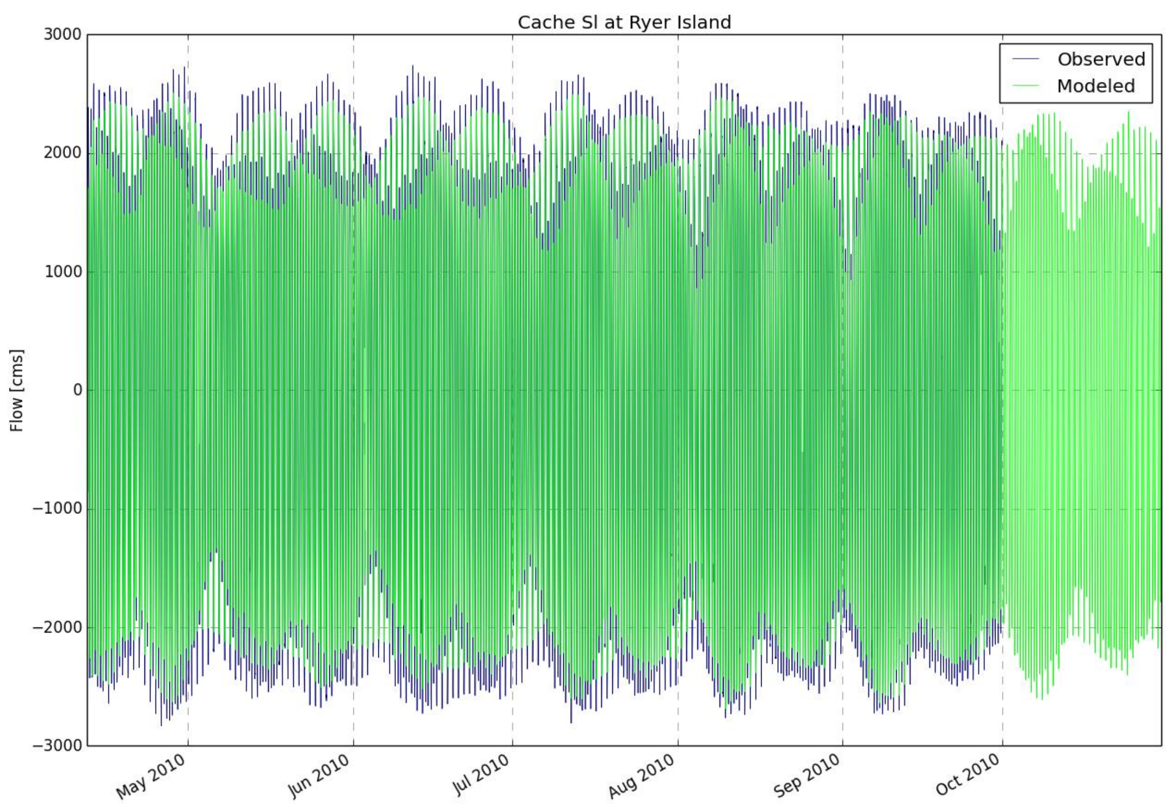

Figure 9-24 UnTRIM results and observed flow at Cache Slough station. 2010 calibration period.

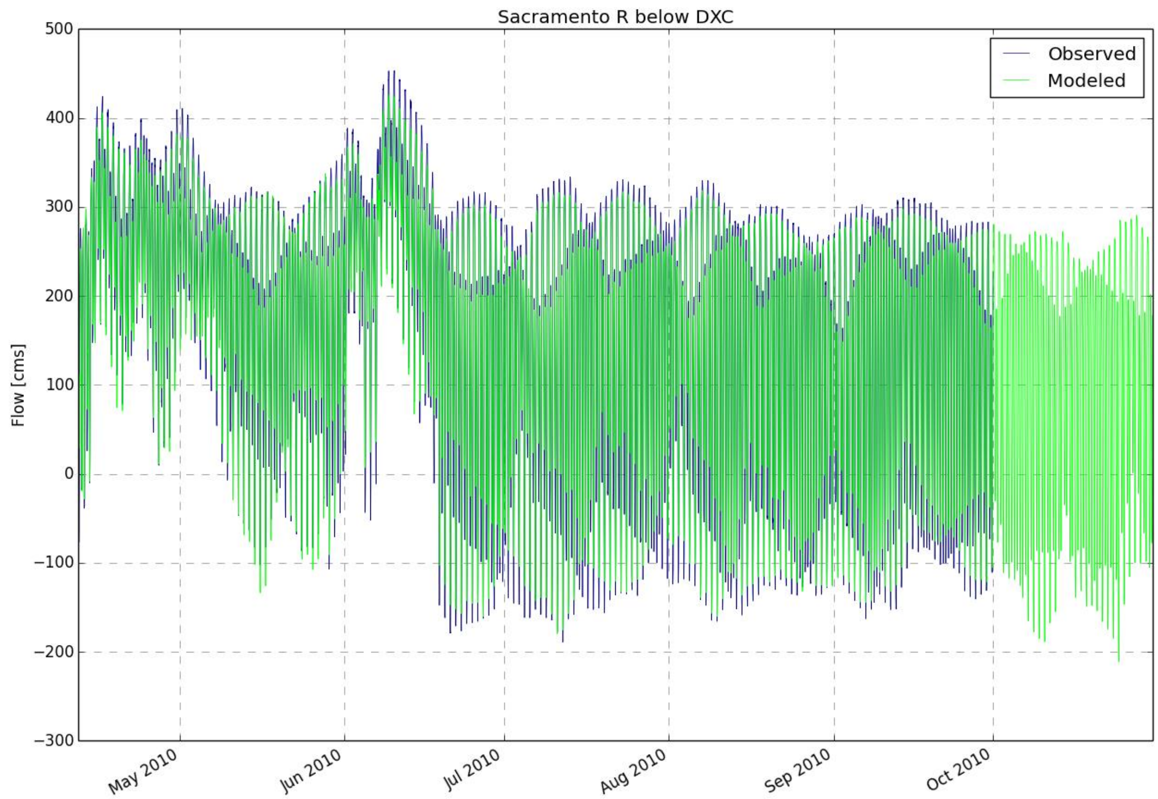

Figure 9-25 UnTRIM results and observed flow at Sacramento River below DCC station. 2010 calibration period.

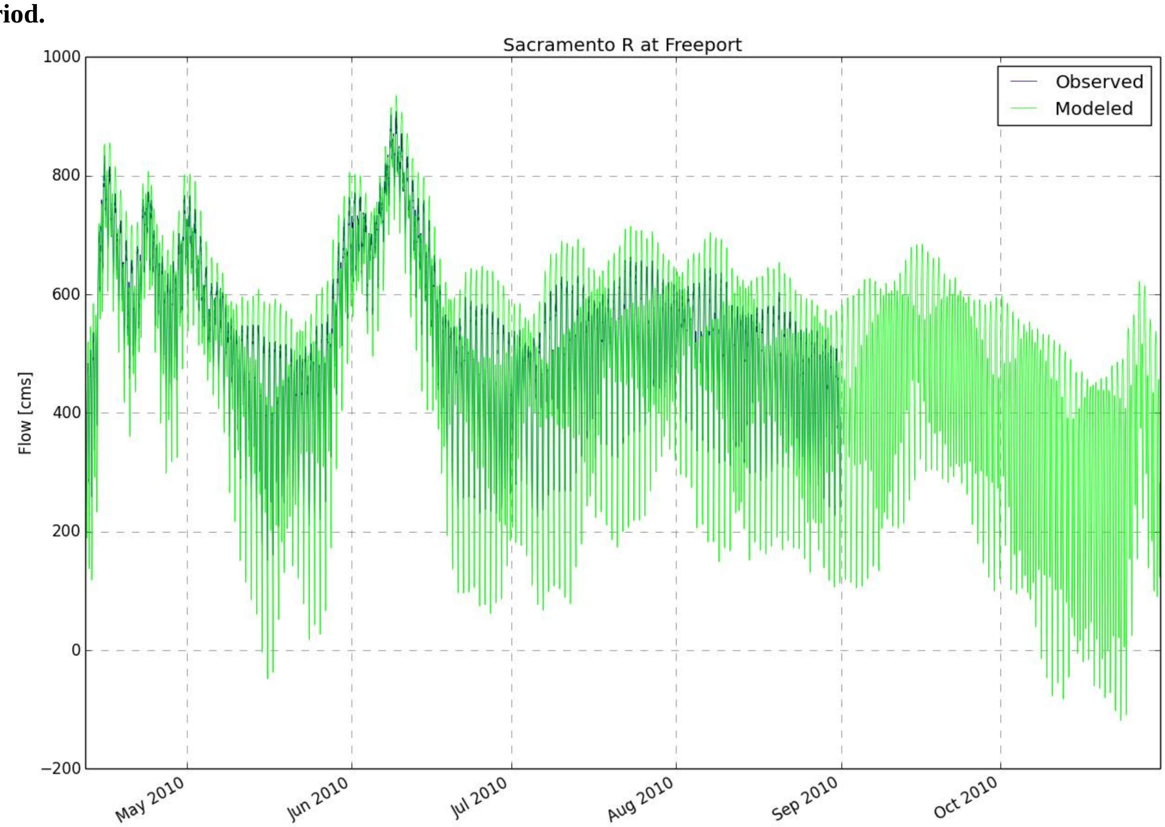

Figure 9-26 UnTRIM results and observed flow at Freeport station. 2010 calibration period.

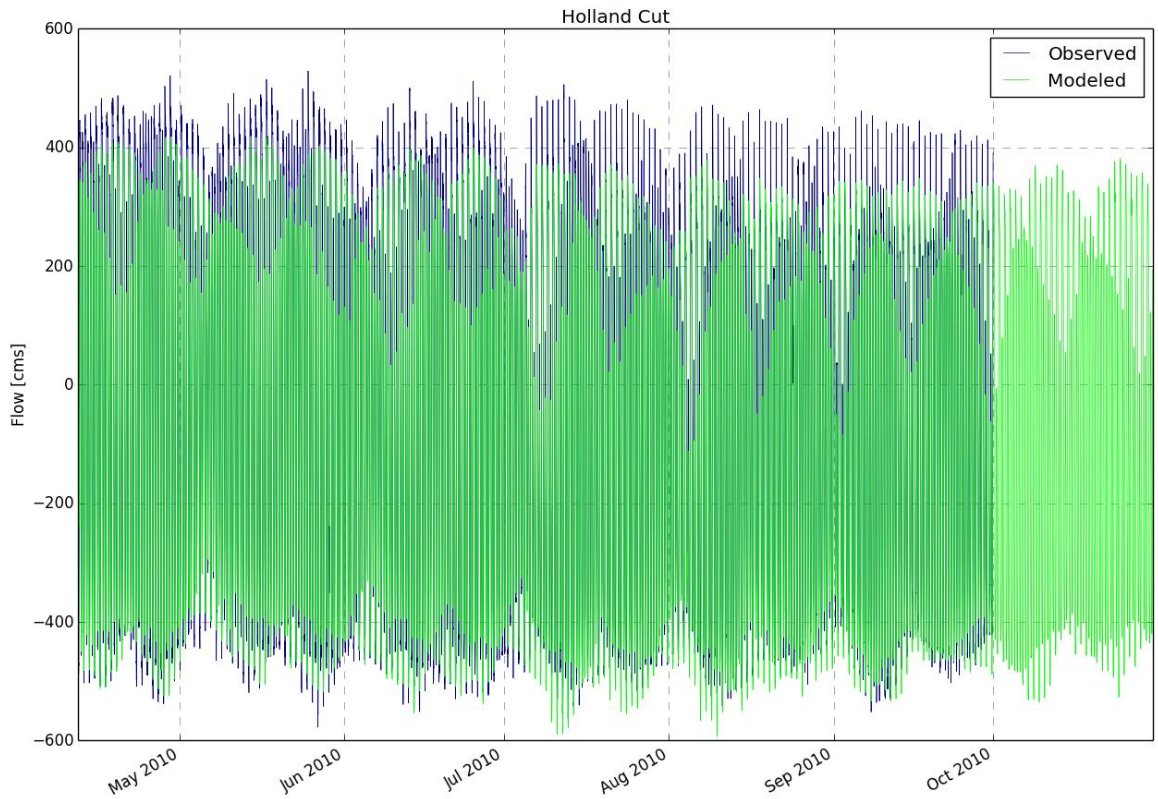

Figure 9-27 UnTRIM results and observed flow at Holland Cut station. 2010 calibration period.

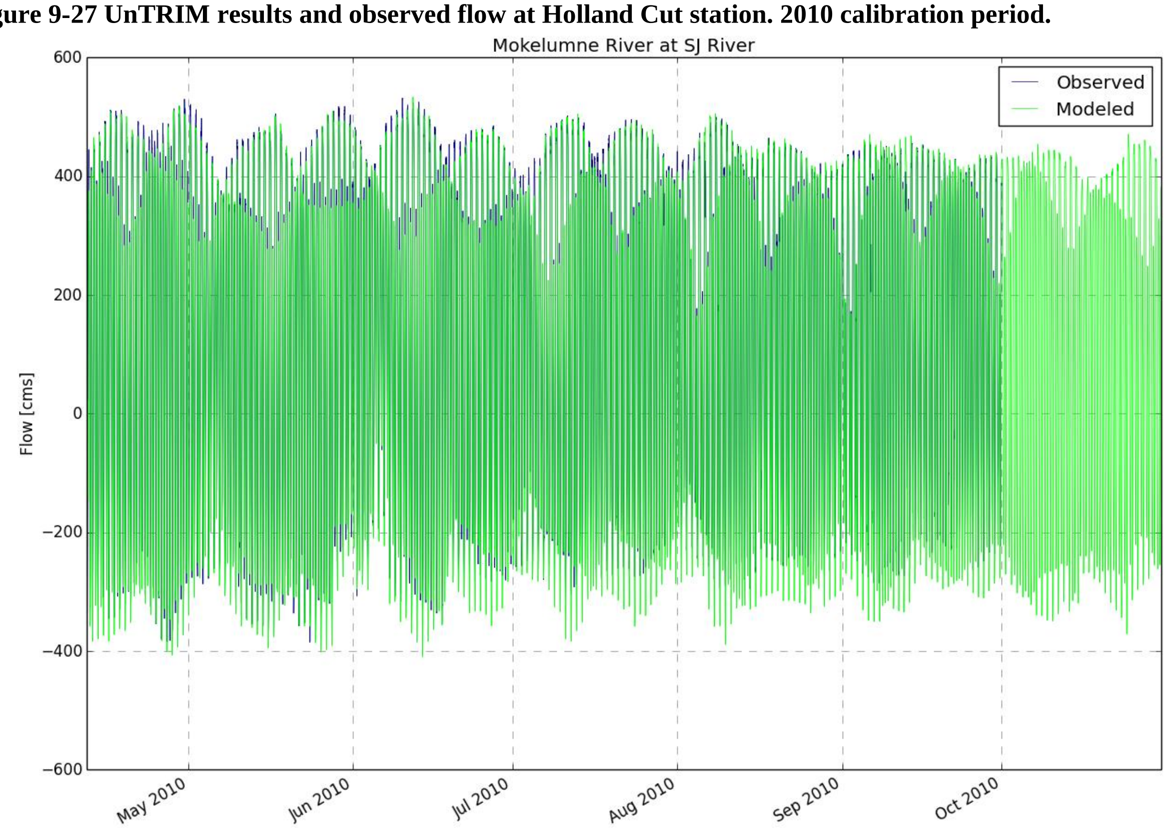

Figure 9-28 UnTRIM results and observed flow at Mokelumne River at the San Joaquin River station. 2010 calibration period.

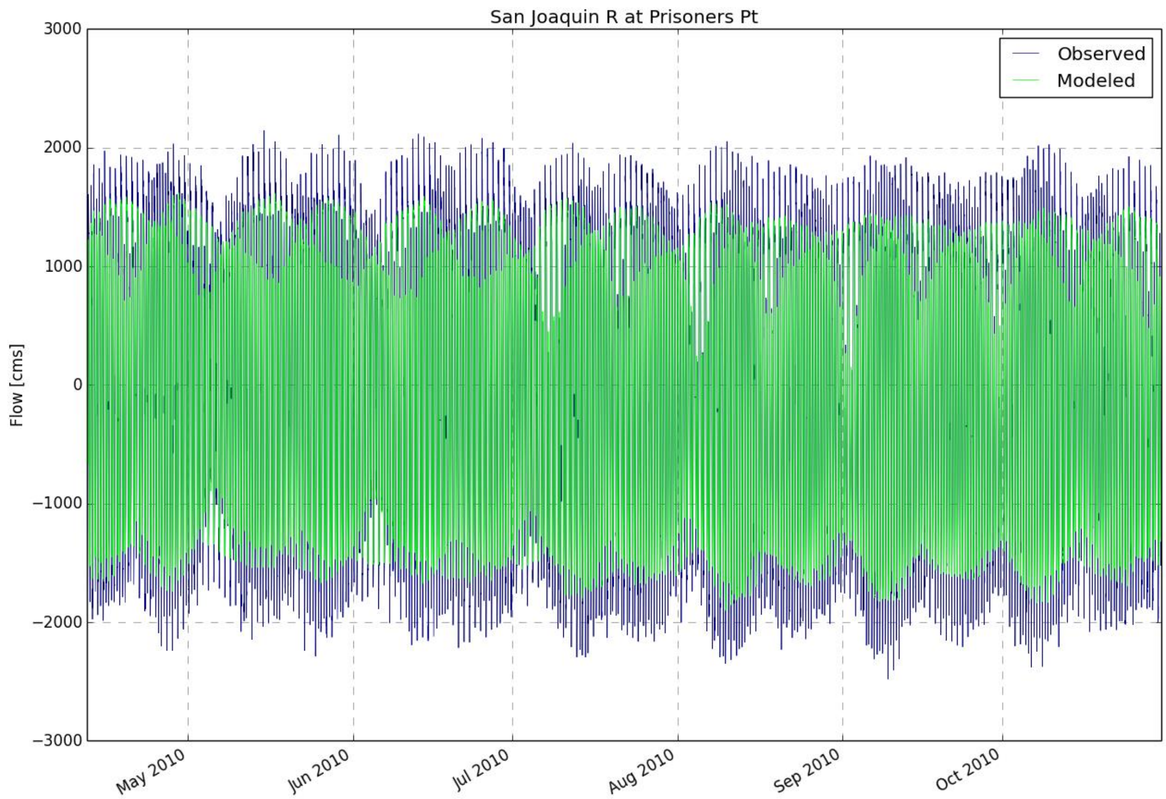

Figure 9-29 UnTRIM results and observed flow at Prisoners Point station. 2010 calibration period.

9.3 Salinity Time Series

Figure 9-30 shows the locations of observed salinity data that were used for model comparison. Observed-modeled time series plots are shown in Figure 9-31 through Figure 9-52. In all of these plots, modeled results are shown in green and are overlaid on observed data, shown in blue. Table 9-3 summarizes the error between the observed and the modeled data.

A salinity initial condition set incorrectly high in some areas of the North and South Delta can be seen in the results. The condition affected the North Delta stations for only a brief period of time. Because of the higher flushing times in the South Delta, the effect of the initial condition can be seen for the first couple of months.

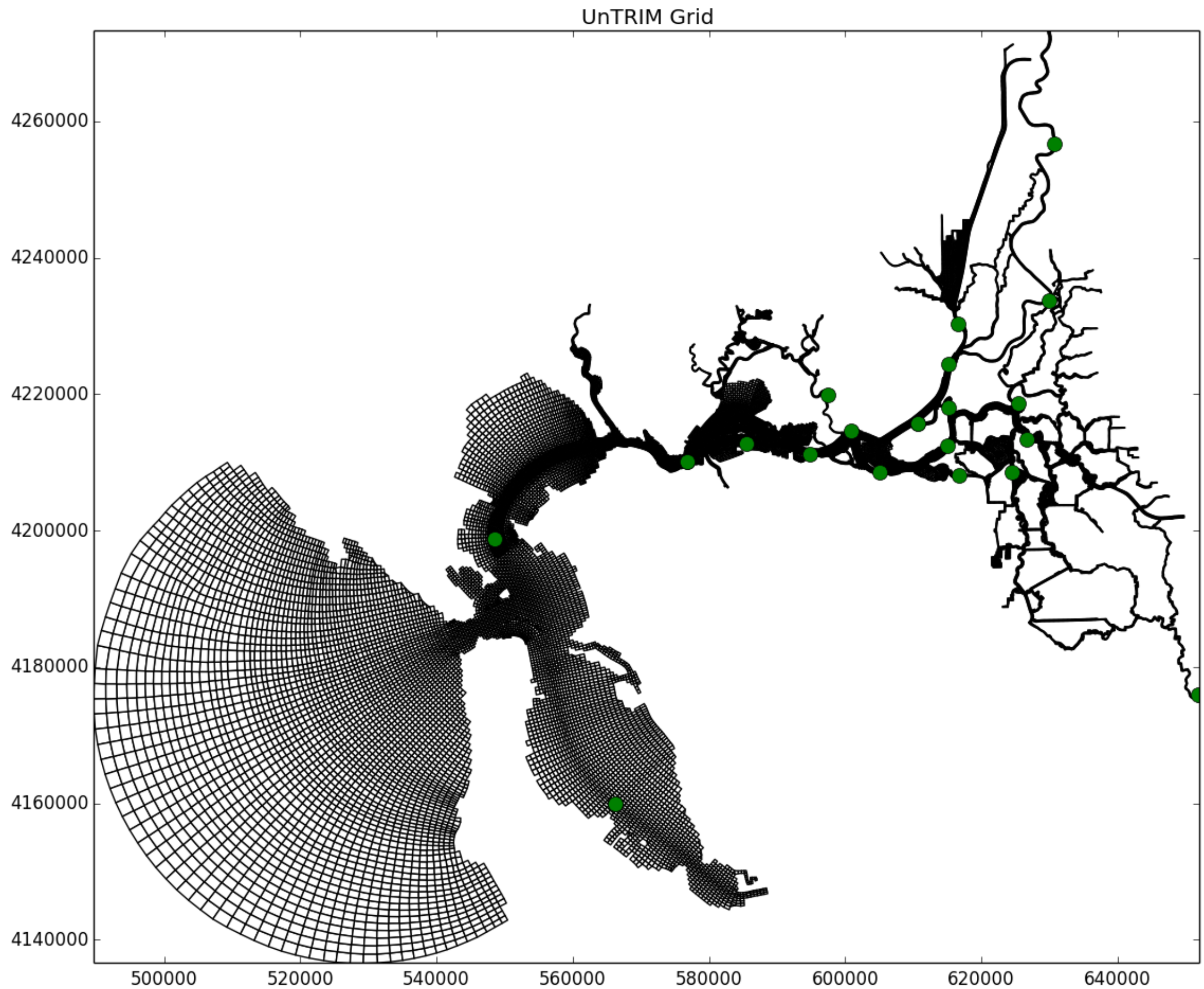

Figure 9-30 UnTRIM model-observed comparison locations for salinity. 2010 calibration.

Table 9-3 UnTRIM salinity error metrics.

Station	MeanE
San Mateo Br Mid	1.489
San Mateo Br Bottom	1.470
Richmond Surface	0.786
Richmond Bottom	0.922
Martinez Surface	-1.286
Martinez Bottom	-2.354
Port Chicago	-0.254
Mallard	-0.409
Mont Sl Nat Steel	0.788
Collisnville	-0.142
Antioch	0.042
Emmaton	0.155
Emmaton Bottom	0.122
SJR at Jersey Pt	0.025
Threemile Sl	0.049
Sac R at Rio Vista	0.001
Cache Sl at Ryer	-0.022
Sac R at Walnut Grove	0.000
Sac R at Freeport	0.008
Dutch Sl	0.066
Holland Cut	0.062
Mok River at SJR	0.018
SJR at Pris Pt	0.032
SJR at Vernalis	0.000

MeanE, Mean Error [PSU] → $1/n \sum_i comp_i - 1/n \sum_i obs_i$
comp = UnTRIM Computed Results
obs = Observed Data

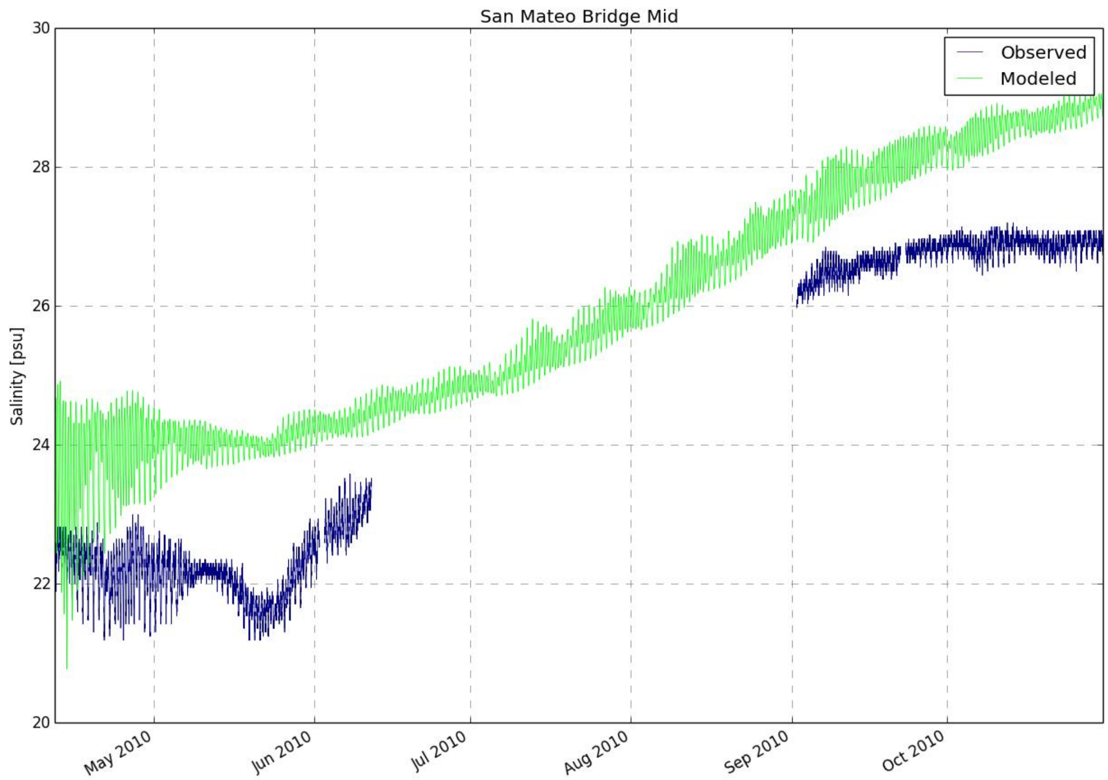

Figure 9-31 UnTRIM results and observed salinity at San Mateo station, surface sensor. 2010 calibration period.

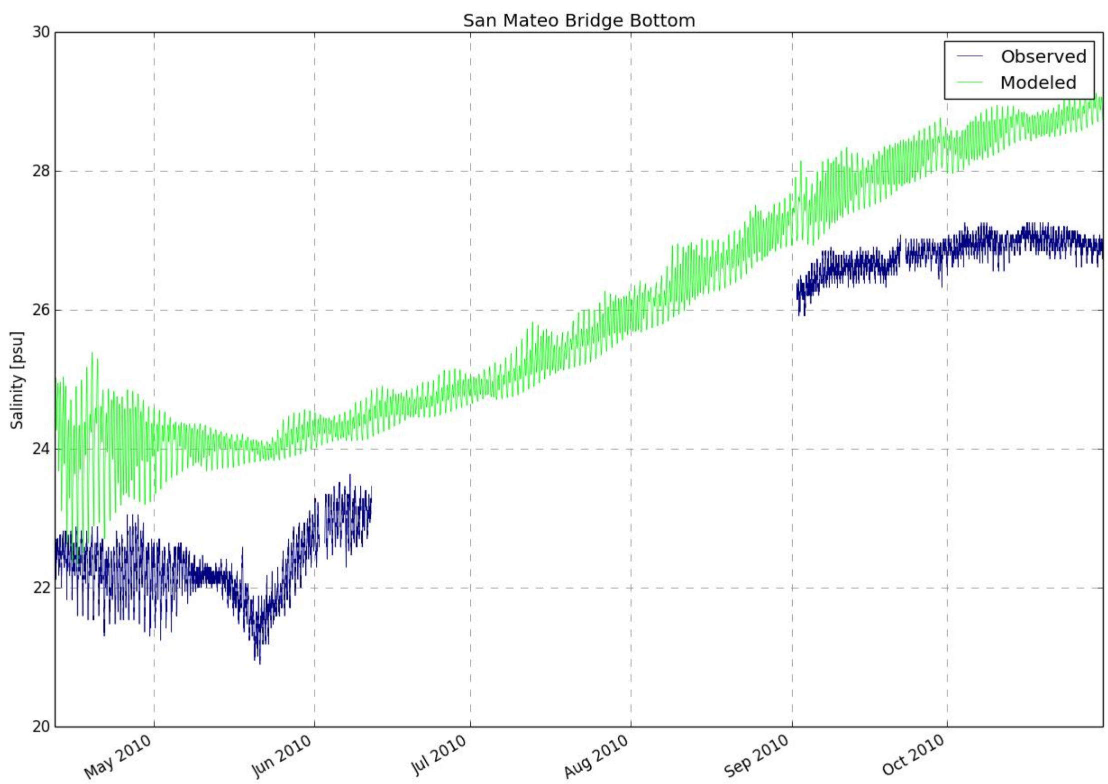

Figure 9-32 UnTRIM results and observed salinity at San Mateo station, bottom sensor. 2010 calibration period.

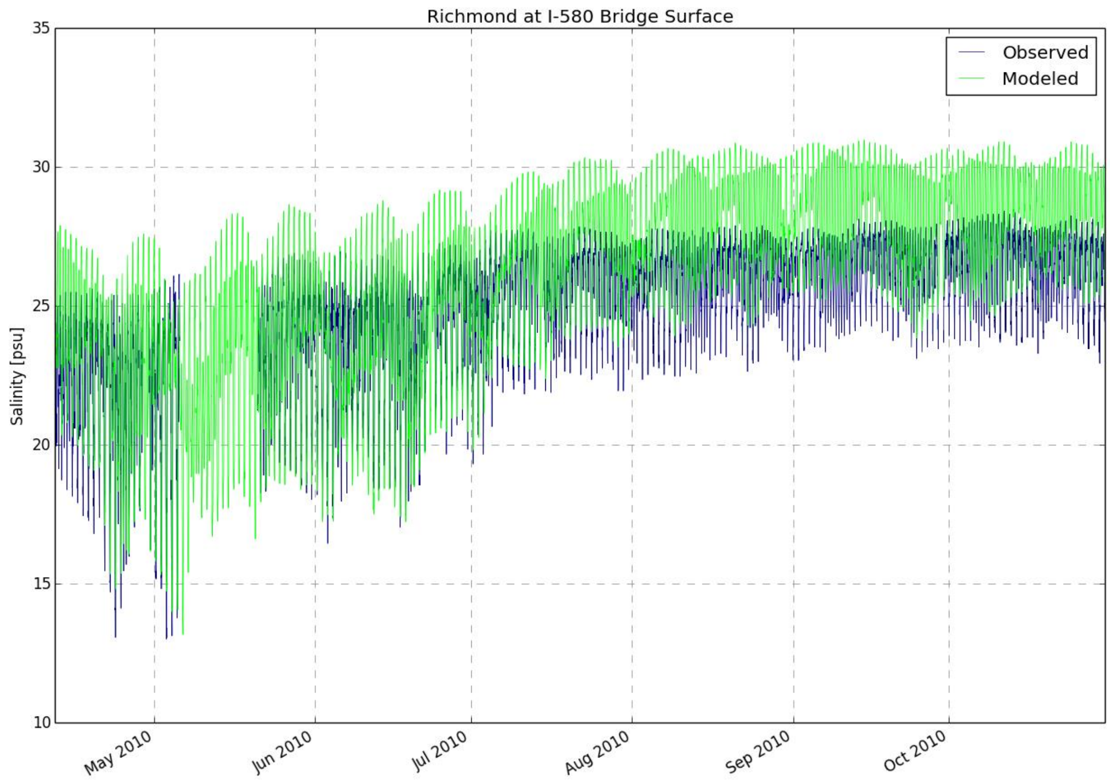

Figure 9-33 UnTRIM results and observed salinity at Richmond station, surface sensor. 2010 calibration period.

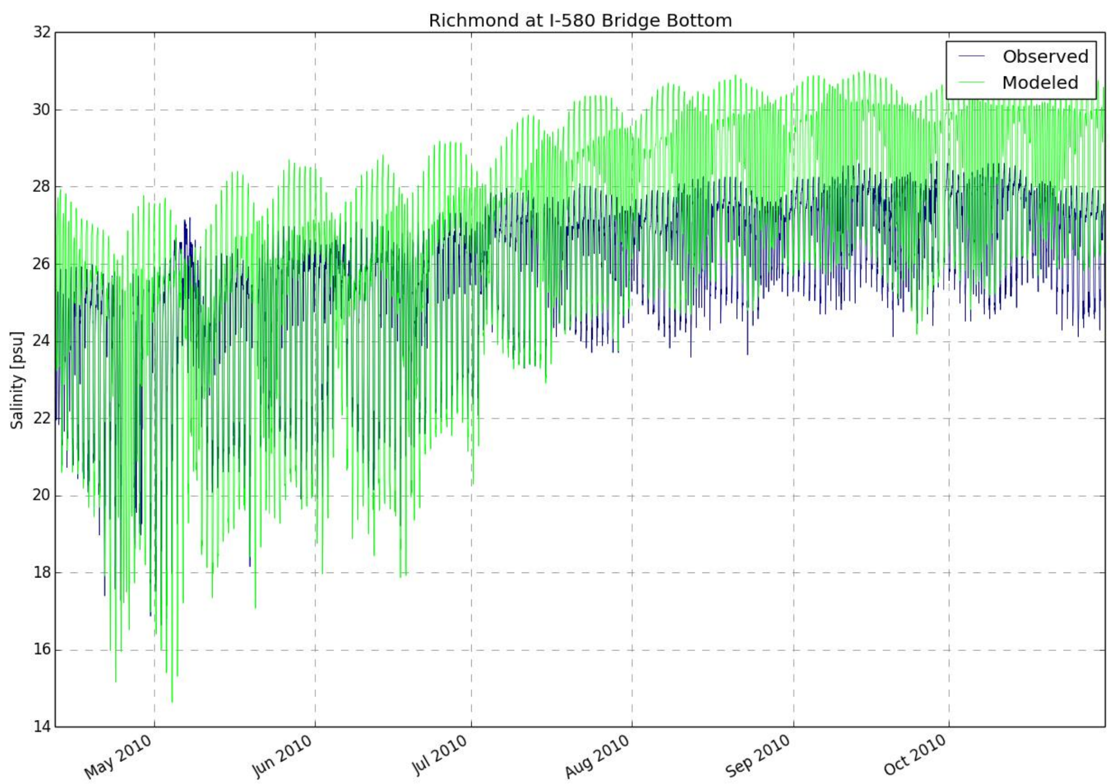

Figure 9-34 UnTRIM results and observed salinity at Richmond station, bottom sensor. 2010 calibration period.

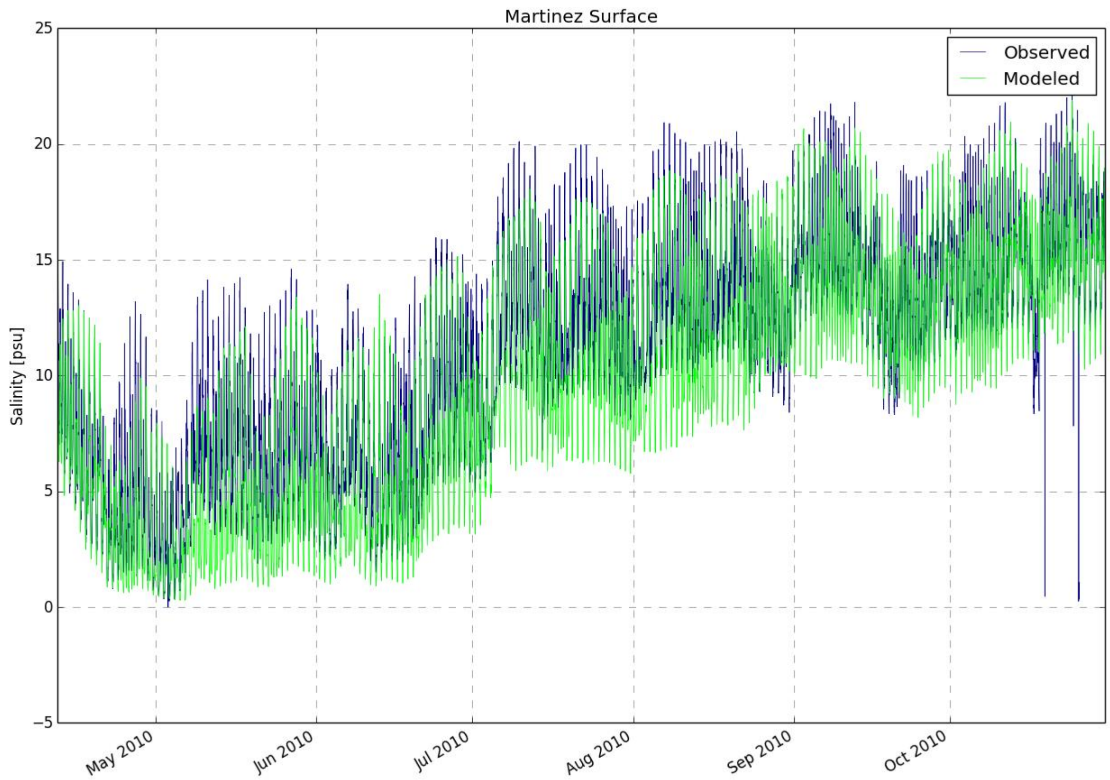

Figure 9-35 UnTRIM results and observed salinity at Martinez station, surface sensor. 2010 calibration period.

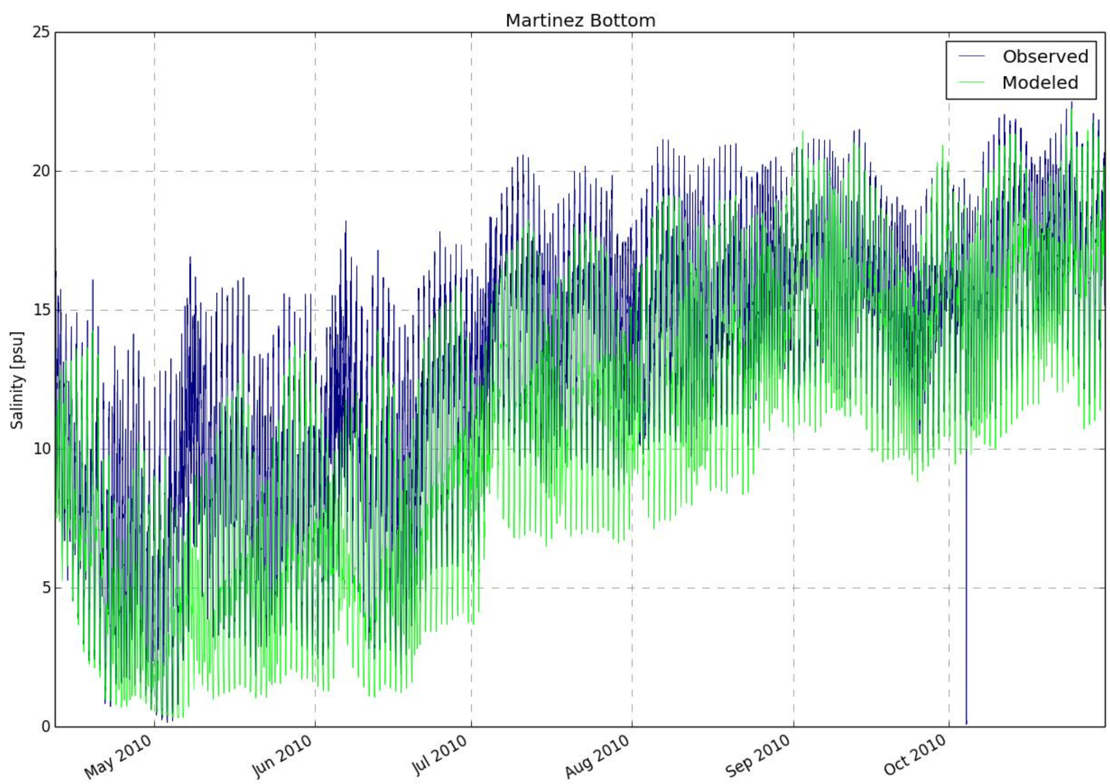

Figure 9-36 UnTRIM results and observed salinity at Martinez station, bottom sensor. 2010 calibration period.

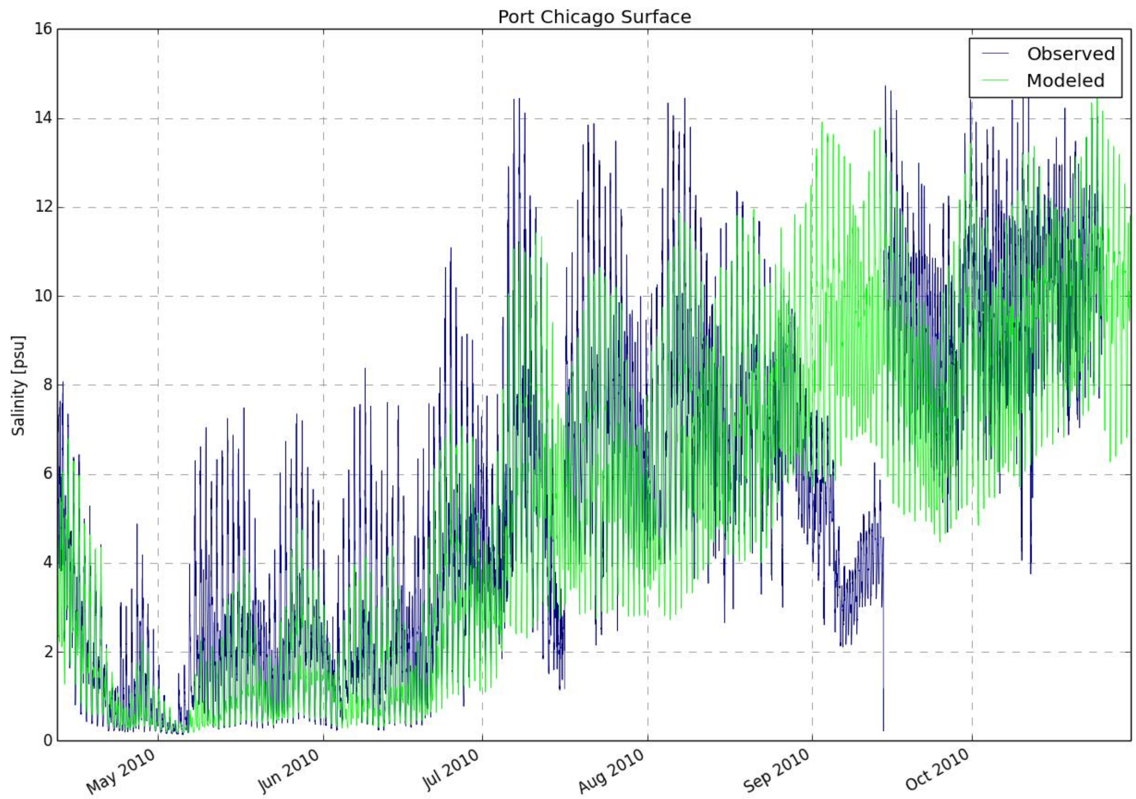

Figure 9-37 UnTRIM results and observed salinity at Port Chicago station. 2010 calibration period.

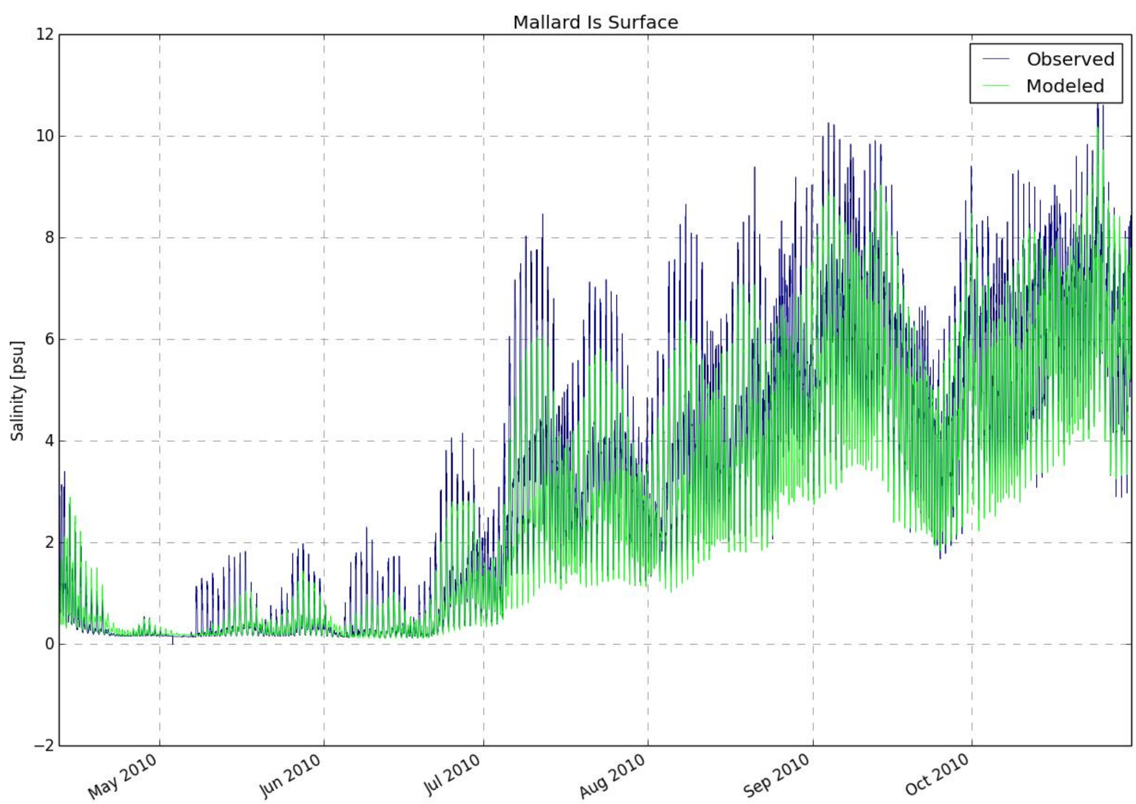

Figure 9-38 UnTRIM results and observed salinity at Mallard Island station. 2010 calibration period.

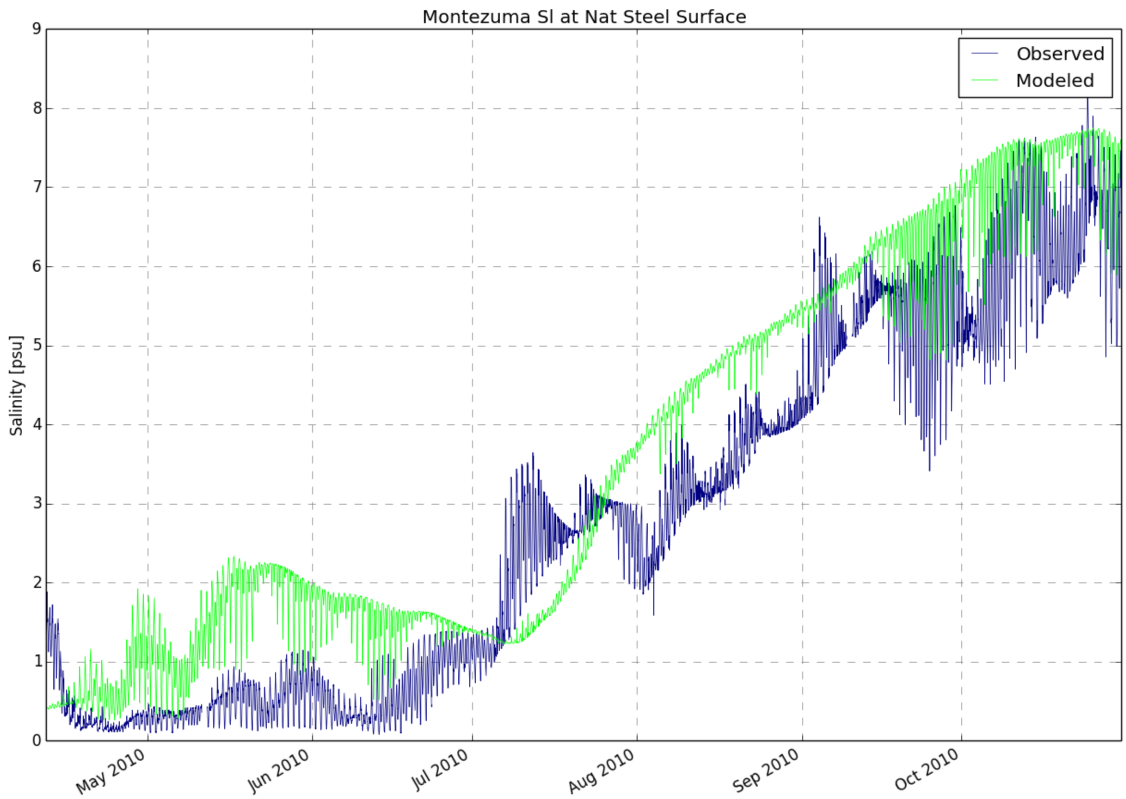

Figure 9-39 UnTRIM results and observed salinity at Montezuma Slough station. 2010 calibration period.

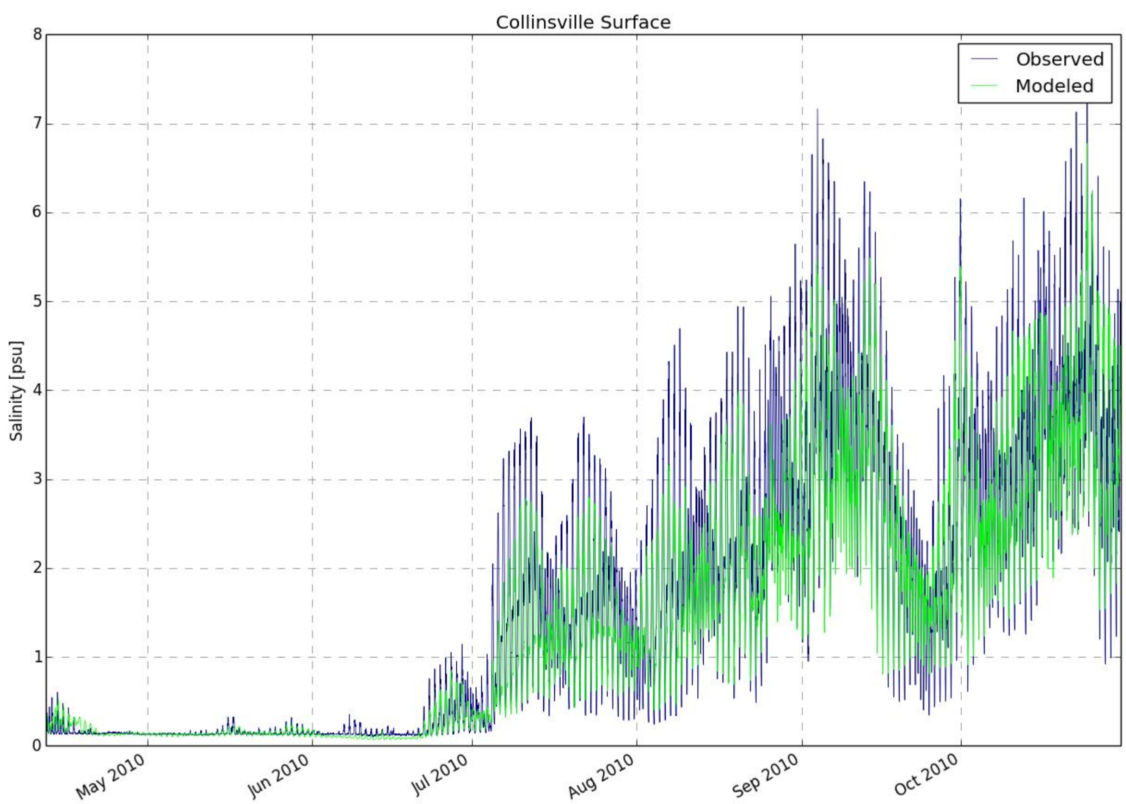

Figure 9-40 UnTRIM results and observed salinity at Collinsville station. 2010 calibration period.

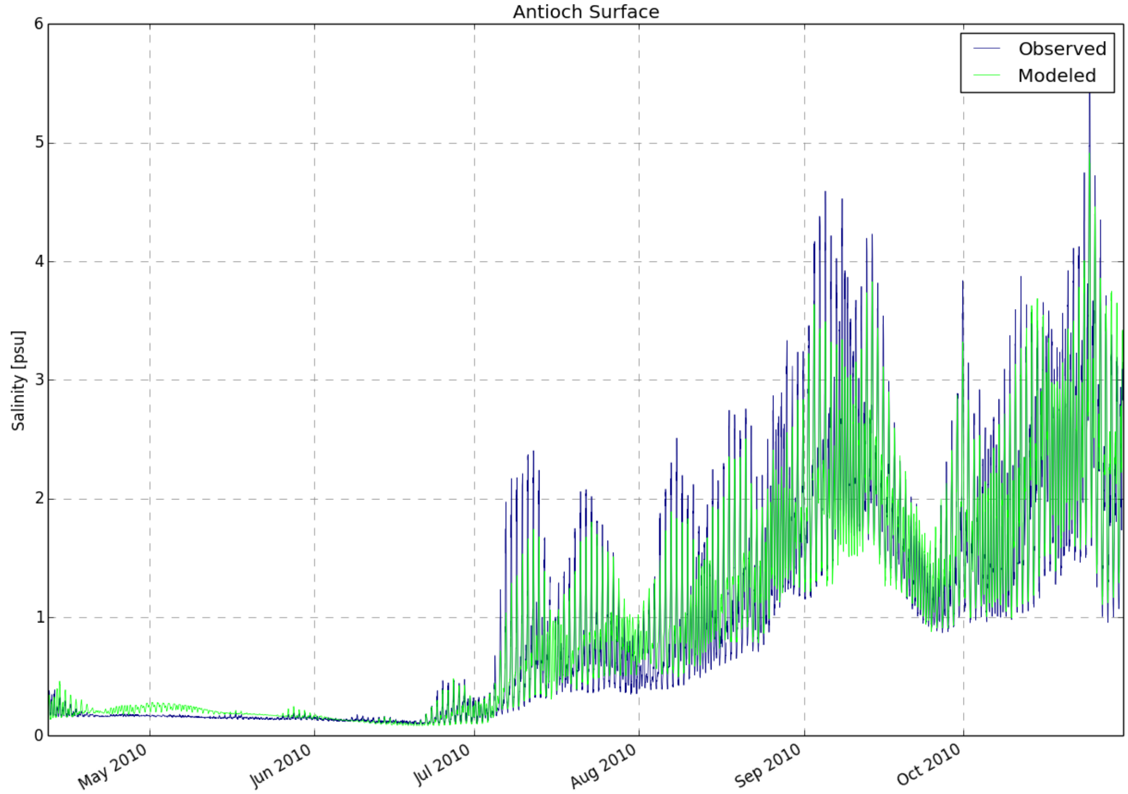

Figure 9-41 UnTRIM results and observed salinity at Antioch station. 2010 calibration period.

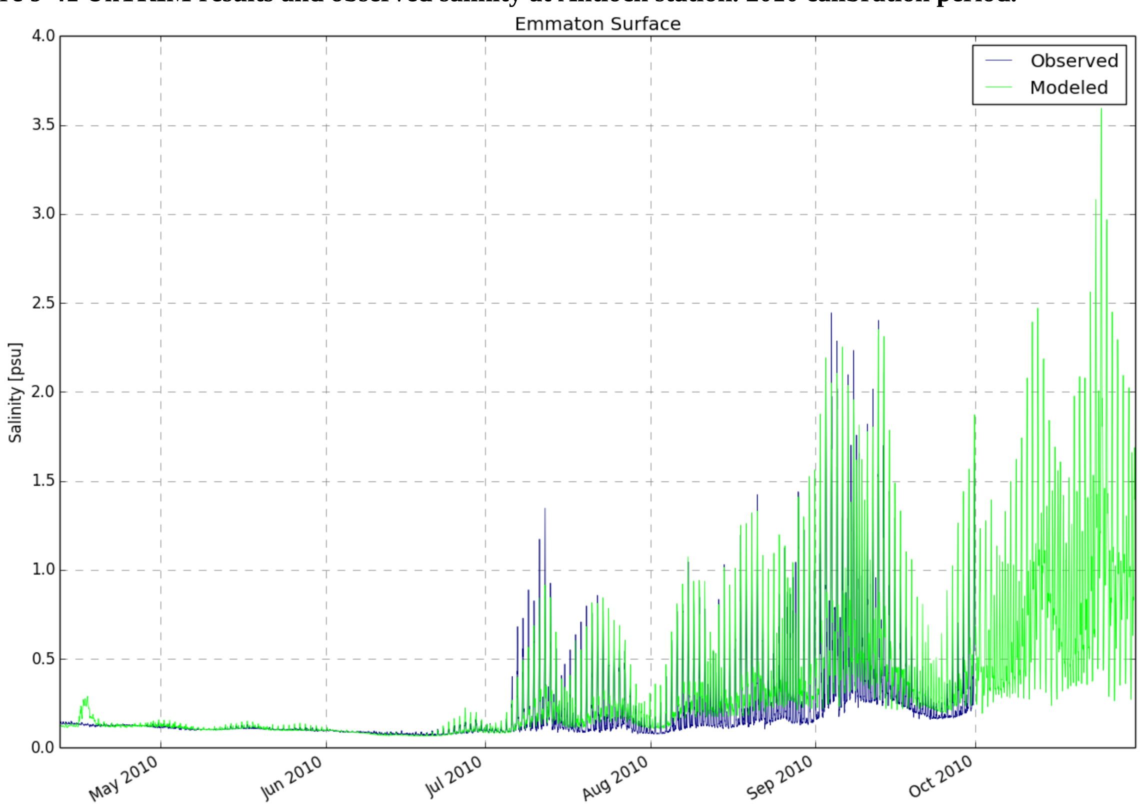

Figure 9-42 UnTRIM results and observed salinity at Emmaton station, surface sensor. 2010 calibration period.

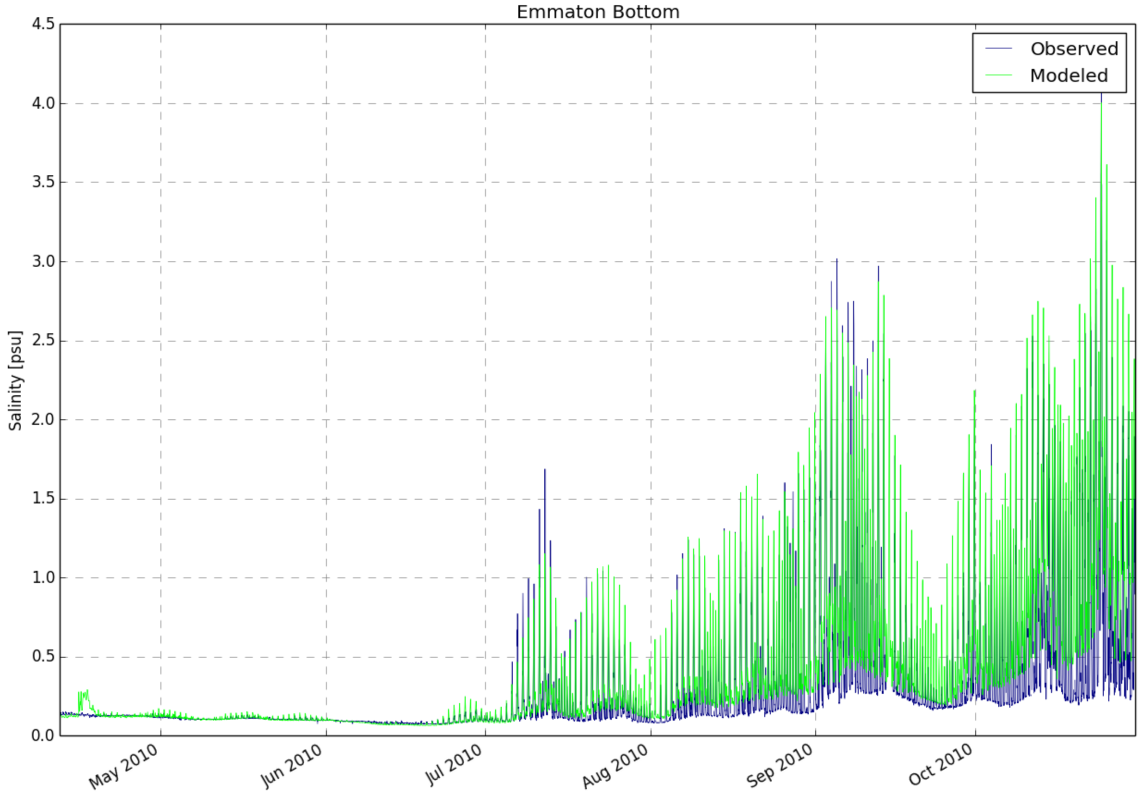

Figure 9-43 UnTRIM results and observed salinity at Emmaton station, bottom sensor. 2010 calibration period.

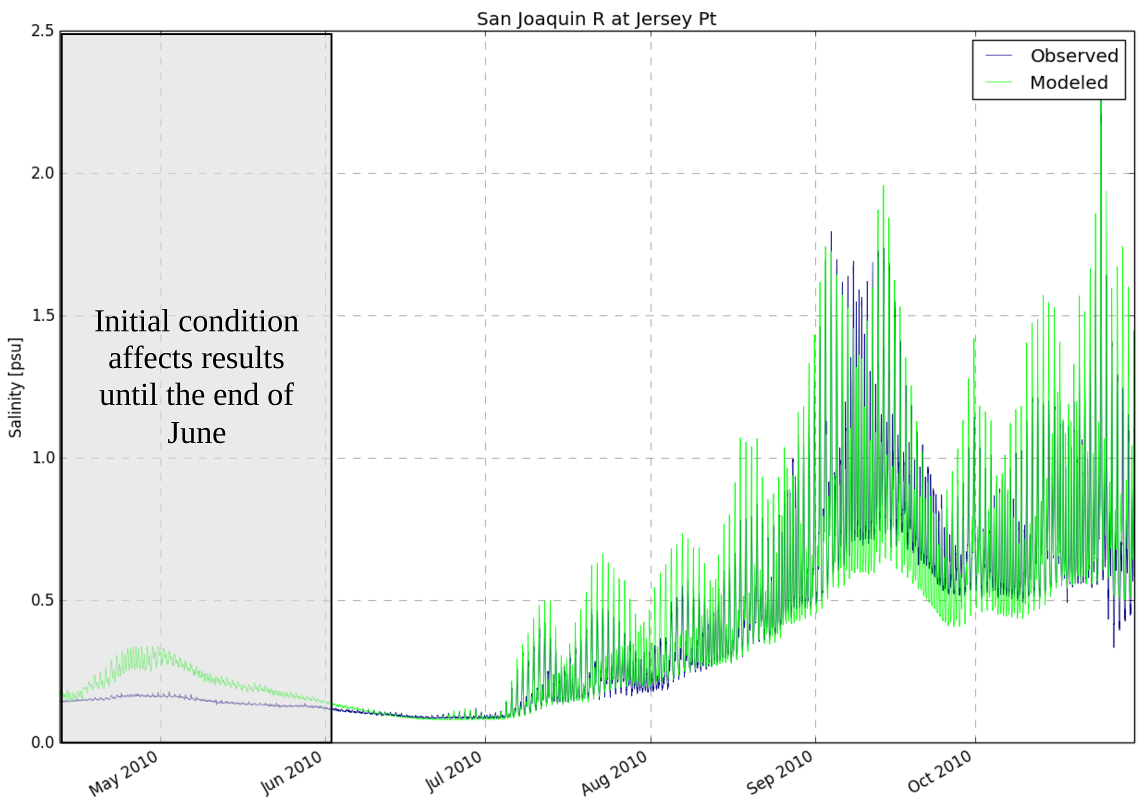

Figure 9-44 UnTRIM results and observed salinity at Jersey Point station. 2010 calibration period.

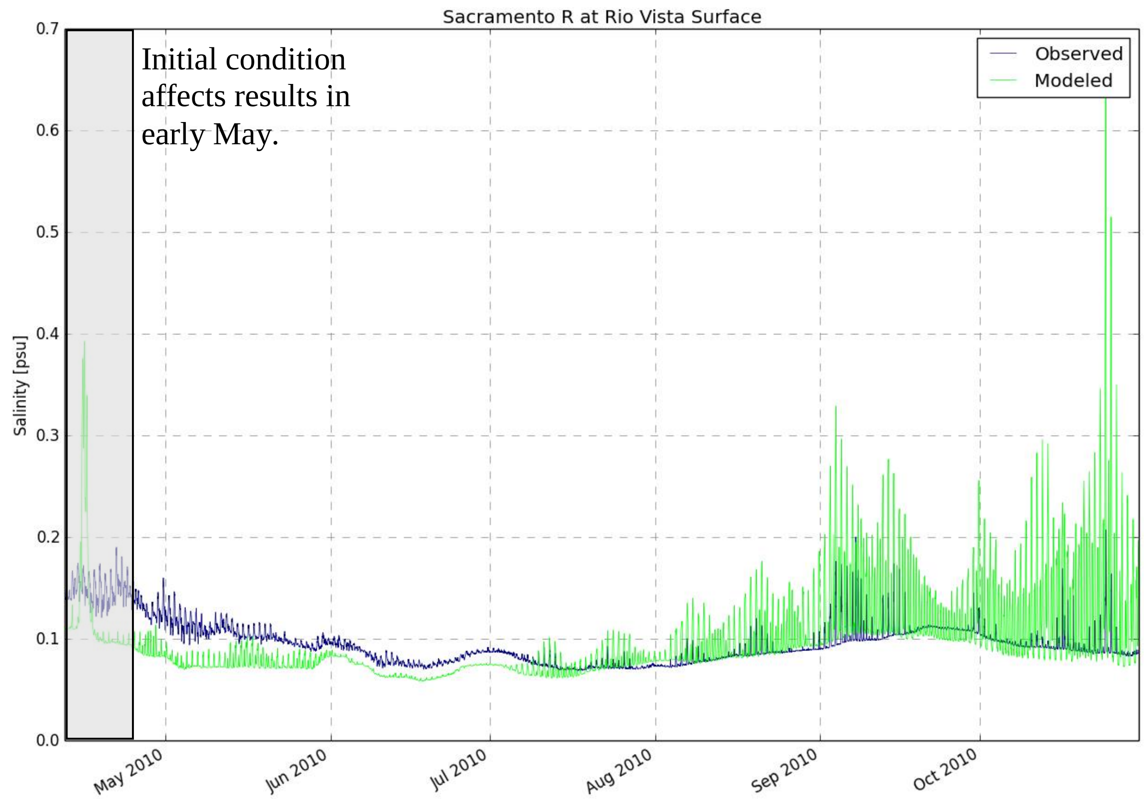

Figure 9-45 UnTRIM results and observed salinity at Rio Vista station. 2010 calibration period.

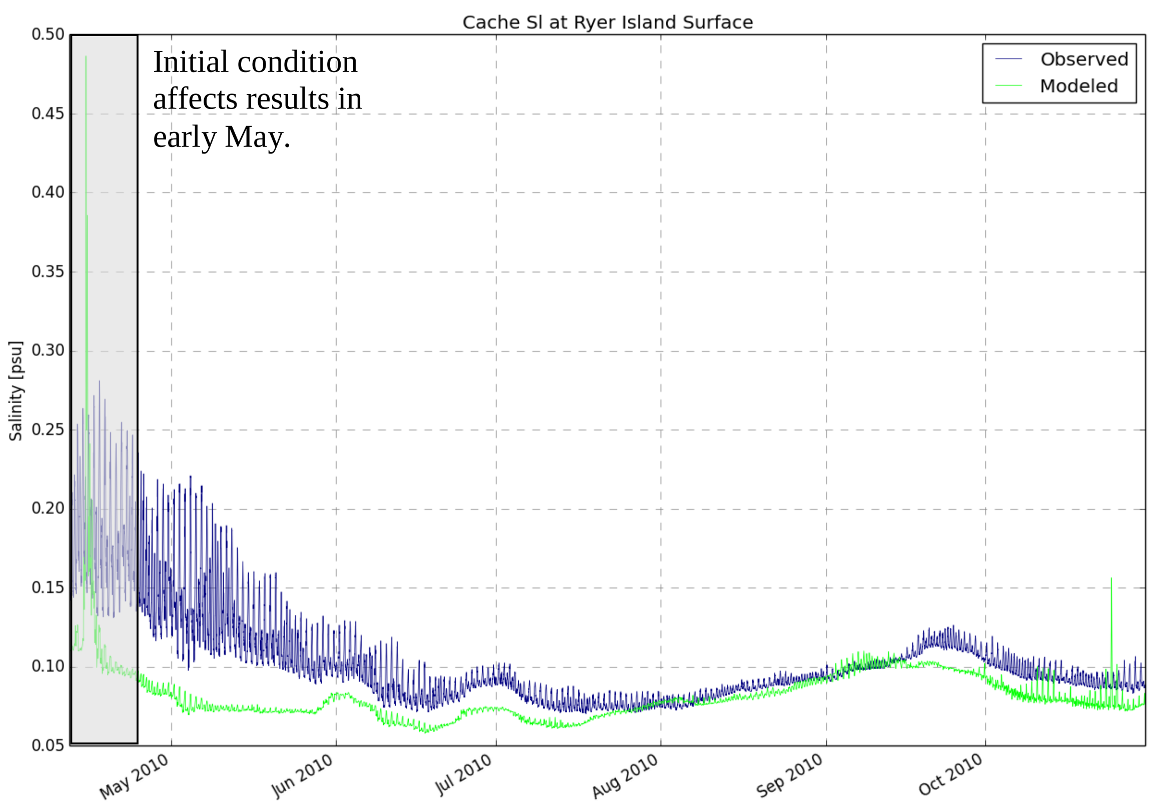

Figure 9-46 UnTRIM results and observed salinity at Cache Slough station. 2010 calibration period.

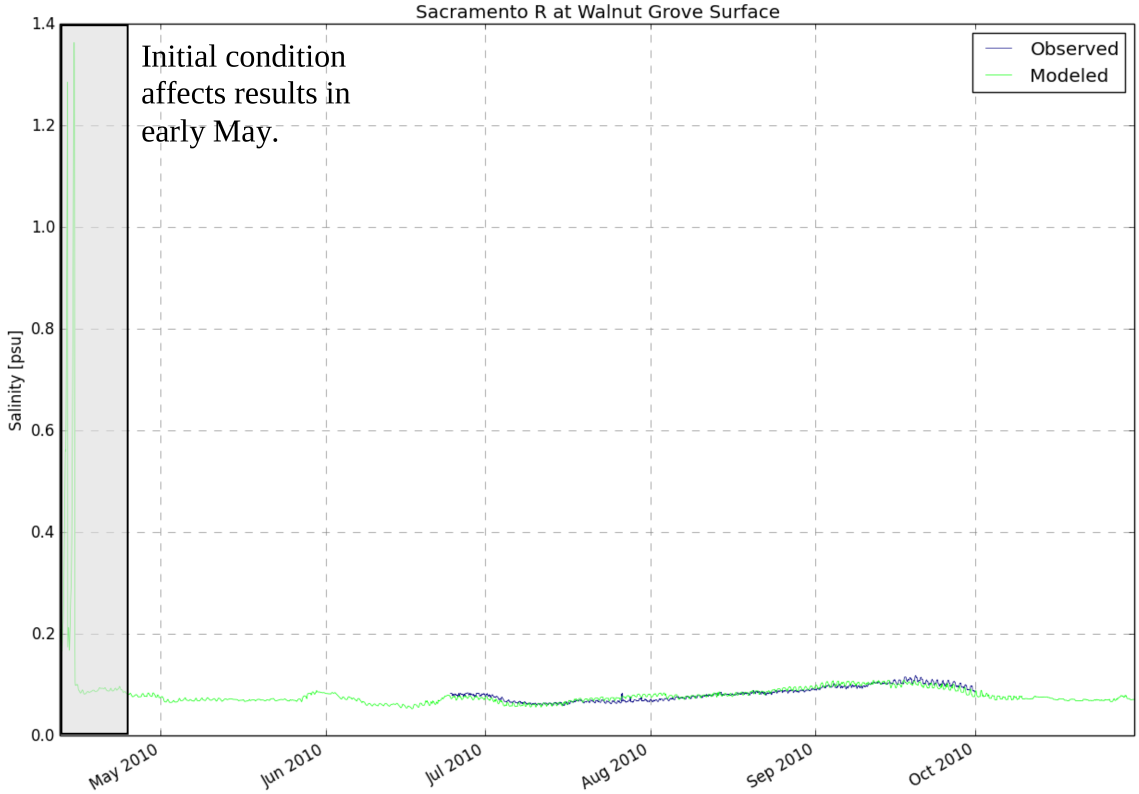

Figure 9-47 UnTRIM results and observed salinity at Walnut Grove station. 2010 calibration period.

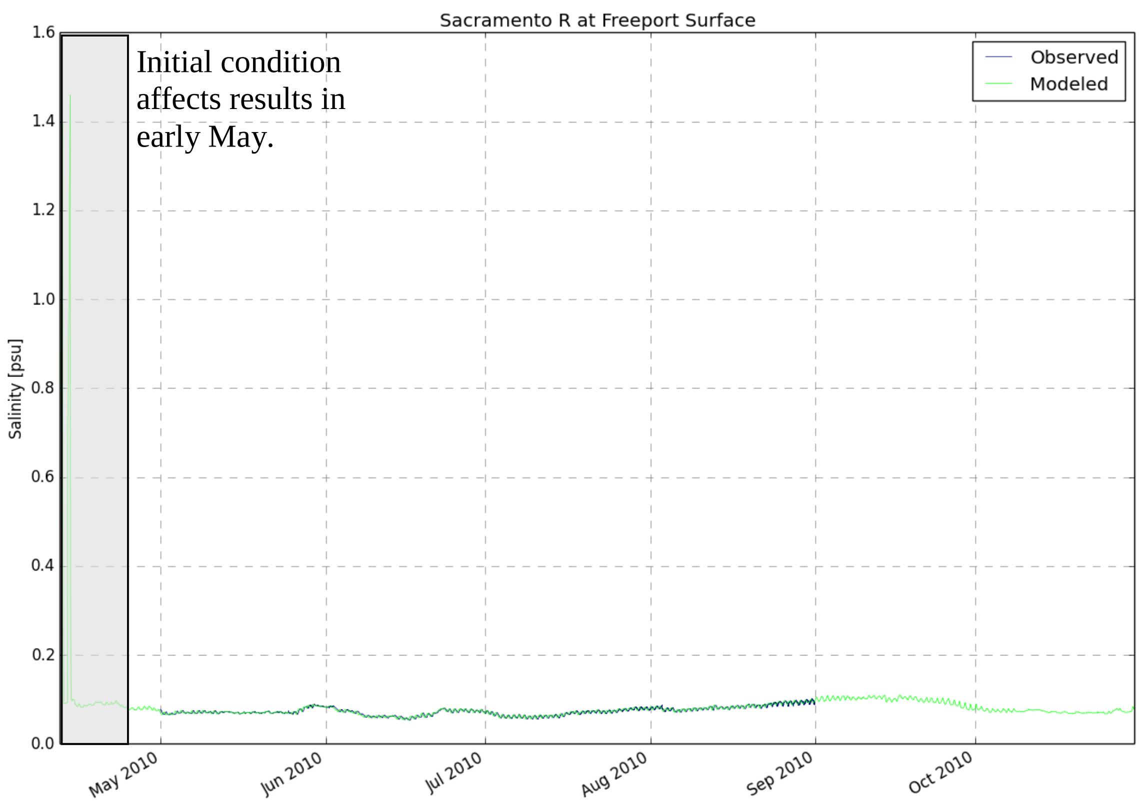

Figure 9-48 UnTRIM results and observed salinity at Freeport station. 2010 calibration period.

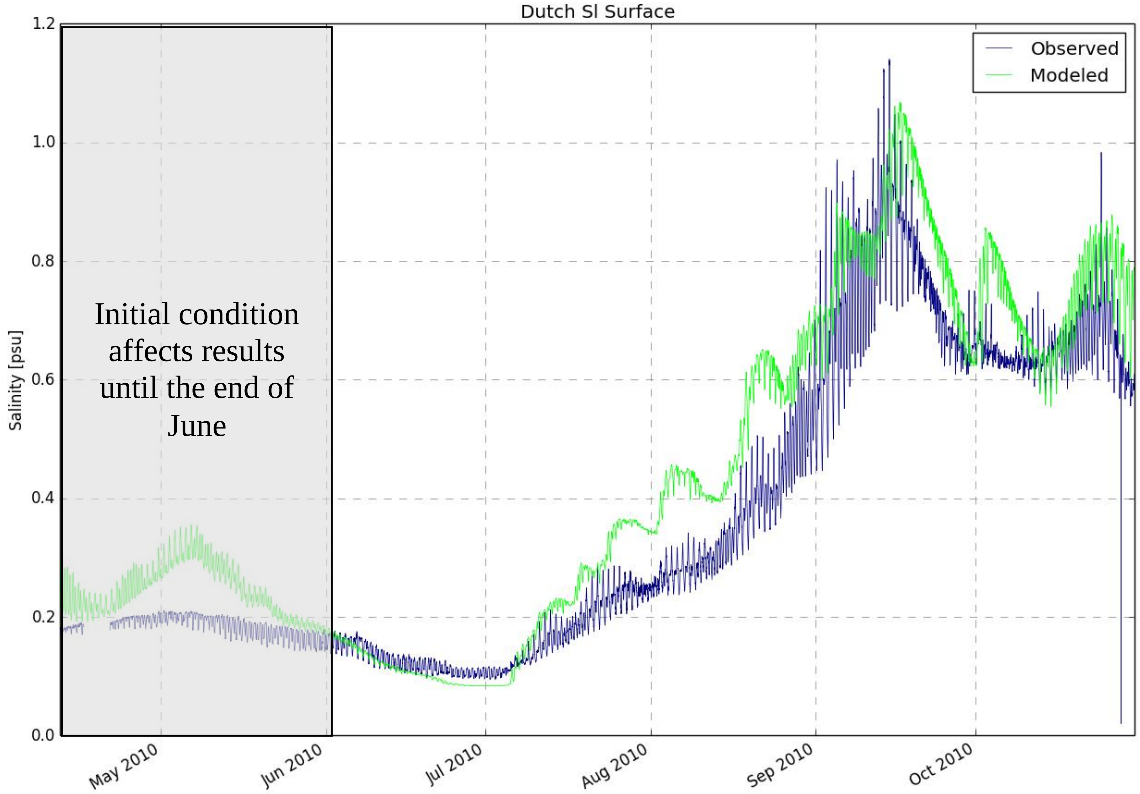

Figure 9-49 UnTRIM results and observed salinity at Dutch Slough station. 2010 calibration period.

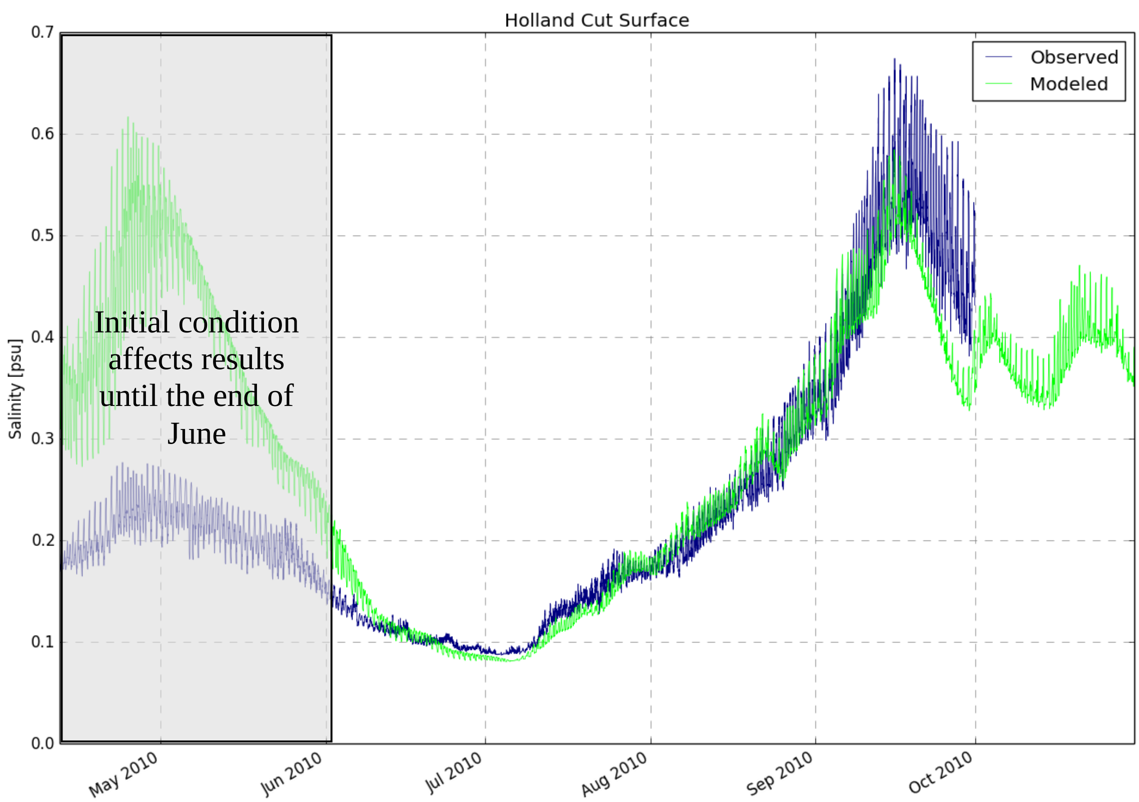

Figure 9-50 UnTRIM results and observed salinity at Holland Cut station. 2010 calibration period.

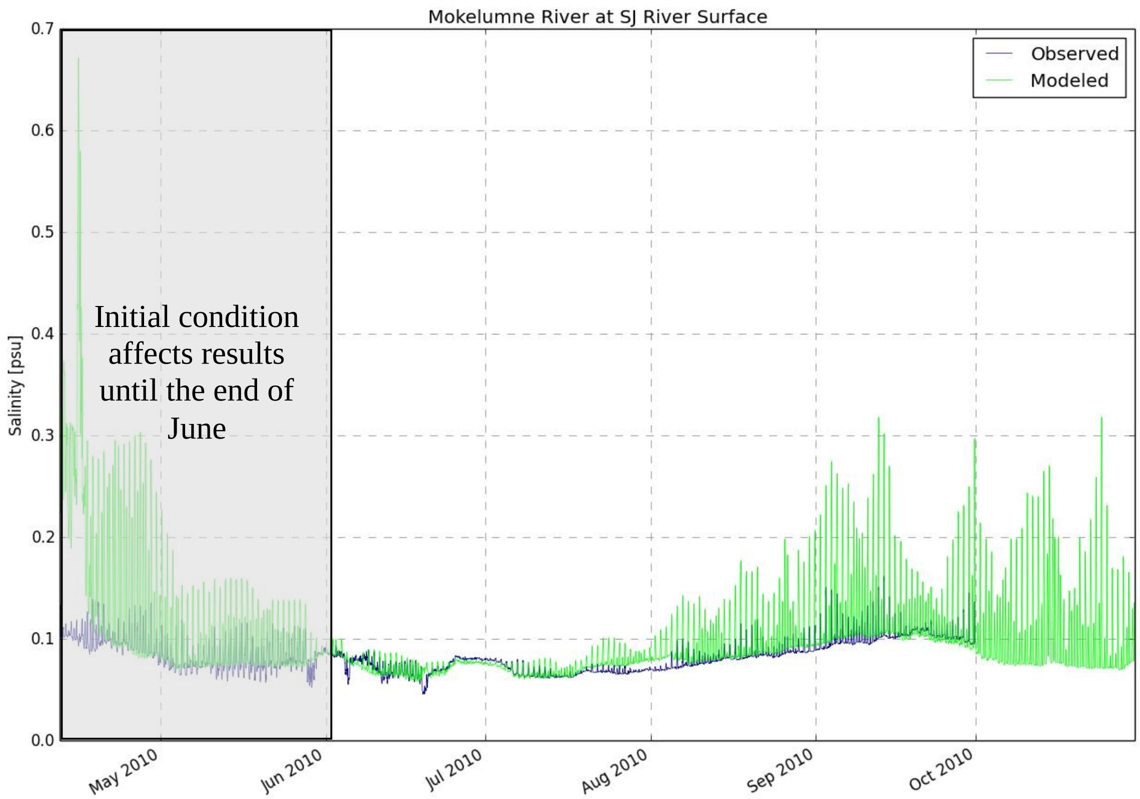

Figure 9-51 UnTRIM results and observed salinity at Mokelumne River at San Joaquin River station. 2010 calibration period.

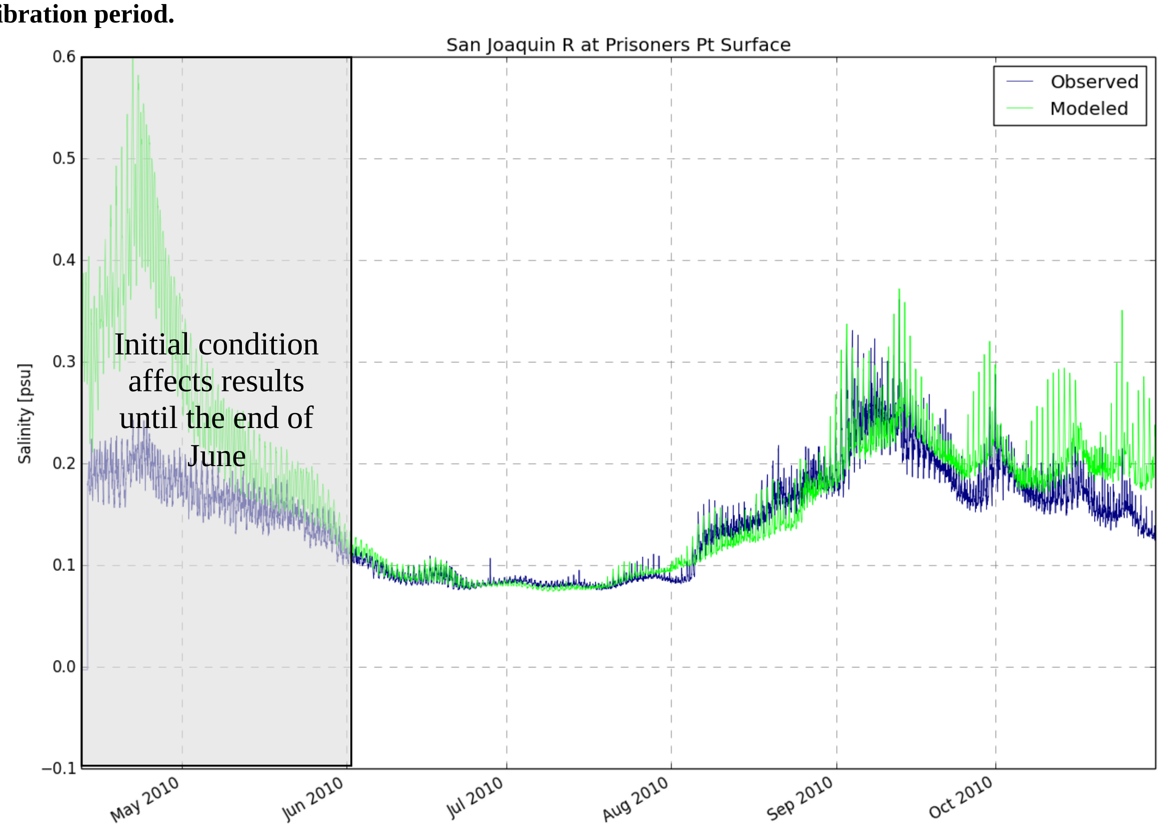

Figure 9-52 UnTRIM results and observed salinity at Prisoners Pt station. 2010 calibration period.

9.4 Polaris Cruise Salinity Transects

USGS Polaris water quality transects are shown in Figure 9-53 through Figure 9-59. In each plot, the observed Bay-Delta salinities are shown in the top subplot. UnTRIM model results are shown for the corresponding times and locations in the bottom subplot. The path of the transect is shown in Figure 4-1 and extends from the Golden Gate (Station 19, data shown at the far left of each plot) to Rio Vista (data shown on the far right of each plot). Salinity contours are shown in intervals of 2 PSU.

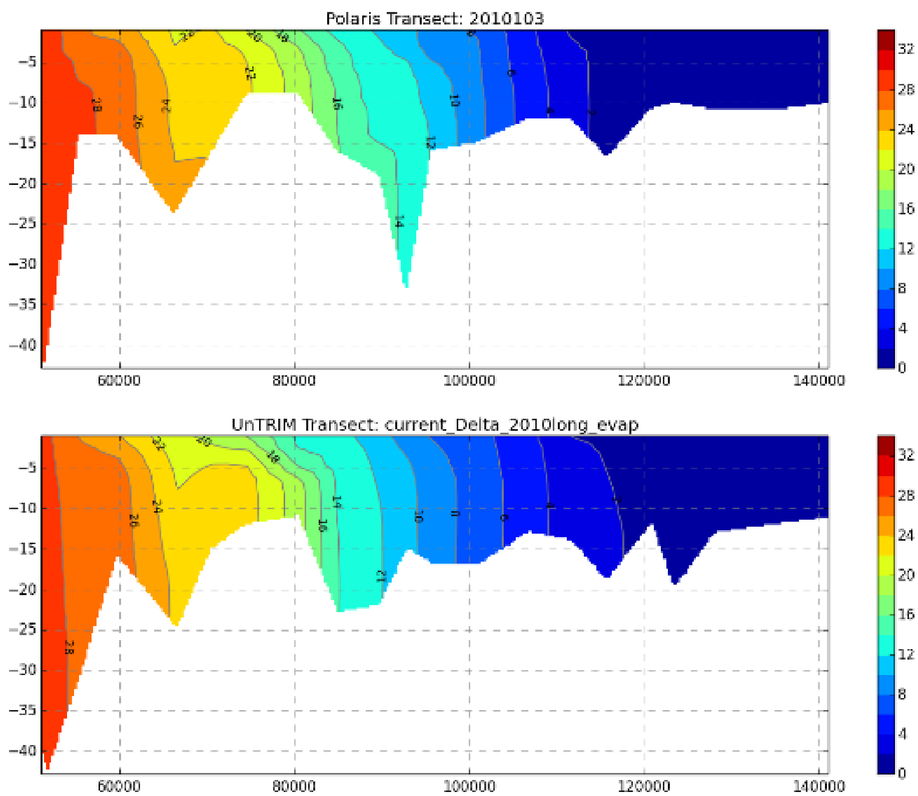

Figure 9-53 Polaris salinity transect (top) and corresponding UnTRIM modeled salinity for 13 April 2010 cruise. Transect extends from the Golden Gate on the left to Rio Vista on the right.

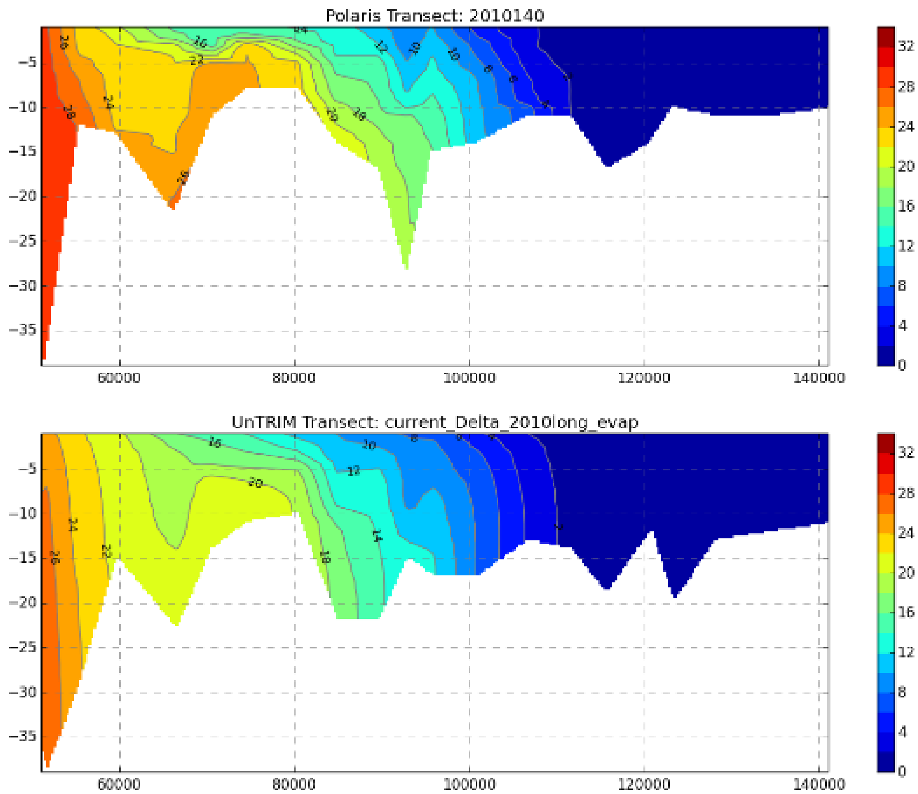

Figure 9-54 Polaris salinity transect (top) and corresponding UnTRIM modeled salinity for 20 May 2010 cruise. Transect extends from the Golden Gate on the left to Rio Vista on the right.

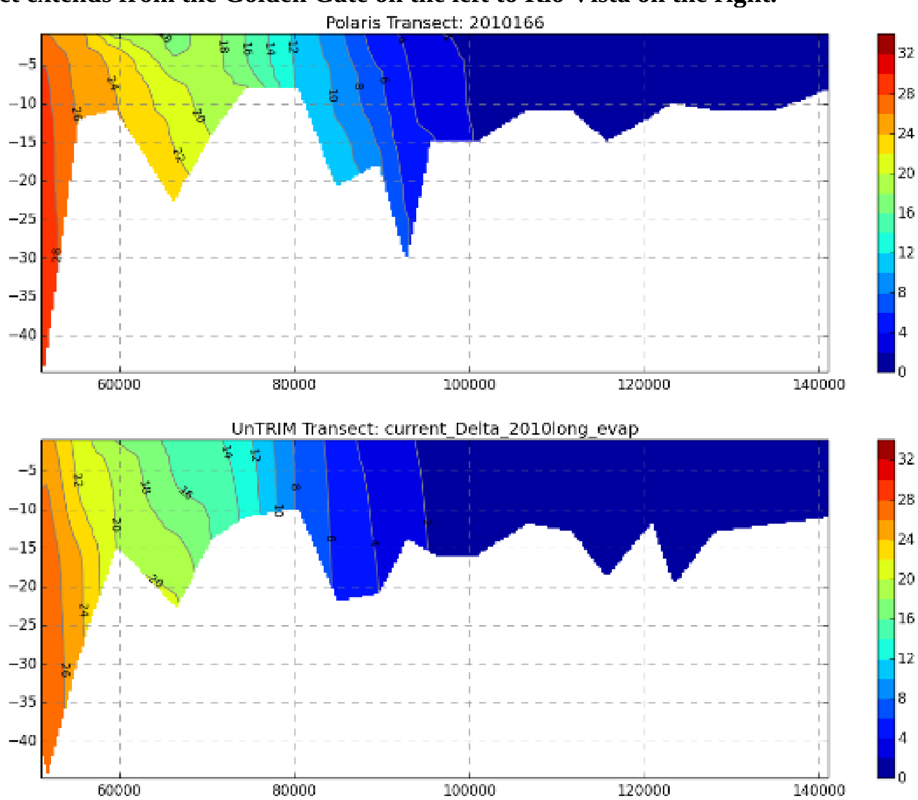

Figure 9-55 Polaris salinity transect (top) and corresponding UnTRIM modeled salinity for 15 June 2010 cruise. Transect extends from the Golden Gate on the left to Rio Vista on the right.

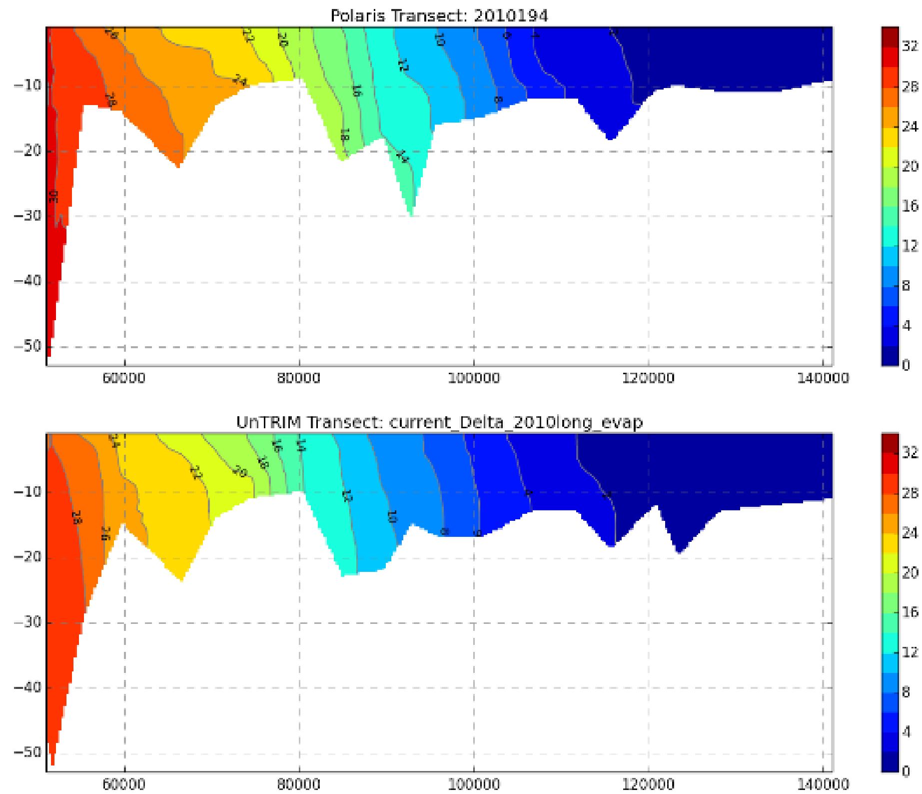

Figure 9-56 Polaris salinity transect (top) and corresponding UnTRIM modeled salinity for 13 June 2010 cruise. Transect extends from the Golden Gate on the left to Rio Vista on the right.

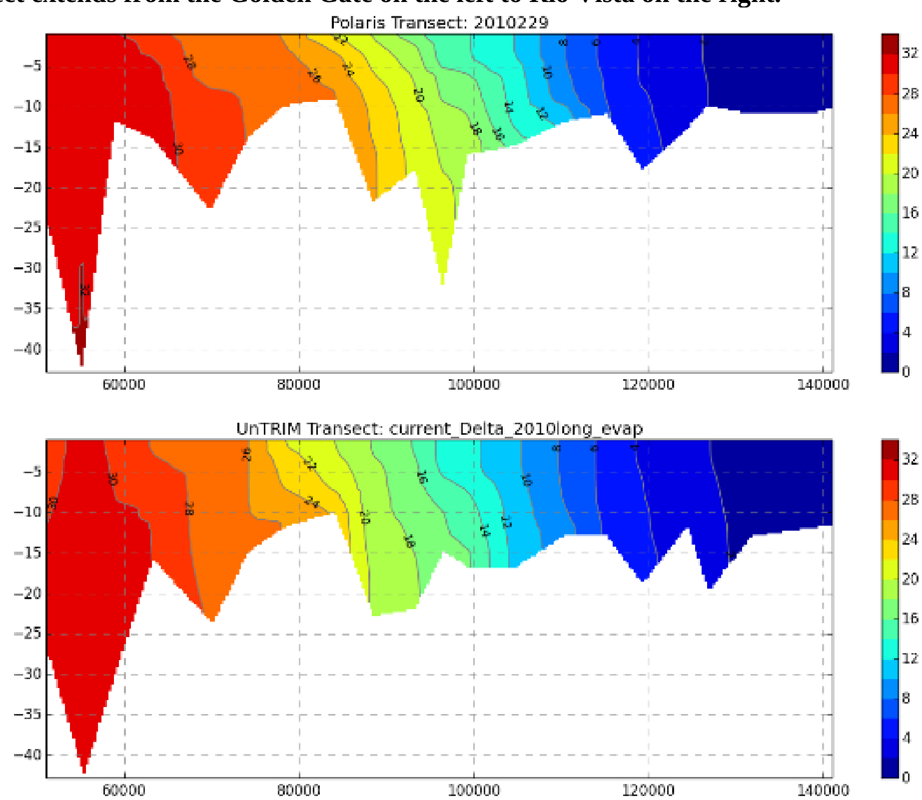

Figure 9-57 Polaris salinity transect (top) and corresponding UnTRIM modeled salinity for 17 August 2010 cruise. Transect extends from the Golden Gate on the left to Rio Vista on the right.

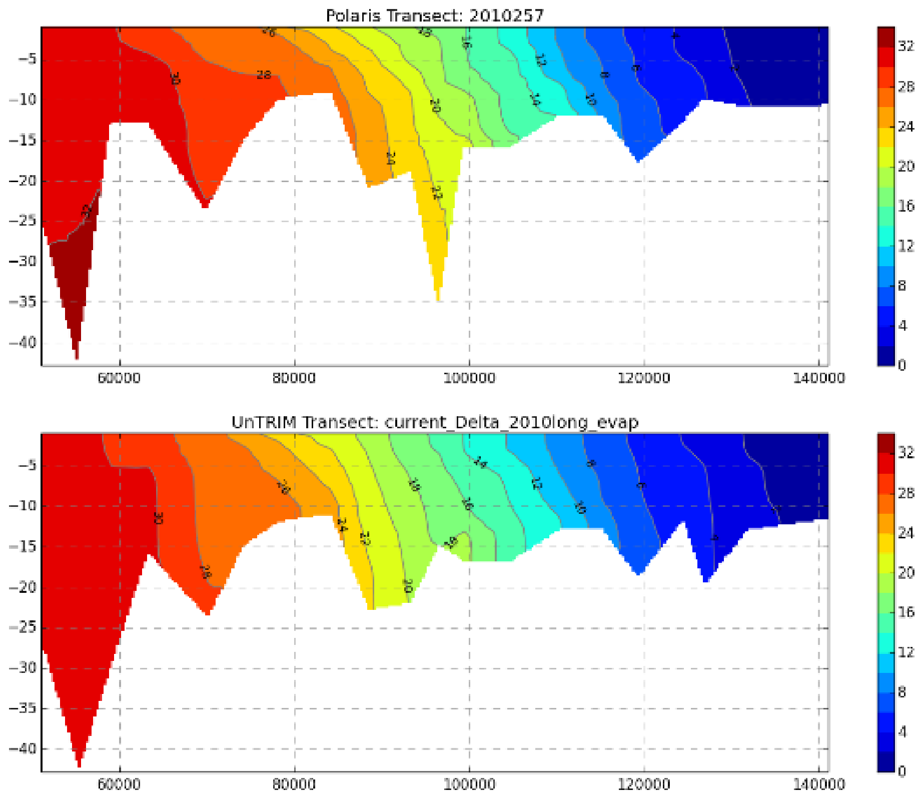

Figure 9-58 Polaris salinity transect (top) and corresponding UnTRIM modeled salinity for 14 September 2010 cruise. Transect extends from the Golden Gate on the left to Rio Vista on the right.

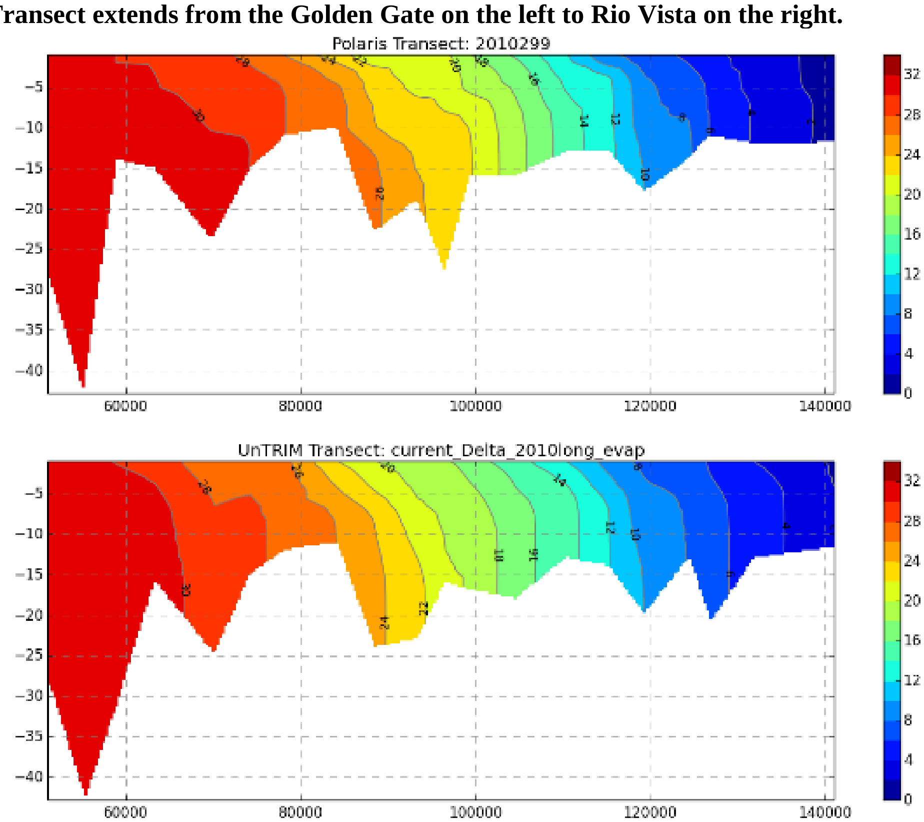

Figure 9-59 Polaris salinity transect (top) and corresponding UnTRIM modeled salinity for 26 October 2010 cruise. Transect extends from the Golden Gate on the left to Rio Vista on the right.

10 Appendix B: Contemporary Bay-Delta Model Calibration Data: 1994 Modeling Period

10.1 Entrapment Zone Study Salinity Transects

Entrapment zone salinity transects are shown in Figure 10-1 through Figure 10-17. In each plot, the observed Bay-Delta salinities are shown in the top subplot. UnTRIM model results are shown for the corresponding times and locations in the bottom subplot. The path of the transect extends approximately from Port Chicago (data shown at the far left of each plot) to Emmaton (data shown on the far right of each plot). Salinity contours are shown in intervals of 2 PSU.

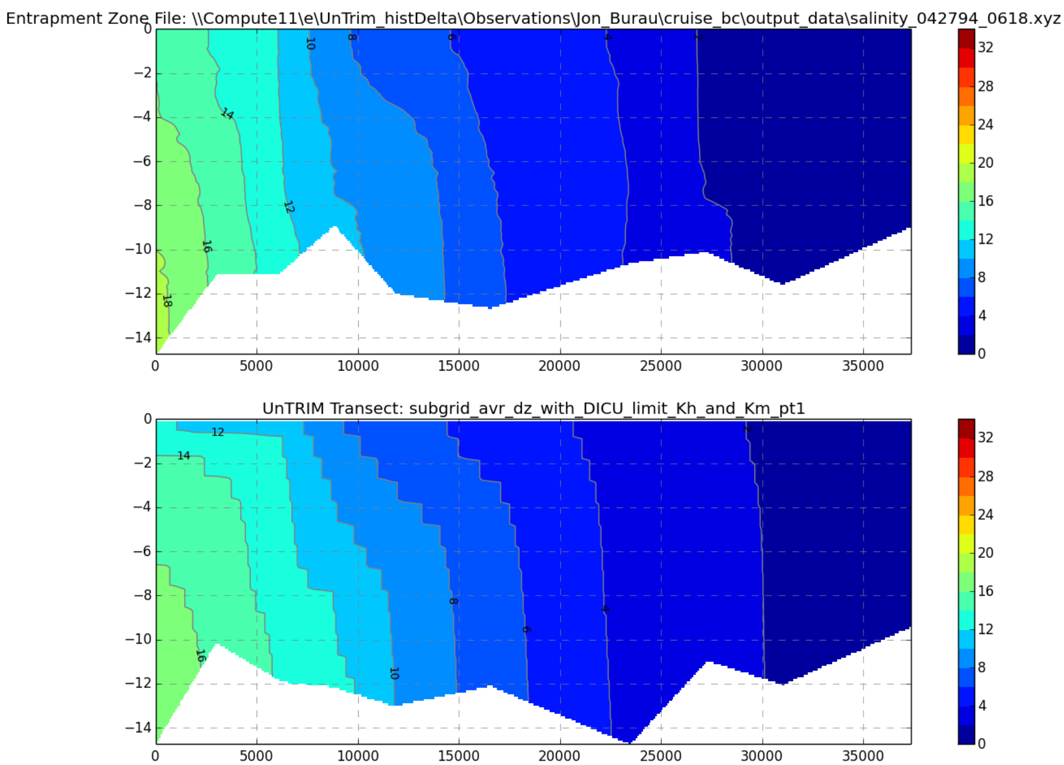

Figure 10-1 Entrapment Zone Study salinity transect (top) and corresponding UnTRIM modeled salinity for 27 April 1994 06:18. Transect extends from Port Chicago on the left to Emmaton on the right.

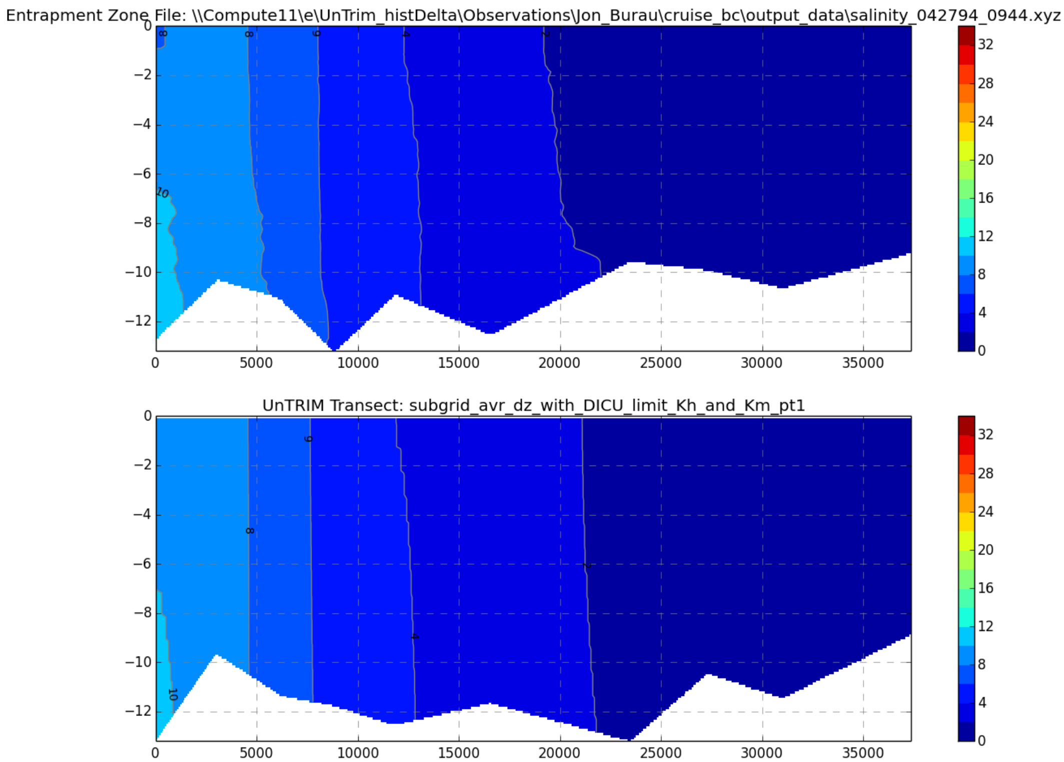

Figure 10-2 Entrapment Zone Study salinity transect (top) and corresponding UnTRIM modeled salinity for 27 April 1994 09:44. Transect extends from Port Chicago on the left to Emmaton on the right.

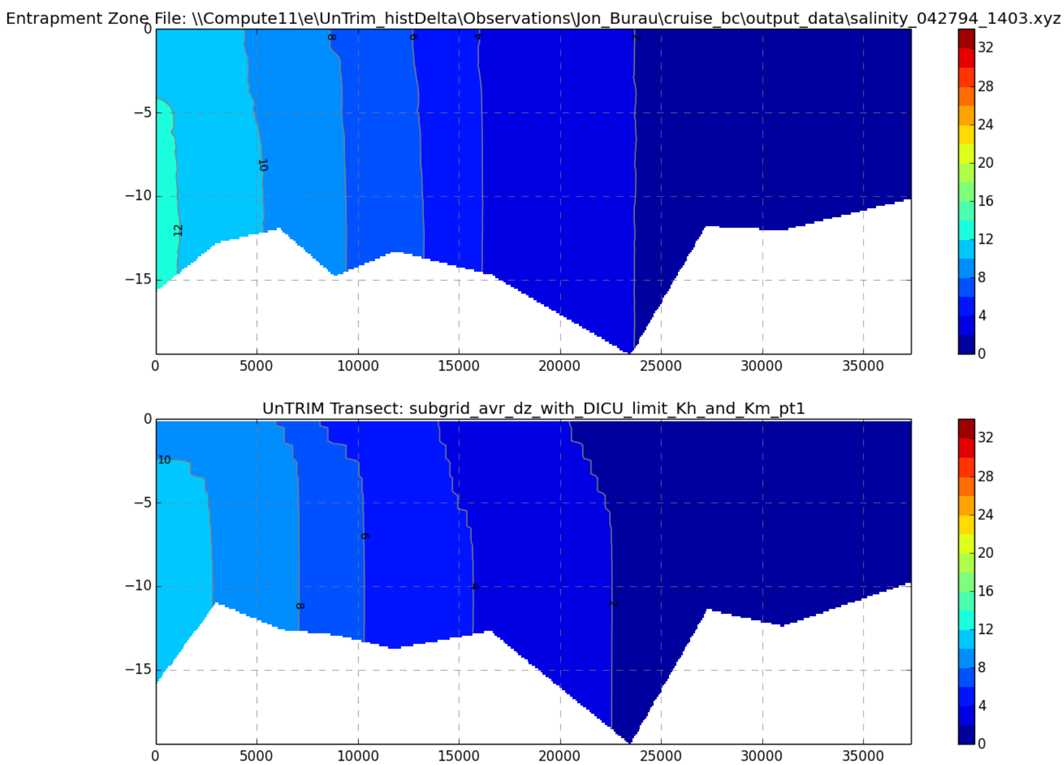

Figure 10-3 Entrapment Zone Study salinity transect (top) and corresponding UnTRIM modeled salinity for 27 April 1994 14:13. Transect extends from Port Chicago on the left to Emmaton on the right.

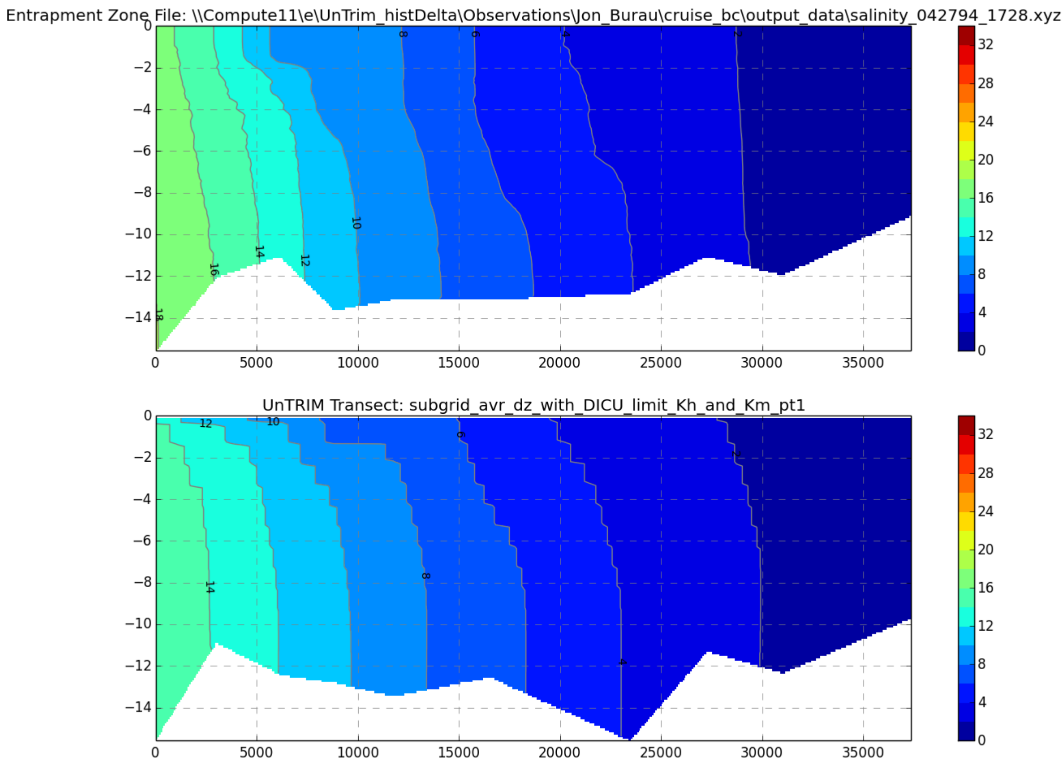

Figure 10-4 Entrapment Zone Study salinity transect (top) and corresponding UnTRIM modeled salinity for 27 April 1994 17:28. Transect extends from Port Chicago on the left to Emmaton on the right.

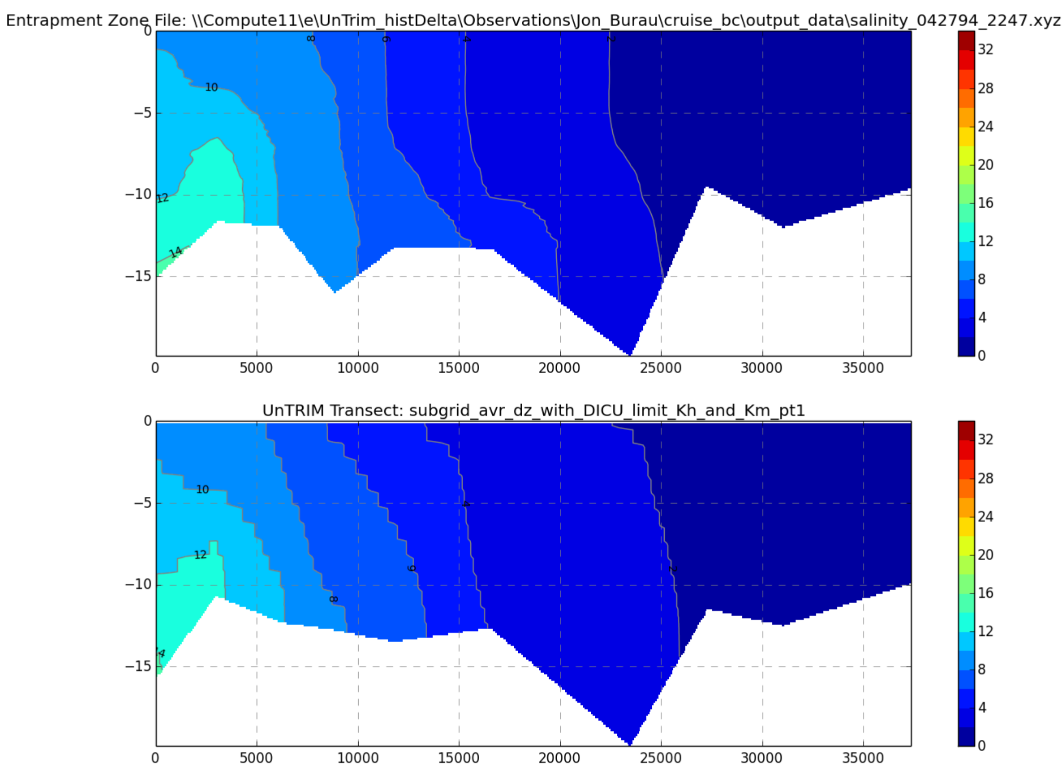

Figure 10-5 Entrapment Zone Study salinity transect (top) and corresponding UnTRIM modeled salinity for 27 April 1994 22:47. Transect extends from Port Chicago on the left to Emmaton on the right.

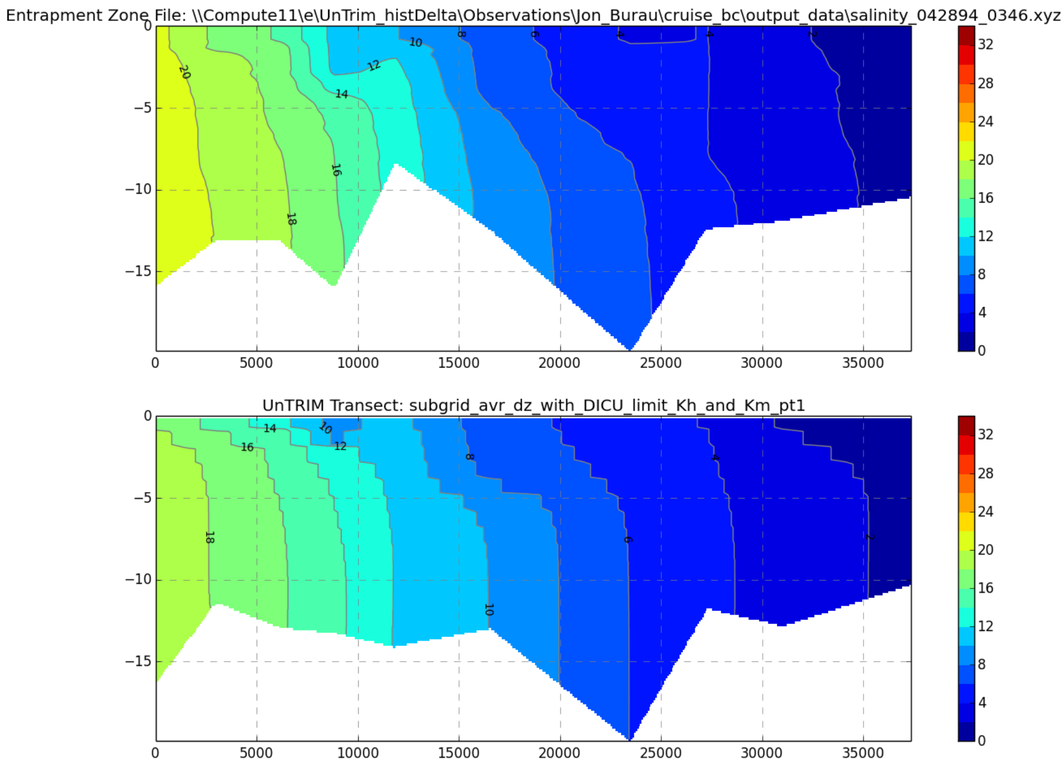

Figure 10-6 Entrapment Zone Study salinity transect (top) and corresponding UnTRIM modeled salinity for 28 April 1994 03:46. Transect extends from Port Chicago on the left to Emmaton on the right.

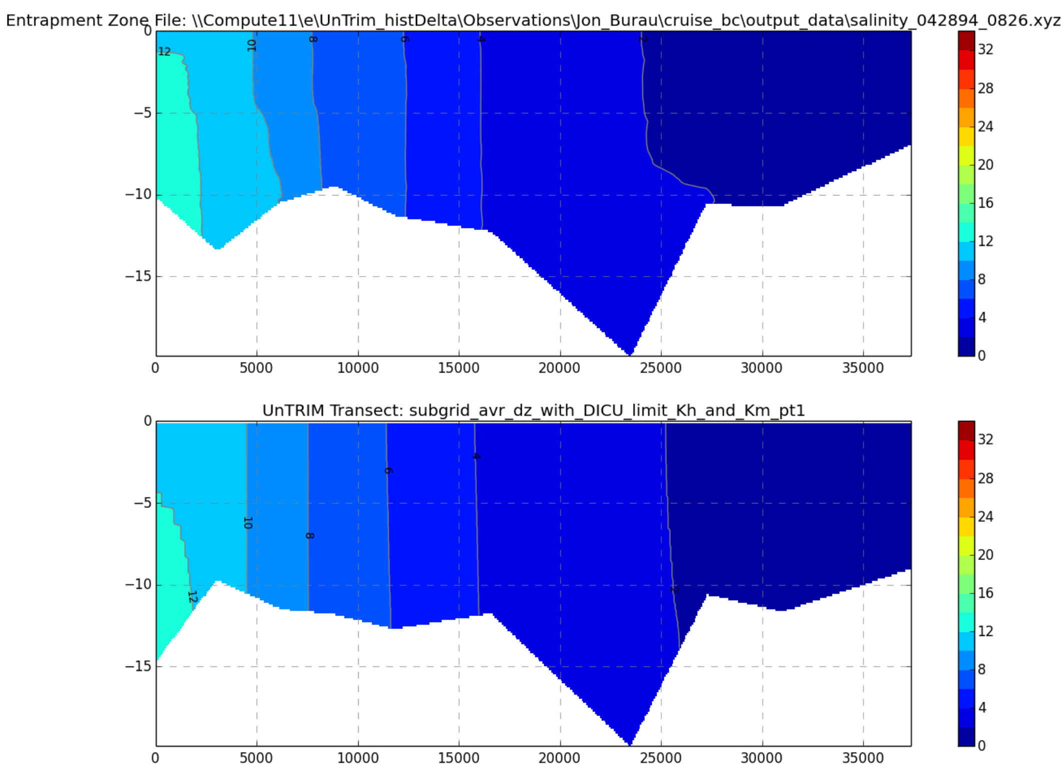

Figure 10-7 Entrapment Zone Study salinity transect (top) and corresponding UnTRIM modeled salinity for 28 April 1994 08:26. Transect extends from Port Chicago on the left to Emmaton on the right.

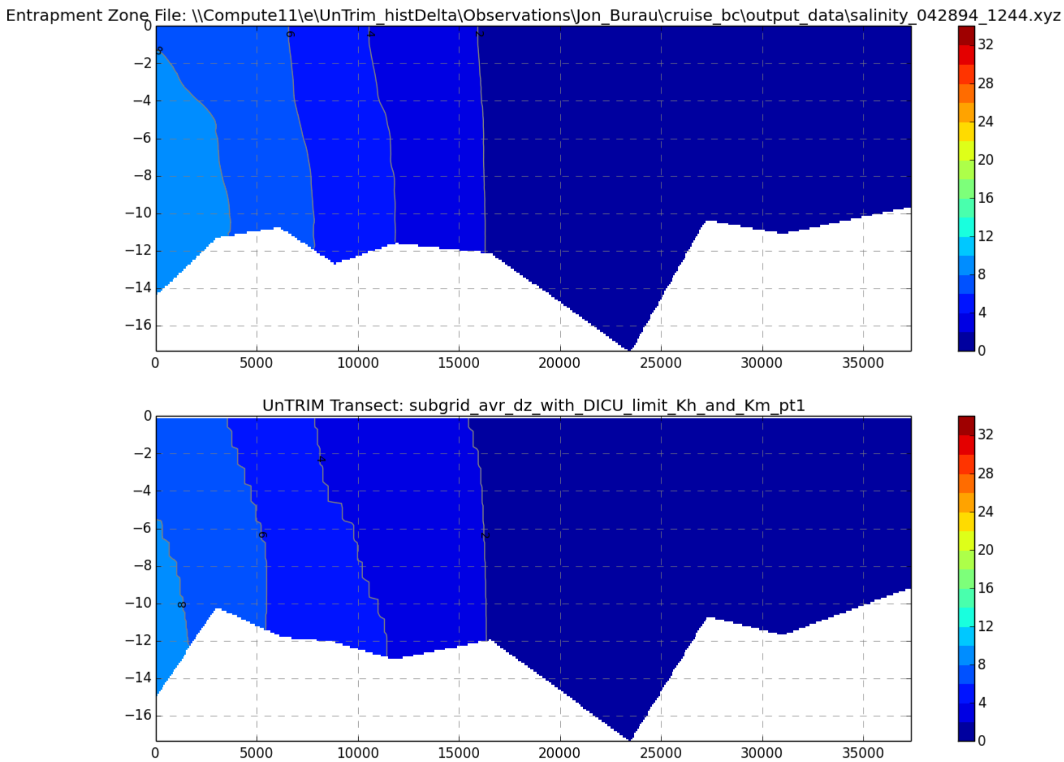

Figure 10-8 Entrapment Zone Study salinity transect (top) and corresponding UnTRIM modeled salinity for 28 April 1994 12:44. Transect extends from Port Chicago on the left to Emmaton on the right.

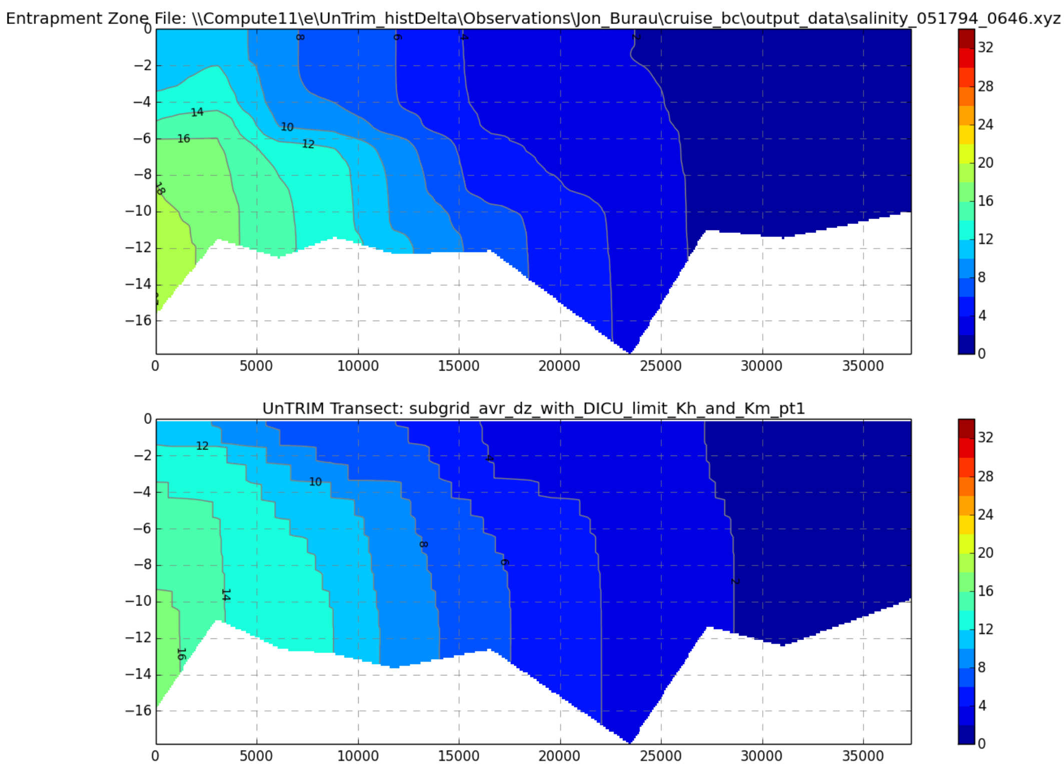

Figure 10-9 Entrapment Zone Study salinity transect (top) and corresponding UnTRIM modeled salinity for 17 May 1994 06:46. Transect extends from Port Chicago on the left to Emmaton on the right.

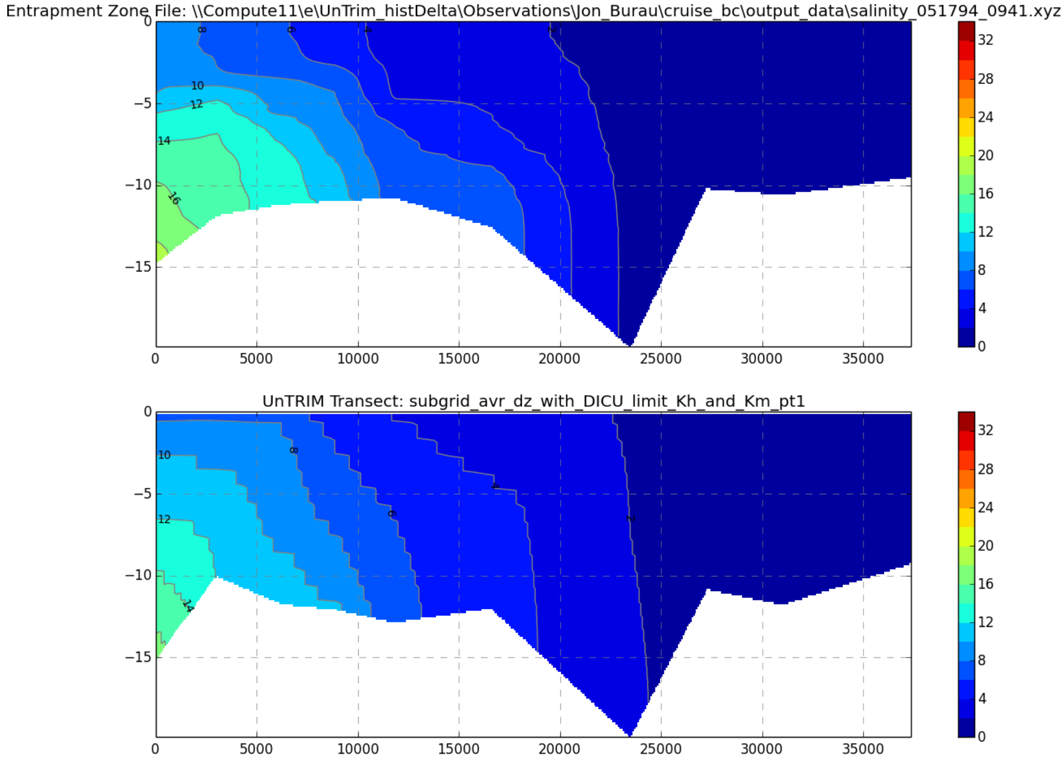

Figure 10-10 Entrapment Zone Study salinity transect (top) and corresponding UnTRIM modeled salinity for 17 May 1994 09:41. Transect extends from Port Chicago on the left to Emmaton on the right.

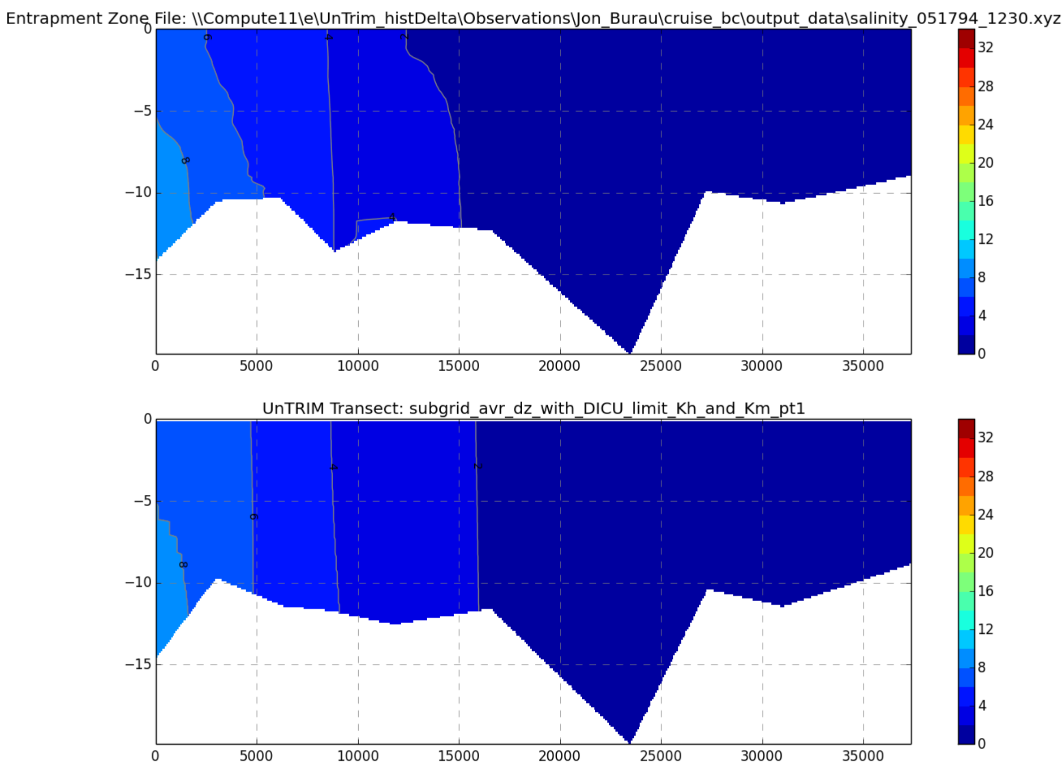

Figure 10-11 Entrapment Zone Study salinity transect (top) and corresponding UnTRIM modeled salinity for 17 May 1994 12:30. Transect extends from Port Chicago on the left to Emmaton on the right.

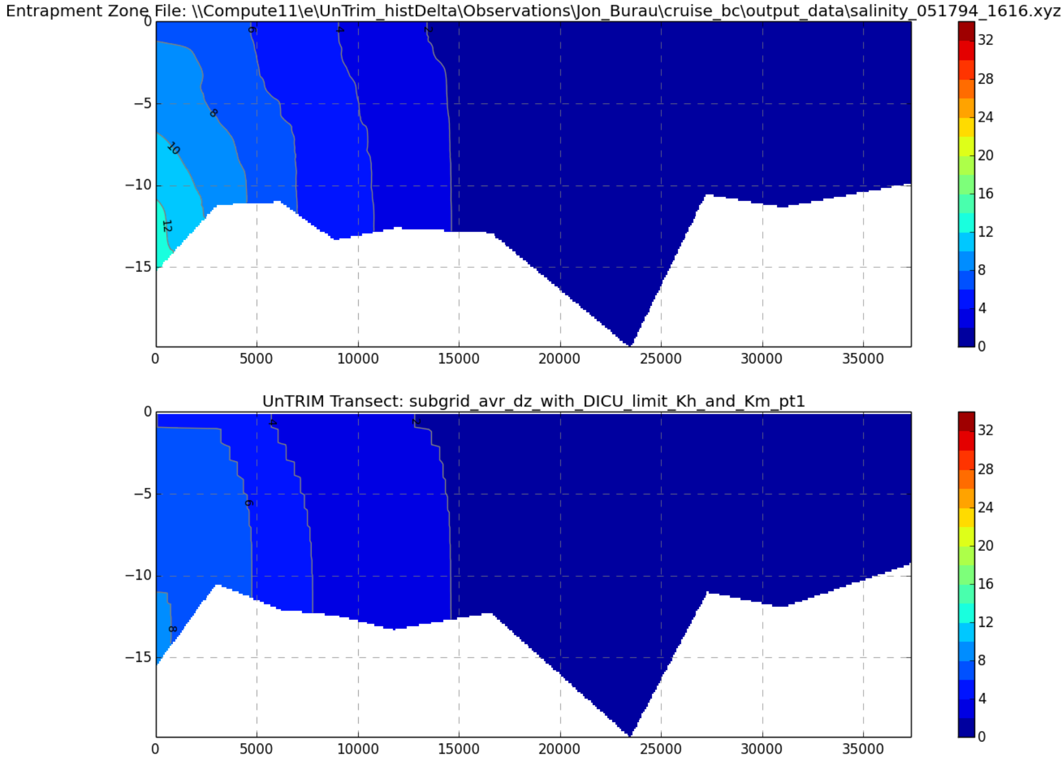

Figure 10-12 Entrapment Zone Study salinity transect (top) and corresponding UnTRIM modeled salinity for 17 May 1994 16:16. Transect extends from Port Chicago on the left to Emmaton on the right.

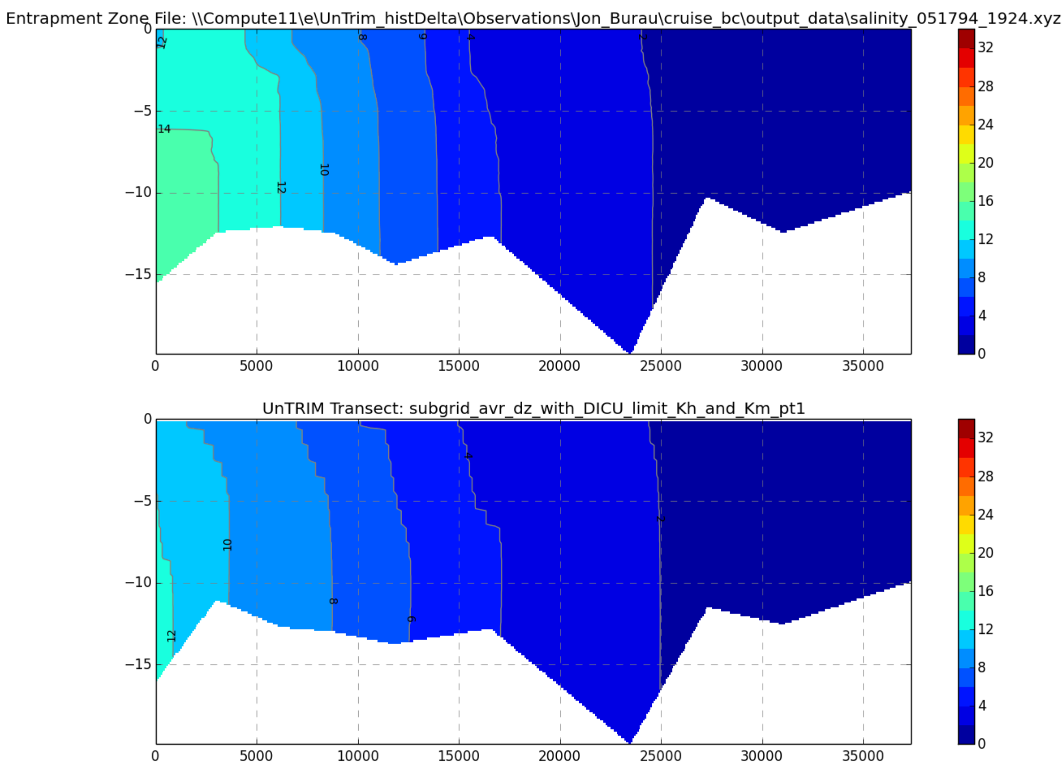

Figure 10-13 Entrapment Zone Study salinity transect (top) and corresponding UnTRIM modeled salinity for 17 May 1994 19:24. Transect extends from Port Chicago on the left to Emmaton on the right.

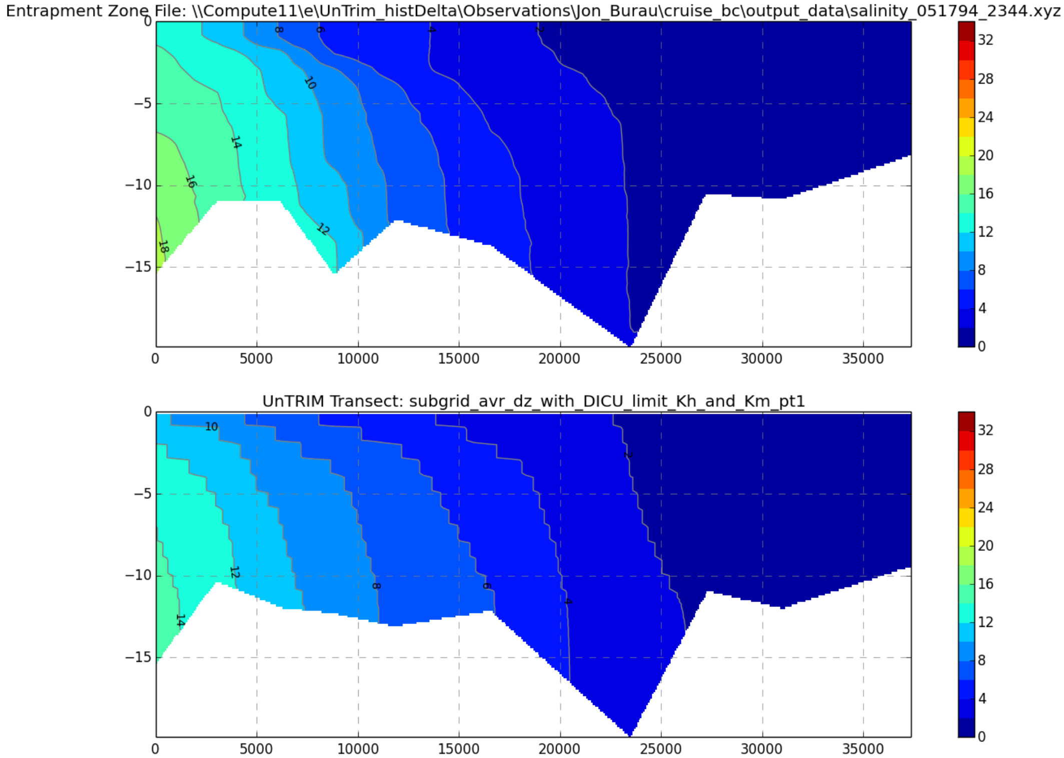

Figure 10-14 Entrapment Zone Study salinity transect (top) and corresponding UnTRIM modeled salinity for 17 May 1994 23:44. Transect extends from Port Chicago on the left to Emmaton on the right.

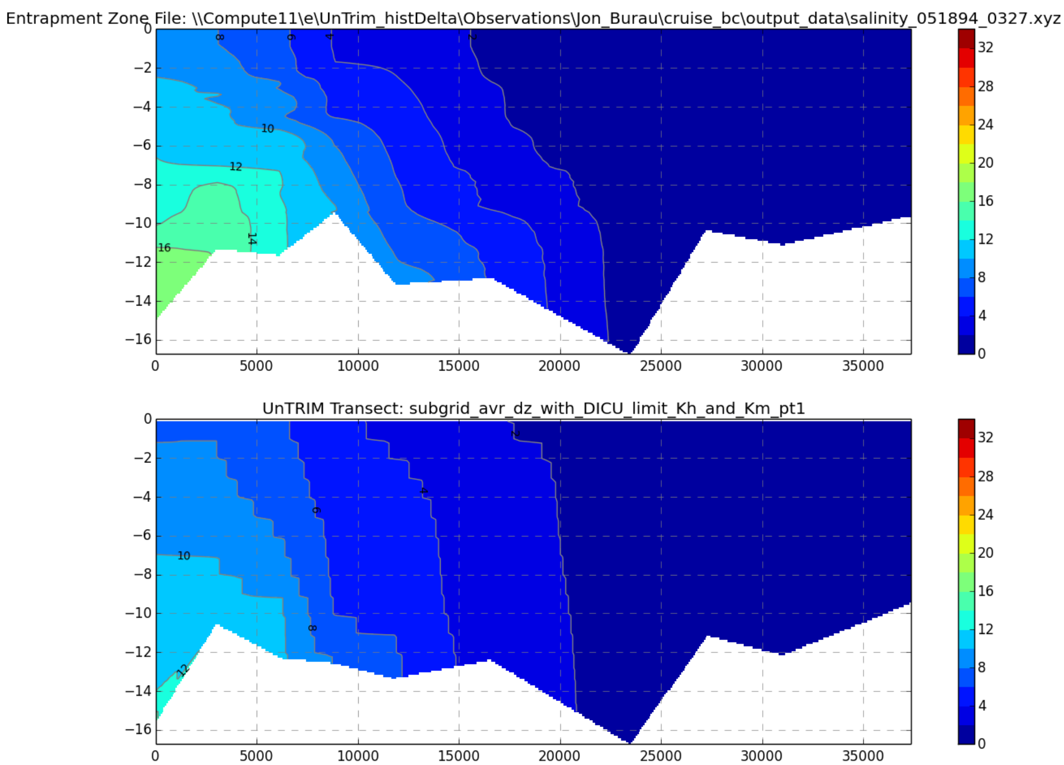

Figure 10-15 Entrapment Zone Study salinity transect (top) and corresponding UnTRIM modeled salinity for 18 May 1994 03:27. Transect extends from Port Chicago on the left to Emmaton on the right.

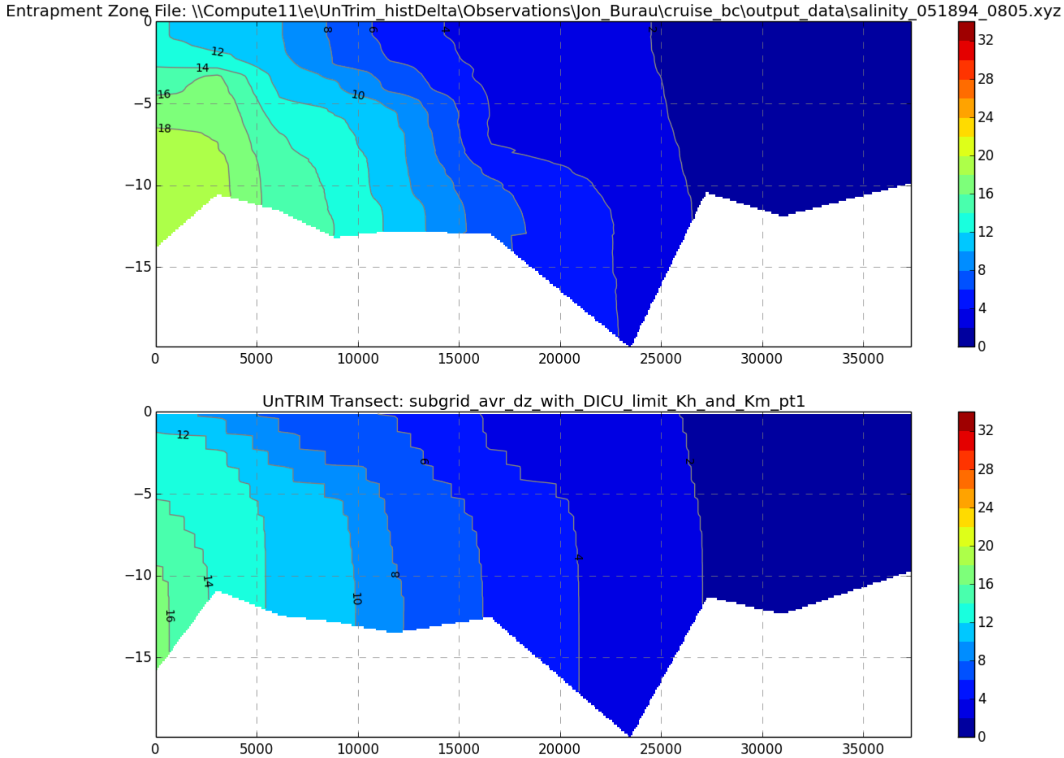

Figure 10-16 Entrapment Zone Study salinity transect (top) and corresponding UnTRIM modeled salinity for 18 May 1994 08:05. Transect extends from Port Chicago on the left to Emmaton on the right.

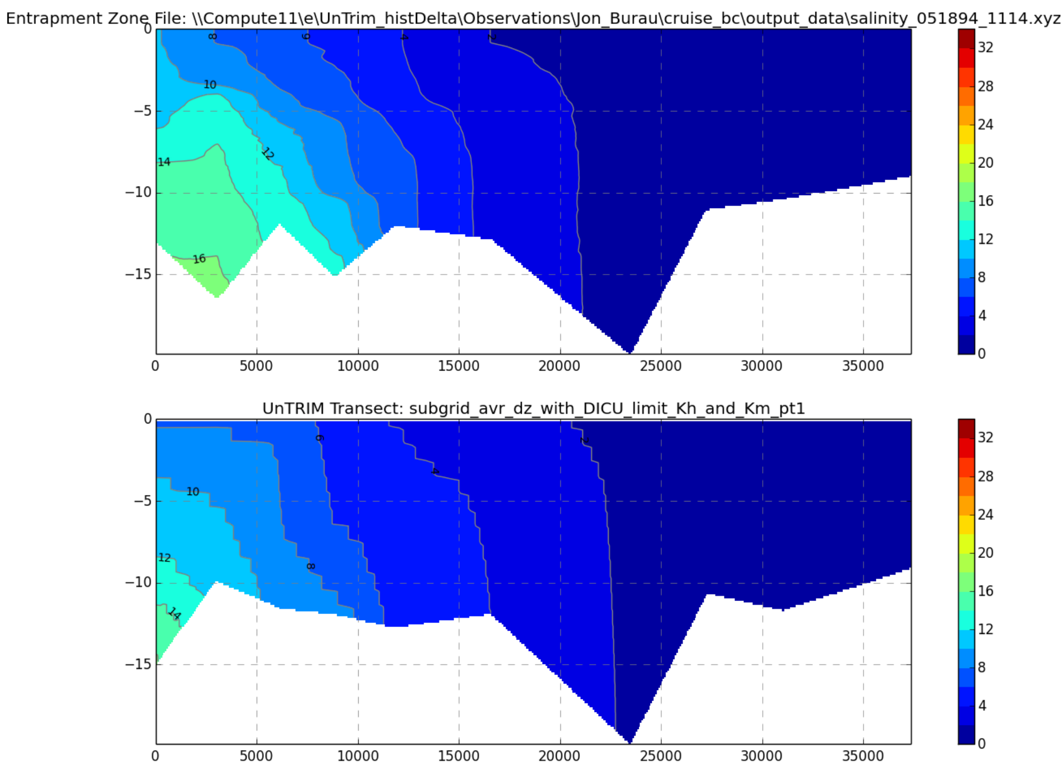

Figure 10-17 Entrapment Zone Study salinity transect (top) and corresponding UnTRIM modeled salinity for 18 May 1994 11:14. Transect extends from Port Chicago on the left to Emmaton on the right.

11 Appendix C: Historical DEM Artifact Types

Phase I modeling of the historical Bay-Delta stopped short of fulfilling the ultimate project objective of characterizing the historical Delta salinity regime due to problems with the historical Delta DEM. The problems stemmed from unrealistic channel geometries and bathymetries which were introduced in the DEM creation process. The resulting UnTRIM grid incorporated these artifacts through the grid creation process, consequently producing unrealistic flow results in the Phase I historical Bay-Delta model runs. The first task of the Phase II work will be to remove the DEM artifacts. A short description of the types of artifacts, along with postulates as to their origins, is given below.

Channel width–depth relationship pinch points: Many lower order streams of the historical Delta lacked available data from which to estimate their depths. In order to create realistic depths for these channels, a regression was developed between the channel width and depth. Width-depth data from channels throughout the Delta were used for this regression. The logic behind this regression was that wider channels were often bigger rivers and would thus be deeper. The regression worked well to predict depths between different channel systems, but created unrealistic channel configurations within the same channel reach. Whereas a river in the real world would respond to a decrease in width with an increase in depth (in order to maintain the same conveyance), the DEM channels decreased both in width and depth. This led to pinch points which greatly restricted flow in major channels throughout the Delta. Examples are shown in Figure 11-1 and Figure 11-2.

Channel width isotropic interpolation: In many locations, channel boundaries were interpolated in the DEM isotropically; i.e., they were not interpolated to follow the contours of the channel centerline. This method produces a ragged-looking edges to the DEM channels, and results in artificial channel constrictions and artificially high channel roughness. An example of this artifact is shown in Figure 11-3. Some constrictions are severe enough to create channel cutoffs (see Figure 11-4).

Artificial groins at junctions: The interpolation method used at channel junctions creates artificial structures resembling groins (Figure 11-5). Similar to actual groin structures, these artifacts restrict flow and increase channel roughness.

Bathymetric data interpolation to assumed parabolic channel bottom junctions: Two methods of setting the cross-channel bathymetry were used in the creation of the DEM: interpolation of historical sounding data and parabolic bottom construction based on the channel width. Sounding data were used as the primary method where available. Transitions between the two methods resulted in abrupt longitudinal changes in channel bathymetry in the DEM. These abrupt changes in bathymetry have consequences for the flow and salinity transport through these areas. Examples of two such junctions are shown in Figure 11-6.

Interpolation effects at edges of DEM: The method of interpolating bathymetries for the marsh plains needs to take into account the edge of the DEM. Interpolation around the DEM edges created some artifacts, including bands of unrealistically high or low elevations. These low elevation areas can result in ponding of water at the edges of the historical model grid. Examples are shown in Figure 11-7 and Figure 11-8.

“**Gridded look” to marsh plains:** Artifacts were created that gave the marsh plain elevations in certain areas of the DEM a “gridded look.” This may be related to the procedure used to create elevation changes as distance from the channel increases. The hydrodynamic results of these artifacts are unrealistic flow and drainage patterns on the affected marsh plain areas. An example is shown in Figure 11-9. The South Delta and Cache Slough Complex are particularly affected by this type of artifact.

Zero slope marsh plain: This DEM artifact relates to areas where the marsh plain elevation has zero or approximately zero slope. Once these areas of the Delta are inundated, they take a very long time to drain because of the lack of any significant slope. Although no example figure is given for this artifact, it is prevalent throughout the marsh plain areas in the DEM.

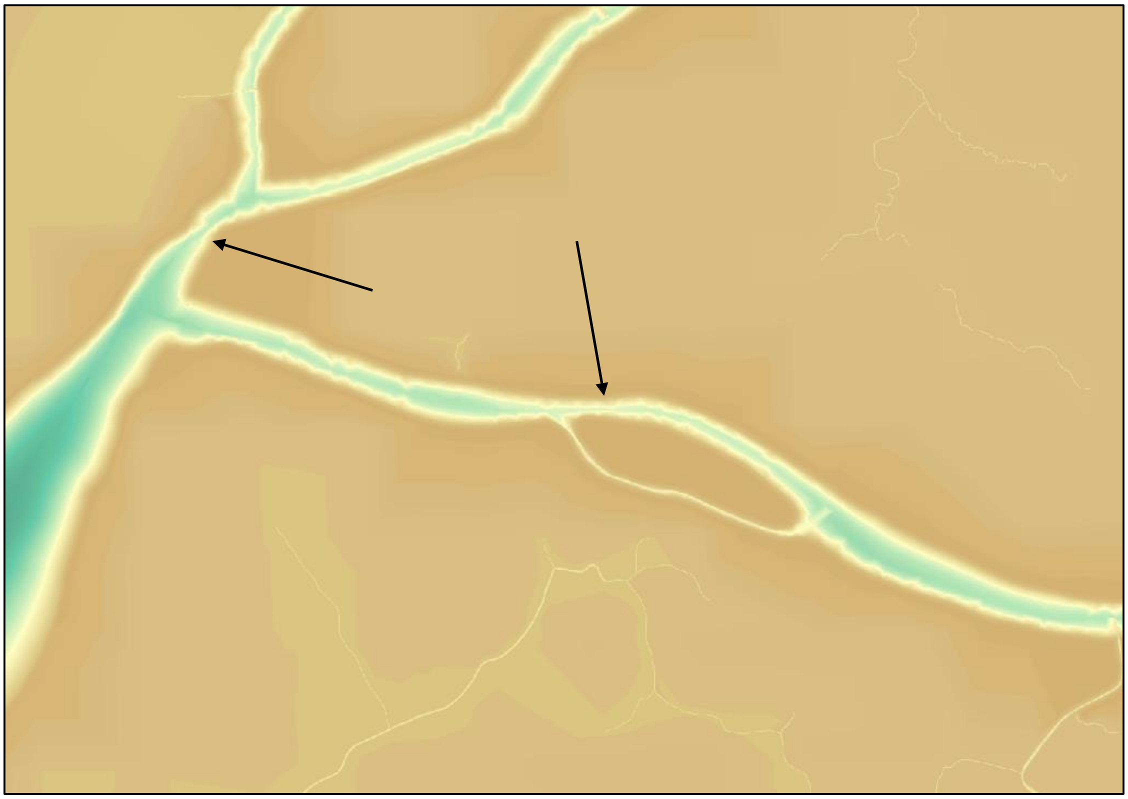

Figure 11-1 Historical DEM artifact example: pinch points caused by use of channel width - depth regression. Grid is shown near Sacramento – Cache Slough confluence.

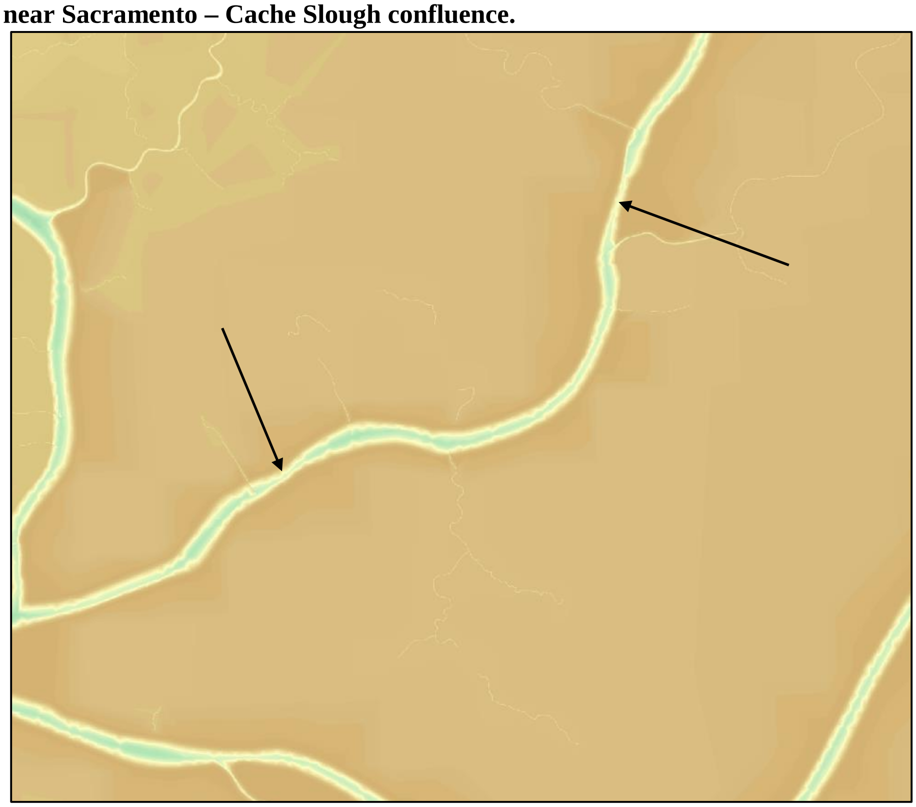

Figure 11-2 Historical DEM artifact example: pinch points caused by use of channel width - depth regression. Grid is shown near Sacramento – Cache Slough confluence.

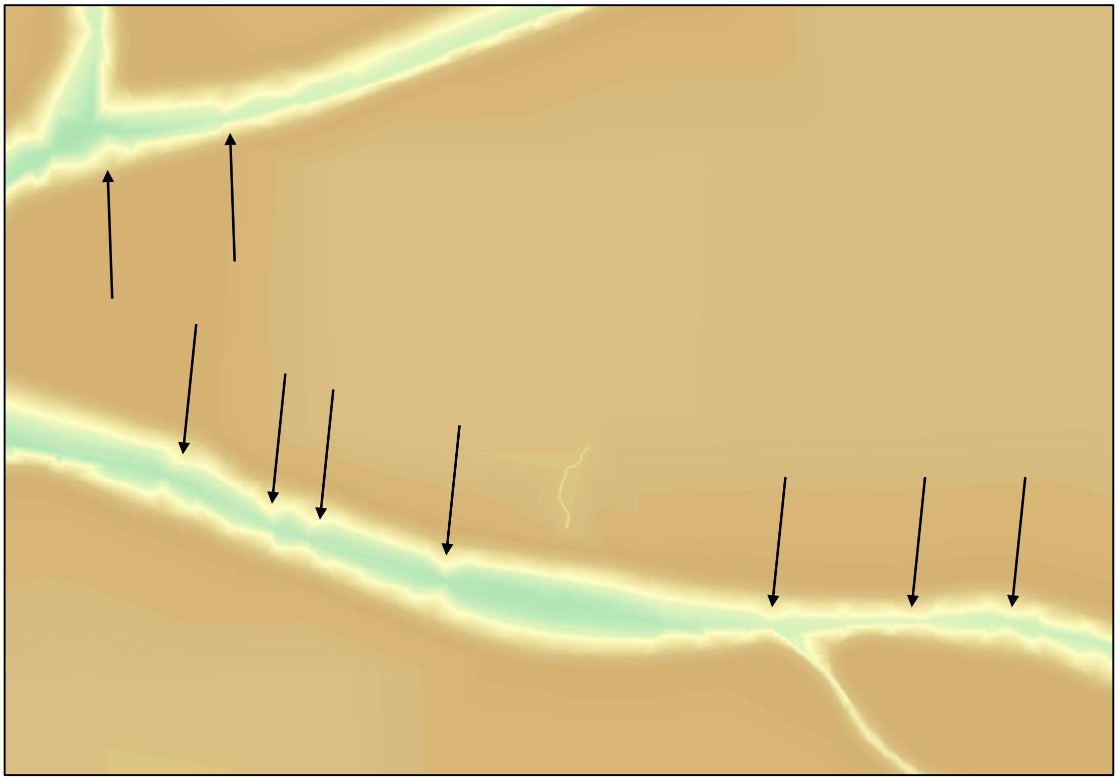

Figure 11-3 Historical DEM artifact example: pinch points caused by isotropic interpolation method. Grid is shown near Sacramento – Cache Slough confluence.

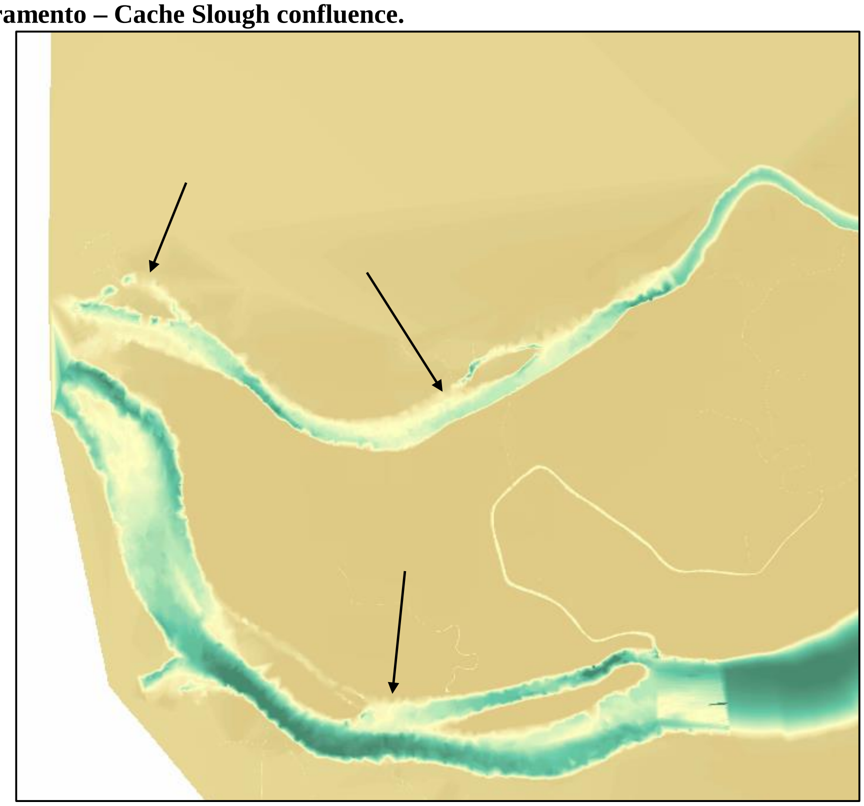

Figure 11-4 Historical DEM artifact example: channel cutoffs caused by isotropic interpolation method. Grid is shown near the Sacramento-San Joaquin confluence.

Figure 11-5 Historical DEM artifact example: artificial groins caused by interpolation near junctions. Grid is shown near Sacramento – Cache Slough confluence.

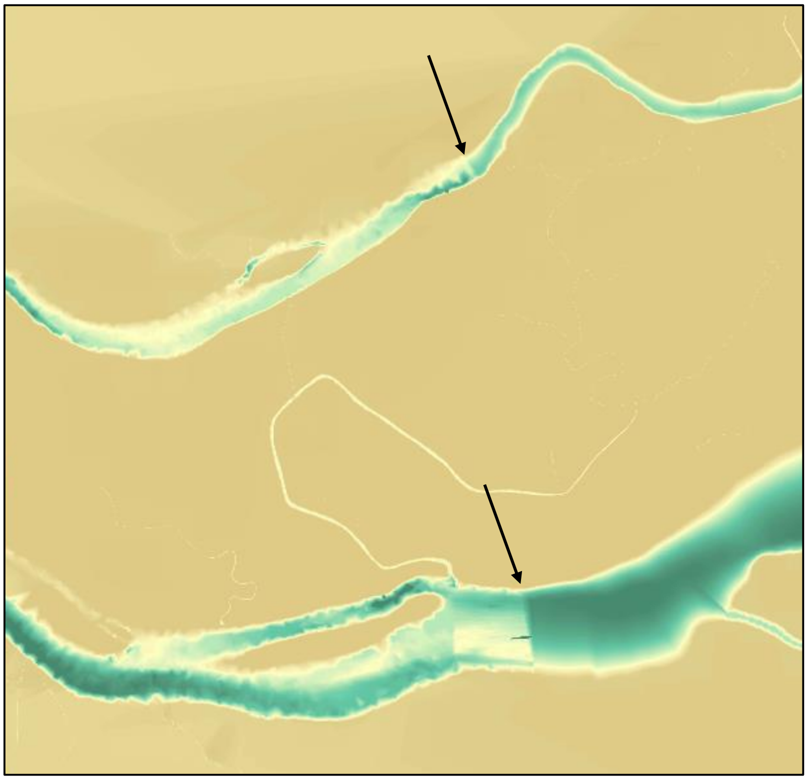

Figure 11-6 Historical DEM artifact example: sharp bathymetric transitions where channel interpolation method transitions from use of measured data to a parabolic channel assumption. Grid is shown near the Sacramento-San Joaquin confluence.

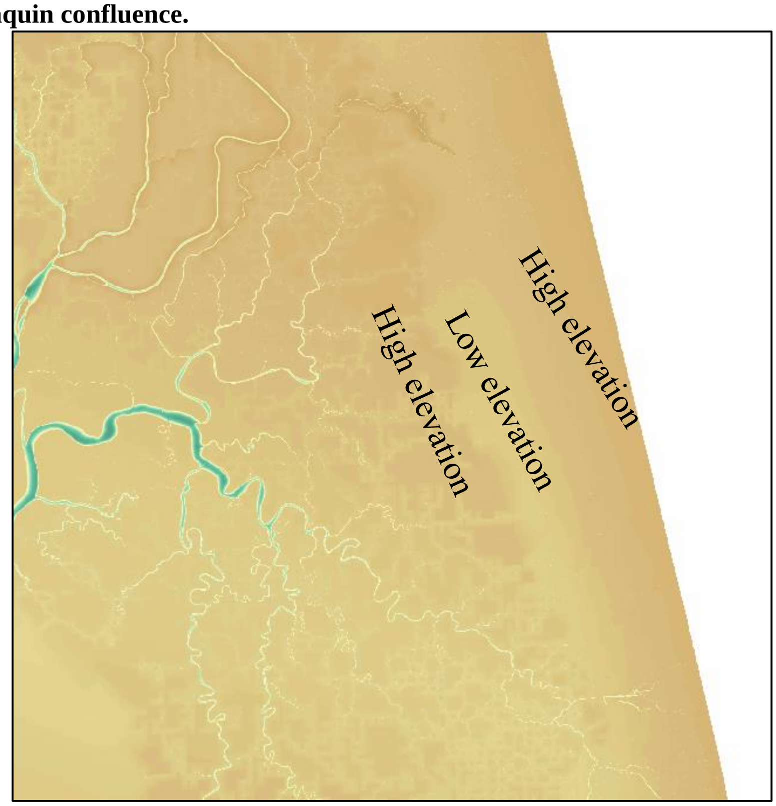

Figure 11-7 Historical DEM artifact example: unrealistic elevation transitions caused by interpolation near DEM boundaries.

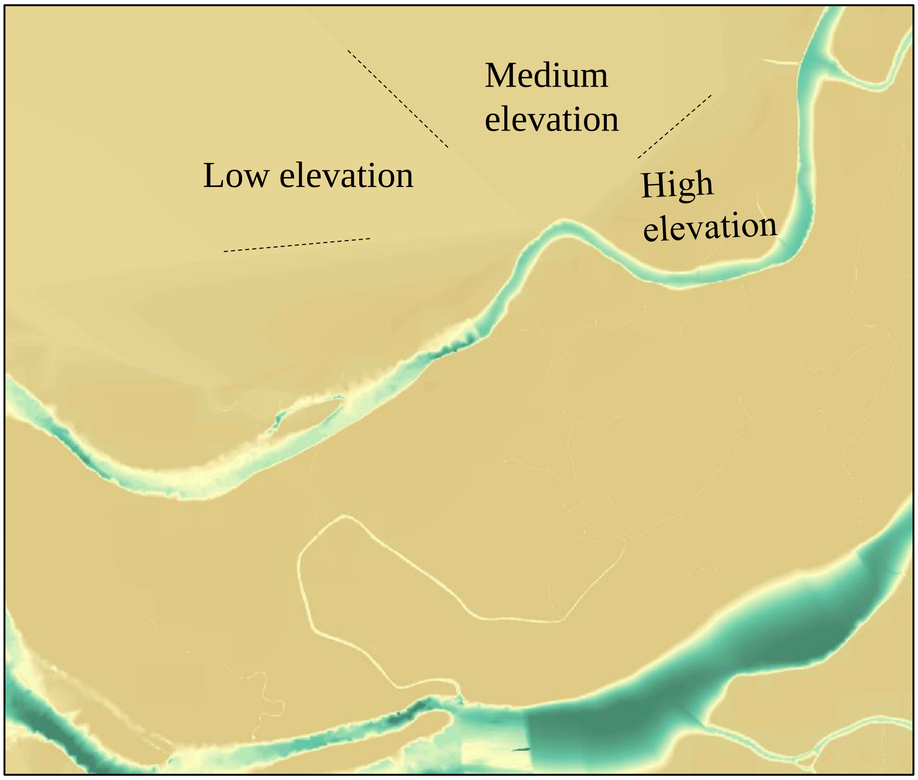

Figure 11-8 Historical DEM artifact example: unrealistic elevation transitions caused by interpolation near DEM boundaries. Grid is shown near the Sacramento-San Joaquin confluence.

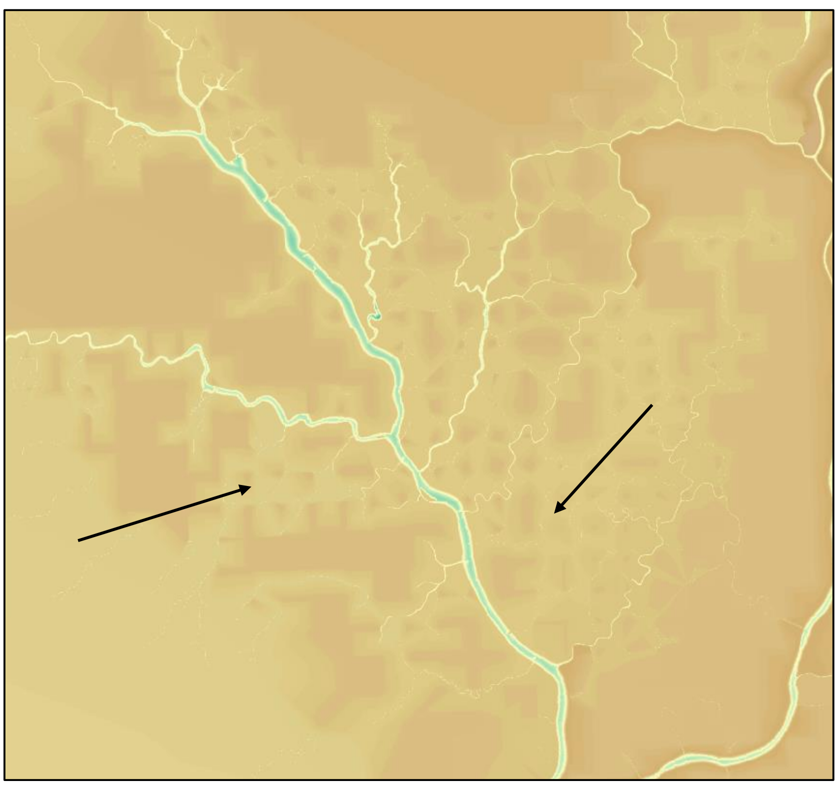

Figure 11-9 Historical DEM artifact example: "gridded look" marsh plain elevations caused by use of buffering to create elevations. Grid is shown near the Cache Slough Complex.